

ISBN 978-83-66216-28-0

G.N. MUSINA, M.K. IBATOV, A.T. TAKIBAYEVA,
ZH.B. RAKHIMBERLINOVA, M.I. BAYKENOV

CHEMICAL TECHNOLOGY IN PRODUCTION

MONOGRAPH



 iScience

WARSAW, POLAND - 2020

KARAGANDY STATE UNIVERSITY NAMED AFTER EA BUKETOV,
KARAGANDA STATE TECHNICAL UNIVERSITY

G.N. MUSINA, M.K. IBATOV, A.T. TAKIBAYEVA,
Zh.B. RAKHIMBERLINOVA, M.I. BAYKENOV

CHEMICAL TECHNOLOGY IN PRODUCTION

MONOGRAPH

Warsaw-2020

*Authors: G.N. Musina, M.K. Ibatov, A.T. Takibayeva,
Zh.B. Rakhimberlinova, M.I. Baykenov.*

Musina G.N., Chemical technology in production / G.N. Musina, M.K. Ibatov, A.T. Takibayeva, Zh.B. Rakhimberlinova, M.I. Baykenov – Warsaw: iScience Sp. z o. o., 2020 - 145 p.

In this book, the optimal conditions for catalytic-cavitation treatment of primary coal tar in the presence of pseudohomogeneous catalytic additives have been determined. Using elemental structural analysis, thermodynamic indicators and the formation enthalpy for the primary tar and its narrow fractions were calculated. The main directions of rational processing of this type of hydrocarbon feedstock were determined. A mechanism for the conversion of hexane, which proceeds according to a free-radical mechanism, initiated by the phenomenon of cavitation has also been proposed.

ISBN 978-83-66216-28-0

© G.N. Musina, M.K. Ibatov,
A.T. Takibayeva, Zh.B. Rakhimberlinova,
M.I. Baykenov, 2020
© iScience Sp. z o. o.

CONTENTS

| | |
|---|----------|
| INTRODUCTION | 5 |
| CHAPTER 1. CONDUCTING A REVIEW OF SCIENTIFIC AND TECHNICAL AND PATENT LITERATURE TO ASSESS THE POSSIBILITY OF PROCESSING THE ORGANIC MASS OF COAL AND A HEAVY OIL RESIDUE..... | |
| 1.1 Processing of coal tar and hydrogenation of coal | 6 |
| 1.2 Catalysts for the processing of heavy hydrocarbon raw materials | 6 |
| 1.3. Physical and chemical processes of cavitation exposure in liquid media | 20 |
| 1.4 Heavy oil residues | 22 |
| 26 | |
| CHAPTER 2. CATALYSTS FOR HYDROGENIZATION OF SOLID HY-DROCARBON RAW MATERIAL | |
| 2.1 Physico-chemical properties of iron sulphides | 34 |
| 2.2 synthesis of iron sulfide solid solutions-catalysts for the hydrogenation of heavy hydrocarbons | 35 |
| 2.3 Hydrogenation of coal in the presence of iron sulfide catalysts | 38 |
| 2.4 Mathematical description of the hydrogenation of coal in the presence of heterogeneous catalysts | 43 |
| 2.5 Optimization of the process of hydrogenation of coal deposits of Karazhar | 52 |
| 2.6 Thermochemical and thermodynamic calculation of iron-containing catalysts..... | 57 |
| 62 | |
| CHAPTER 3. DEVELOPMENT OF AN EXPERIMENTAL METHODOLOGY AND ANALYSIS OF THE RECEIVED PRODUCTS | |
| 3.1 Source materials and methods for the study of coal tar | 64 |
| 3.2 The method of catalytic cavitation treatment of primary coal tar and hexane..... | 64 |
| 3.3 Methods of viscometric measurements..... | 70 |
| 3.4 Methods of pycnometric measurements | 71 |
| 3.5 Equipment and methods for the hydrogenation of coal and a mixture of model organic compounds | 72 |
| 3.6 Methodology of elemental analysis | 73 |
| 3.7 Methods of processing experimental data..... | 73 |
| 3.7.1 Calculation of the structural and chemical indicators of primary coal tar..... | 74 |
| 74 | |

| | |
|---|------------|
| 3.7.2 Calculation of the heat of combustion and the enthalpy of formation | 76 |
| 3.7.3 Calculation of thermodynamic parameters..... | 78 |
| CHAPTER 4. CATALYTIC PROCESSES. HYDRAULIC EXPOSURE TO HEAVY OIL AND HEAVY HYDROCARBON RAW MATERIALS | 83 |
| 4.1 Catalytic methods for removing metals from crude oil..... | 83 |
| 4.2 Chemical composition of the products of catalytic hydrogenation (coal, high-viscosity oil, petroleum bitumen) | 86 |
| 4.3 Influence of the nature of catalysts on the chemical composition of liquid products | 88 |
| 4.4 Paramagnetic properties of coal, products of their catalytic hydrogenation | 94 |
| CHAPTER 5. KINETICS OF CATALYTIC HYDROGENIZATION OF HEAVY HYDROCARBON RAW MATERIALS AND HIGH-VELOCITY OIL | 99 |
| 5.1 Macrokinetics of the process of coal hydrogenation | 102 |
| 5.2 Investigation of the kinetics of thermal destruction of coal Kenderlyk and Shubarkol deposits..... | 106 |
| 5.3 The kinetics of hydrogenation of Karazhambas high-viscosity oil..... | 112 |
| 5.4 The kinetics of the process of hydrogenation of high-viscosity oil (fraction <200 °C | 117 |
| 5.5 Kinetic model of high-viscosity oil hydrogenation | 119 |
| 5.6 Kinetics of demetallization of highly viscous oil | 124 |
| CHAPTER 6. DEVELOPMENT OF THE THEORY OF THE ORGANIC CAVITATION OF COAL AND A HEAVY OIL RESIDUE..... | 127 |
| 6.1 Influence of catalytic-cavitation treatment on the individual chemical composition of the primary coal tar..... | 127 |
| 6.2 Catalytic cavitation treatment of a model object (hexane) in the presence of β -FeOOH, Fe (OA) 3 nanocatalysts..... | 133 |
| CONCLUSION | 136 |
| LIST OF USED SOURCES | 137 |

INTRODUCTION

The primary coal tar obtained in the process of semi-coking is very similar in structure and appearance to the functional groups and structural fragments with the organic mass of the original coal. For the primary coal tar is characterized by the presence of organic substances with a wide range of molecular weights. Primary coal tar is characterized by a high content of phenols 20-30 %, represented by o-cresol, p-cresol and 1,3,5-xylenol. Primary coal tar is obtained under conditions that exclude their high temperature pyrolysis, which allows the tar to be used as a raw material for industrial organic synthesis and is of great interest for creating the scientific foundations of the process of fossil coal destruction.

Coking tar is used in industry, which consists mainly of polycyclic aromatic hydrocarbons and high-molecular compounds, but the primary coal tar in Kazakhstan and the CIS countries do not find industrial use for the production of commercial products and organic raw materials. In industry benzene, toluene, naphthalene, phenols, as well as pyridine bases are obtained from a coke-chemical tar using hydrotreatment extraction. To obtain the above chemicals from the coke tar, repeated fractionation operations, hydrotreating are used, therefore, the use of cavitation in the presence of pseudohomogeneous catalytic additives (PHCA) for processing the primary CT with the aim of increasing the yield and improving the quality of the chemical products obtained is a big task that has a practical significance. Heavy oil residue (HOR) is the residue in the refining process. Due to the high content of metals, sulfur and asphaltenes, it is not used in the oil refining industry. In this regard, the primary processing of coal tar and HOR by direct hydrogenation is an urgent task that confronts researchers working in this field.

1. CONDUCTING A REVIEW OF SCIENTIFIC AND TECHNICAL AND PATENT LITERATURE TO ASSESS THE POSSIBILITY OF PROCESSING THE ORGANIC MASS OF COAL AND HEAVY OIL RESIDUE

1.1 Processing of coal tar and hydrogenation of coal

In the Republic of Kazakhstan and abroad, chemical products from coal are produced, mainly, using the processes of thermal destruction of coal — coking and semi-coking. Coal (coke) tar, consisting mainly of condensed aromatic hydrocarbons and other high-molecular compounds, is the most difficult to process high-boiling hydrocarbon feedstock [1].

In industry, the tar is subjected to dehydration and distillation into separate fractions, from which phenols, pyridine bases, benzene, naphthalene, and other chemical products are obtained by alkaline and acidic extraction, crystallization, and hydro purification methods. Currently, the processing of the tar is carried out in order to obtain commercial products which quality conforms to the requirements of the standards. The light fraction of the tar is usually processed with heavy benzene, the middle fraction is used as a source of raw materials for the production of phenols, nitrogenous bases, the naphthalene fraction is considered as a source of valuable phenolic raw materials.

Extraction of phenols and bases is based on their acidic and basic properties and ability to form with aqueous solutions of alkalis (for example, NaOH) and sulfuric acid, respectively, water-soluble salts phenolates:



Phenols are weak acids. In the coking industry, the dephenolization of coal tar fractions is carried out with an aqueous solution of sodium hydroxide. The technology for producing phenols from a fraction includes a series of phased operations.

To extract phenols from hydrogenation products, the authors of [2] propose 70% aqueous solutions of lower alcohols, ethanol, as an extractant. The content of phenols in the coal tar fraction ranges from 5 to 20%. The report shows studies of the process in a continuous countercurrent using aqueous ethanol as the extractant. Liquid coal hydrogenation products served as the raw material for dephenolization (60240 and 100 240°C fractions with a phenol content of 9 to 12,5%).

Analysis of the literature [2-6] has shown that the use of ethanol as an extract for suppressing phenols from coal products is more promising than using traditional extractant — sodium hydroxide. Extraction of phenol with

sodium hydroxide is associated with a number of technological problems: a multistage process, the use of mineral acids, etc. However, it should be noted that in the literature there is such fragmentary information about the extraction of phenols from coal tar with the help of tanol.

As can be seen from the literature review [2-6], the extraction of phenols from primary coal tar is not fully considered and requires further research.

Pitch fractions of tar with b.p. above 350°C are used directly as a binder in the production of electrode products or is preliminarily subjected to oxidation to increase the softening temperature and increase the yield of pitch coke [7].

Each stage of chemical separation of their products is accompanied by the use of repeated distillations, high consumption of heat and reagents and loss of valuable products, such as naphthalene. A number of valuable chemical products, for example, 2,6-dimethylnaphthalene, due to the low content and high cost of isolation is not currently performed.

Currently, in connection with the tightening of the quality requirements for raw materials for organic syntheses, the growing need for benzene and naphthalene, research and experimental work are being actively carried out to improve the hydro-processing processes of coke chemical raw materials.

The semi-coking tar is a "primary" tar formed during the thermolysis of fossil coal in the temperature range of 400–600°C, while the organic components are practically not subjected to secondary transformations. During high-temperature processing (coking), the "primary" tar is subjected to secondary thermal transformations when passing through a layer of coal charge and high-carbon material, at a temperature of 800-900°C [1, 2].

In the industrial conditions of the semi-coking process, the secondary impact on the primary tar is insignificant, and its physicochemical and technical characteristics are close to those for primary coal tar. The yield of high-temperature coking tar does not exceed 3-3.5% per load, which is significantly lower than the output of the "primary" 8-10% [34]. For example, the tar yield in semi-coking of the Cheremkhovo coal is 8–9% by dry weight of the mixture, the density is 999-1058 kg/m³. The tar contains (%): nitrogen-containing bases 1.9-2.9, phenols 20-33% [1].

The components of the primary tars are similar in structure and character to the fragments of the organic mass of coal. Tars are characterized by the presence of compounds in a wide range of molecular weights, relatively unstable compounds with heteroatoms, with phenolic hydroxyls and double bonds [1]. Aromatic compounds are represented by highly substituted hydrocarbons having from one to four rings [2]. The primary peat

gum contains low molecular weight aliphatic hydrocarbons, which can be used in the production of motor fuels and lubricating oils after cleaning. In general, the composition of the tar will be determined by the final temperature of the process. As the temperature increases, the tar is enriched in carbon and nitrogen (Table 1).

Table 1
Outlet and elemental with remaining tars of semi-coking peat

| Indicat or | до 350°C | 300- 350°C | 350- 400°C | 400- 450°C | 450- 500°C | 500- 550°C |
|---|-------------|---------------|---------------|---------------|---------------|---------------|
| Tar yield,% for dry peat | 1,11 | 2,27 | 3,31 | 1,95 | 0,89 | 0,71 |
| The elemental composition of the tar | | | | | | |
| C | 77,15 | 79,35 | 79,93 | 77,85 | 79,10 | 80,66 |
| H | 10,77 | 10,51 | 10,63 | 8,78 | 8,92 | 9,17 |
| N | 0,61 | 0,68 | 0,66 | 0,88 | 1,10 | 1,14 |
| O + S | 11,47 | 10,46 | 8,78 | 12,49 | 10,88 | 9,03 |

The composition of the semi-coking tar includes phenols. The need for phenols is constantly growing due to the expanding production of phenol-formaldehyde tars, synthetic detergents, disinfectants and many other products.

When semi-coking peat are formed in significant quantities of tar (pitch). Tar is a valuable chemical raw material enriched with phenols. Their content on the tar is 16-20 % (1.6-2% by weight of peat). So, with the semi-coking of peat, the yield of phenols is (%): monatomic 0.127, polyatomic 0.281. Phenols of semi-coking contains, along with phenol, significant amounts of o-cresol, p-cresol (80-85%). Also, they contain a lot of 1,3,5-xylenol, which is a scarce raw material for the production of fire-resistant turbine liquid – trixylenyl phosphate [5].

A distinctive feature of the primary tars from high temperature tars is the absence of 1 fraction, representing a high-carbon component, insoluble in quinoline. This fraction is formed from the vapors of the tar compounds in the space of the coke oven batteries at temperatures above 800°C [4].

At present, there are no technologies for processing semi-coking tars in the coal industry to produce a wide range of marketable products. In the process of processing tars there are difficulties associated with the coking of equipment. This leads to frequent stopping of process units.

As an example, to solve the complex task of processing a semicoking tar, industrial experience can be used to process a weakly pyrolyzed tar from combustible shale [5, 6] and various semi-coking tars and the production of molded coke [6].

Coal tars have a (pitch coke) one of the products of the process of coking coals. It is a viscous black liquid with a characteristic phenolic odor, the density is 1120-1250 kg/m³, the output during coking is ~ 3% by weight of coal.

Coal tar and has a complex chemical composition: aromatic, heterocyclic compounds and derivatives boiling away over a wide range of temperatures. In addition, the tar contains a number of unsaturated compounds and saturated hydrocarbons of the fat and hydroaromatic series. The composition of coal tar from different factories is of the same type, it depends not on the composition of the coal, but on the mode of the process. Currently, more than 400 individual compounds have been isolated from coal tar.

Primary processing of coal tar is carried out at coking plants. The resin is subjected to distillation into narrow fractions (Table 2) in installations that include a tube furnace and distillation columns to separate the distillate into fractions [7]. Individual substances are extracted from the coal tar fractions by crystallization or by treatment with reagents (for example, an alkali solution in the extraction of phenols). Due to the large number of components in the fractions by one rectification, it is impossible to obtain any component with a sufficiently high yield; therefore, obtaining separate products from the tar is achieved by a combination of different methods.

The heavy fraction is the residue after the craving. It is used as absorbers of benzene products from coke oven gas, for preserving wood, producing carbon black, and other purposes. Peck (the residue after separation of coal tar into fractions) is used to make electrode coke, coatings, and bonding materials.

A variety of pharmaceutical preparations are synthesized by being based on the processing of coal tar streptocid, sulfidin, pyramidone, phenacetin, aspirin; plastics, individual products (naphthalene, anthracene, to a lesser extent phenols) are manufactured [8].

Table 2
Composition coal tar

| Fraction | Yield, masses. % | Temperature range of boiling, °C | Density (at 20°C), kg/m ³ | Emittable substances |
|----------|---------------------|--|--|----------------------------|
| Light | 0,2-0,8 | h.k.-170 | 900-960 | Benzene and its homologues |
| Phenolic | 1,7-2,0 | 170-210 | 1000-1010 | Phenols, pyridine bases |

| Fraction | Yield, masses. % | Temperature range of boiling, °C | Density (at 20°C), kg/m³ | Emittable substances |
|--------------------|------------------|----------------------------------|--------------------------|---|
| Naphthalene | 8,0-10,0 | 210-230 | 1010-1020 | Naphthalene, thioneften |
| Heavy (absorption) | 8,0-10,0 | 30-270 | 1050-1070 | Methylnaphthalenes, acenaften |
| Anthracene | 20,0-25,0 | 270-360 (up to 400) | 1080-1130 | Anthracene, phenanthrene, carbazole, etc. |
| Peck | 50,0-65,0 | Above 360 | 1200-1300 | Pyrene and others. Highly condensed |

Industrial processing of low-pyrolyzed tars is focused on the production of fuels, phenols, technical mixtures.

On an industrial scale, a number of technological schemes for the processing of semi-coking tars has been carried out. For example, industrial distillation of low-temperature tar was carried out in England at Balzover Plant [8]. The following products are obtained (%): light oil 2, medium oil 38, heavy oil 30, peck 25, water and losses 5. The composition of the obtained oil distillates is given in table 3 [9].

Table 3

The composition of the composition of the narrow fractions of semi-coke tar

| Indicators | Light oil | Medium butter | Heavy oil |
|-----------------|-----------|---------------|--|
| Content, mass.% | | | |
| Phenols | 12 | 45 | 35 |
| Hydrocarbons | 86 | 52 | 65 |
| including: | | | |
| saturated | 21.5 | 12.0 | Complex mixture of hydrocarbons of various types |
| olefinic | 34.5 | 14.0 | |
| aromatic | 30.0 | 26.0 | |
| Grounds | 2.0 | 3.0 | |

The light and medium oil fractions are further subjected to dephenolization and purification with concentrated sulfuric acid. After purification, the oils can be used as components of fuels. The oil fraction ($t_b = 200-314$ °C) is used as a flotation reagent for the enrichment of coal.

The dephenolization of oil fractions in this technology is carried out by alkaline extraction. Further processing of the selected phenols is similar

to the processing of raw phenols from high-temperature tar.

The proposed technology allows to obtain high-quality fuel products, phenols, binders. The main disadvantage of this technology is the high cost of the process, due to the use of highly efficient corrosion-resistant equipment.

The technology of shale tar processing was proposed at the "Slantsy" SPP (Kohtla-Jarva) [9]. According to this technology, mechanical impurities are removed from the tar in heat sinks under pressure; corrosive components (phenols and chlorides) are removed by washing with water and dispersed. During the distillation of the tar, the gasoline and diesel fractions, distillate fuel oil and the residue ($tb > 350^{\circ}\text{C}$) are selected. The output and characteristics of the fractions are given in table 4.

Table 4
Characteristics of shale tar distillates

| Product Name | The yield of the tar, % | Density, g / cm ³ | Fractional composition | | | | | |
|----------------------|-------------------------|------------------------------|--------------------------|-----|-----|-----|-----|-----|
| | | | Boils up to 0 C, (vol.%) | | | | | |
| | | | 170 | 200 | 250 | 300 | 320 | 360 |
| The original tar | | 0.97 | 14 | 23 | 33 | 41 | 46 | 55 |
| Gasoline fraction | 1.0 | 0.81 | 92 | - | - | - | - | - |
| Diesel fraction | 9.0 | 0.89 | - | 30 | 77 | - | - | - |
| Distillate fuel oil | 30.0 | 0.99 | - | - | 7 | 35 | 54 | 84 |
| Distillation residue | 59 | 1,035 | - | - | - | 2 | 5 | 15 |

The gasoline fraction after defenolation is used as a component of motor gasoline. The diesel fraction after defenolation mixed with the fuel oil fraction is a good wood preservative.

Heavy residue is used as a raw material for coking, as well as for the production of road bitumen. The resulting coke has a low ash content (0.5-0.6%) and used for the manufacture of electro-carbon and graphitized products for electrometallurgy. For preparation of road bitumen residue was subjected by heat treatment with oxygen. The resulting road bitumen is characterized by good adhesion to the mineral filler [10-12].

Phenols are extracted by extraction with butyl acetate and can be used as a raw material for the production of epoxy tar, tanning agents, rubber

modifiers [13-14].

The disadvantage of this processing scheme is also the incomplete use of phenol resources, since monatomic phenols, the content of which in the tar is 10%, are not extracted at all. During medium-temperature processing of Cheremkhovo gas coals, about 150 thousand tons of heavy tar is released annually. The tar is defenolized and used for fuel needs [15-16].

The ICE (Moscow) proposed scheme of production and fuels and aromatics-based and lowmedium pyrolyzed coal tar. The technology provides distillation, coking, hydrogenation purification, dewaxing and destructive hydro-aromatization [17].

In work [17], it was proposed to stabilize highly reactive coal tar compounds by means of a hydrogenation refining process. The process was carried out without prior distillation and in the presence of a hydrogen donor (tetralin). Hydrogenation refining of the tar was carried out in the presence of crystalline compounds of Mo, Ni, Fe, and other metals of nanoscale. The catalyst was introduced in the amount of 0.030.1% per metal. Hydrogenation of the tar was carried out at a temperature of 425 0 C and a hydrogen pressure of 5.0 MPa, a bulk flow rate of raw materials of 0.9 h ⁻¹.

Hydrogenation is a multi-step process involving the hydrogenation of the feedstock and its subsequent cracking under hydrogen pressure. Since molecular hydrogen itself is not very active, the process is carried out in the presence of catalysts, with heating and high pressures. The presence of these factors and the use of a solvent (paste-forming agent) greatly facilitate the processing of solid fuels, which are highpolymer substances. At the initial stage, the dissolution occurs. The resulting coal solution is the feedstock for hydrogenation. Further processing of the coal solution is absolutely analogous to the hydrogenation of heavy petroleum products and tars. This results in a predominantly mixture of hydrogenated compounds with a lower molecular weight than the original fuel. Depending on the process conditions and the degree of conversion of the organic mass of the fuel by hydrogenation, it is possible to obtain high-quality motor fuels (gasolines, diesel, jet, boiler rooms), raw materials for the chemical industry (aromatic hydrocarbons, phenols, nitrogenous bases), and also gases containing hydrogen and predominantly saturated hydrocarbons [18].

Raw materials for hydrogenation can be coal or tars obtained by semi-cooking of coal or shale. The choice of raw materials is associated with the need to solve a number of technical and economic problems. Hydrogenation of the tar is a relatively simple process, since the removal of the solid phase becomes less complicated, the consumption of hydrogen and pressure decrease. However, the yield of tar in the calculation of OCM is small; there are problems of utilization of significant amounts of char and

other products, the consumption of coal for the production of 1 ton of liquid fuel increases. At the same time, the direct hydrogenation of coal is complicated because of the need to transport and process large quantities of ash sludge.

Particular attention is paid to the processing of shale tar (in foreign literature it is often and inaccurately called "shale oil") by methods of hydrogenation. The incomparably higher than during coal processing, the output of shale tar (calculated on the organic mass of fuel) makes it tempting to turn it into oil-like products using hydrogenation methods. Shale tar differs from oil by its higher viscosity, density, high content of oxygen and nitrogen, and high pour point. Using hydrocracking, as shown, in particular, in works performed in the USA, it is possible to prepare gasoline, jet, diesel and liquid boiler fuel of high quality from shale tar with a yield of 65–80% to the feedstock [18].

The hydrogenation is carried out in the liquid and gas phases. The purpose of liquid-phase hydrogenation is to transform the highmolecular components of black or brown coal, high-boiling oil refining residues and tars into an average oil suitable for further continuous processing in the gas phase. It is also possible to jointly hydrogenate different raw materials, but the starting materials must be of the same type (similar in structure), since coking can occur in the reaction volume otherwise. In the gas phase, hydrogenation of medium oils of various origin in any ratio is allowed.

The results of direct hydrogenation of coal and the composition of the products of hydrogenation depend on the amount of hydrogen entering into the reaction: a product is formed with a certain ratio of heavy and medium oil, gasoline and gas with a relatively small amount of residual coal. The composition of products is also dependent on the hydrogenation conditions (pressure, temperature, contact time), the used catalysts and the properties of the solvent (passer).

Liquid-phase hydrogenation can be carried out under conditions of destruction (splitting) or purification. With destructive hydrogenation (a single or multi-stage catalytic process, a special case of which is hydrocracking), the main goal is to split the molecules of the original fuels to form hydrocarbons of lower molecular weight, and the addition of hydrogen to the product and the removal of heteroatoms (nitrogen, oxygen, sulfur) is only a means for achieve this goal. As a result of destructive hydrogenation, gasoline, medium and heavy oils are formed, along with it gas which is a by-product is released.

In refining hydrogenation (a single-stage catalytic process), the addition and reduction reactions are the goal, and splitting is considered only as an inevitable concomitant phenomenon. As a result of refining

hydrogenization of coal, bitumen is obtained [19].

Now let us consider in more detail the consideration of the mechanism of the process of catalytic hydrogenation of coal; Considering the mechanism of catalytic hydrogenation of PKS does not make sense, because compounds included in its composition are closer in structure and type of functional groups to fragments that make up the organic mass of the original coal.

Let's start with the chemical structure of coal. Coal is a complex natural formation with increased polydispersity and morphological heterogeneity. From the point of view of the hydrogenation process, it is especially important to emphasize the heterogeneity of its chemical composition, molecular distribution of the organic mass and the macromolecular (supramolecular) structure.

If we exclude minerals, ash, and occasional pollution in coal, its structure can be represented by two different, but interrelated "phases". The first one is a smaller part of the whole coal sample (no more than 20%; it depends on the degree of coalification and the petrographic group) and consists of molecules of various sizes (on average, of relatively small mass) that are not connected to each other, as well as with the rest of the coal with strong bonds [20].

The main part of the OCM consists of the macromolecular phase formed by a three-way-stitched mesh ("coal matrix"). The crosslinked structure cannot be extracted, and even in the best solvents for coal it only swells, but does not dissolve (in the absence of a destructive effect). The size of the macromolecular chains forming the net varies from 400 to 4000 conv. unit masses between cross links (bonds) depending on the technique used for the destruction of the structure of coal, extraction and methods for determining the molecular masses. Such an idea of the crosslinked phase is most suitable for the vitrinite of the coals of the lower and middle stages of metamorphism.

The composition and dimensions of macromolecular chains in coal are different, so they cannot be characterized using a repeating unit (monomer), as in classical polymers. For coals, the special term "structural unit" ("cluster") is proposed, implying that it reproduces the average composition and some structural parameters of the coal mass. The structural unit plays the role of a "monomer" and is a flat carbon layer of several condensed nuclei containing various aliphatic radicals as substituents, which can be closed into nonaromatic cycles, and functional groups. The molecular mass of the structural unit is 200-500 conv. unit depending on the nature of the coal and the petrographic component [21].

It is believed that the main types of chemical groups that carry out

the cross-linking of macrochains and the linking of structural units are ether, methylene and sulfide groups. Depending on the degree of coal metamorphism, electronic donor-acceptor interactions (EDAinteractions) contribute to the binding of macrochains, which are the result of the presence in the macromolecular chains of a large number of various polar functional groups and bridge bonds consisting of methylene fragments and heteroatoms.

The structure of the organic mass of coal can be represented as a self-coherent multimer with a three-dimensional structure, [18-19]. According to this concept, OCM consists of a set of macromolecules of different composition, connected by multiple nevaletnye bonds, the main role among them is played by electron donor – acceptor (EDA) interactions, including hydrogen bonds. An analysis of the literature on the effect of a mixture of solvents [20–21] on OCM sites showed that each of the components separately act simultaneously on OCM sites with different EDA characteristics. Given the value of EDAinteractions in intermolecular bonds, an important role is played by the selection of the solvent, which must also be a good donor and an active extractant [22].

In the work of Torgashin A.S., Kuznetsov P.I. and others [23], it was shown that in the course of low-temperature hydrogenation of brown coal, as the OCM converts, along with destruction, the process of its discharge also occurs, which is reflected in a gradual decrease to swelling. The authors of [23] found that during the thermal transformation of coal in a hydrogen donor solvent, the structural elements of the OCM differentiate. A clearly marked staged process has been established, which is due to the different reactivity of the structural components of the organic mass. Components have the highest reactivity, containing paraffinic chain and oxygenates.

The least reactive graph is a graphite-like component. Using a dispersed iron-containing catalyst, the ratios of the rates of degradation and structuring can be adjusted.

The obtained semi-quantitative ideas about the chemical structure of coals shows the complexity of the chemical composition and the variety of chemical bonds with different strengths that exist in OCM, therefore the hydrogenation process is also very complicated, and the overall change in the initial amount of coal is the result of many successive, parallel and side effects, including reverse reactions. The possible reactions of the process include the breaking and saturation of C – C, C– O, C – S and C – N bonds with hydrogen, the hydrogenation of aromatic rings, isomerization, condensation and dehydrogenation.

It is almost impossible to describe the mechanism of the process of coal hydrogenation by a combination of any elementary stages. You can only talk about the predominant group of reactions, and not the only possible one.

Therefore, multicomponent mixtures of substances of various classes are considered as intermediate compounds and end products: gases consisting of CO₂, CH₄, C₂H₆, CO, etc.; oils (maltens) substances soluble in hexane or pentane; asphaltenes, soluble in benzene, but not soluble in pentane; preasphaltenes substances soluble in pyridine, carbon disulfide or alcohol benzene, but not soluble in benzene. The polarity of the resulting substances increases in the range of oils <asphaltenes <preasphaltenes. In many cases, an insoluble high molecular weight product, semi-coke, is also formed. Studies using chromatographic separation techniques have shown that oils are composed of saturated hydrocarbons and non-polar alkyl aromatic substances; asphaltenes from polar aromatic substances, nitrogen-, oxygen and sulfur-containing heterocycles and simple phenols; preasphaltenes from multifunctional molecules with more than 40% of heteroatoms, including polyphenols. Oils have a molecular weight of 150–400 conventional units, asphaltenes from 300 to 1100 and preasphaltenes more than 1500 conventional units.

Data on the kinetics of coal conversion show that at least two stages of the transformation of coal with different rate constants proceed successively. It was found that the order of the reaction of coal conversion (conversion was determined by the amount of dry residue after extraction of products with benzene) varies not only from one stage to another, but also to a small extent and within each stage. Approximately the reaction orders can be taken equal to 1 for the first stage, from 0.5 to 2 for the second.

Order variations are further evidence of the occurrence of various types of reactions during hydrogenation (with different temperature coefficients) even within any single stage. The process indicates not only the interaction of many reactions, but also the possible effect of intermediate products. Within the limits of such complexity it is possible, however, to assume that one group of related reactions characterizes the main direction of the process leading to the destruction of OCM.

The magnitude of the activation energy of the hydrogenation process is calculated from the change with the temperature of the pseudofirst-order rate constant. The values found for various coals under various conditions are relatively small (for reactions of thermal breaking of chemical bonds) and lie within 40–250 kJ/mol. The most characteristic feature of the activation energy of the process is its increase with the depth of coal conversion. The explicit involvement of many reactions in the process of liquefaction proves that the measured activation energies are of limited value due to the different temperature coefficients of these reactions and the complexity of the structure of the reaction forms.

Based on the available data on the study of the chemical structure

and the process of hydrogenation of coal, it is possible to present a qualitative model of the process. It is most likely that hydrogenation liquefaction of coal begins, first of all, with breaking donor acceptor bonds between macromolecules and thermal homolytic breaking of alkyl bridges of the benzyl $\text{ArCH}_2\text{CH}_2\text{Ar}$ type and ether groups of the ArCH_2OAr type (there are very few alkyl alkyl ethers in OCM and aryl-aryl esters are stable). On model compounds and polymers, it was shown that under conditions of coal liquefaction, the rates of C – C, C – O and C – S bond breaking are comparable (in the absence of catalysts).

The resulting free radicals are stabilized as a result of hydrogenation reactions of hydrogen-donor solvent with molecular hydrogen or hydrogen to form low-molecular products, or recombine into poorly soluble high-molecular substances [24].

Let us make a deeper emphasis on the stabilization of cleavage products. As stabilizers, not only molecular hydrogen and solvents with donor ability can be used, but also various additives that can disintegrate under the process conditions with release of low molecular weight highly active radicals and coal substance, depending on its structure and chemical composition, can exhibit donor properties hydrogen.

It is known that in the presence of substances whose thermal decomposition proceeds by a radical mechanism, the process of conversion of coal into liquid hydrocarbon fractions is intensified. Synthetic polymeric materials that are characterized by a high hydrogen content (up to 14 wt.%) can be used as such substances, and therefore can act as a source of hydrogen, necessary for the conversion of coal into liquid hydrocarbons. It is worth noting that the process of joint transformation of plastmass and coal can be considered as an effective method of utilization of industrial and household waste with the simultaneous production of popular hydrocarbon products [24].

The share of the importance of active hydrogen sources on the intensity and depth of the process of destructive hydrogenation of solid and heavy fuels and other organic raw materials depends on many factors — elemental, structural, and mineral composition, temperature, pressure, composition of the gas phase, activity and selectivity of catalysts, and duration of the process. Moreover, molecular hydrogen and hydrogen donors in addition to affecting the hydrogenation process affect the physical properties of coal and paste, which can both increase and decrease the rate of liquefaction.

In addition to the stabilization of radicals formed during thermal decomposition, hydrogen is consumed for: OCM hydrocracking, the formation of gases, solvent regeneration, the hydrogenation of aromatic and

olefinic structures, the removal of heteroatoms, the shift of reversible reactions towards saturated structures, the decrease in compaction yield.

With increasing temperature, the solubility of hydrogen in organic solvents increases, but at the same time the rate of thermal decomposition of OCM and the consumption of hydrogen to stabilize intermediate products increase. Therefore, as the temperature increase, accelerating the process flow of the destructive hydrogenation, to prevent formation of undesirable by-products it is necessary to increase the hydrogen concentration due to growth of its partial system pressure, i.e. the rate of hydrogen supply to the reaction zone should be proportional to the rates of thermal decomposition of OCM and other reactions occurring with its consumption [22].

It should be noted that with the hydrogenation of young coals, the rate of hydrogen consumption at short contact times is quite high at relatively low consumption, but with increasing conversion time, the consumption increases. Thermodynamic conditions are less favorable for cyclic structures and therefore the hydrogen pressure is necessary to compensate for the shift in thermodynamic equilibrium. The composition and yield of the products of the process of destructive hydrogenation is determined by the consumption of hydrogen [24].

It has been established that the mechanism of hydrogen transfer from the gas phase to liquefaction products is largely determined by the process conditions and, first of all, by the composition of solvents (paste formers) and catalysts [25].

In addition to hydrogen CO – H₂O, CO – H₂, H₂S and others have become increasingly important as a reducing medium.

The solvents used in the liquefaction process must have certain properties:

1. to have a boiling point above 260–300 °C in order to be in the liquid phase when the paste is heated to a temperature of 400–450 °C.
2. to have a high proton-donor activity, mainly dependent on the presence of partially hydrogenated poly-aromatic compounds. Proton donors reduce coke formation and the number of functional groups in fragments of depolymerized OCM. The donor properties of the solvent components increase with an increase in the hydrogen content [25].

In the work [26], it was shown that in the medium of a protodonator solvent (tetralin) the hydrogenation process proceeds quite effectively. The degree of conversion of coal at 430 °C without the use of catalytic additives reached 86%. In the presence of fuel oil containing solvent with weak protodonator properties, the conversion under the same conditions was only 33.6%.

In [27] isopropyl alcohol (IPA) was chosen as the proton donor

additive. With the introduction of IPA in the reaction mixture, there is a slight decrease in the yield of liquid cracking products from 92.90 to 87.13 90.49%, an increase in the share of solid products from 6.72 to 7.63 8.52% and gaseous from 0.38 up to 1.88 4.35 wt. %, respectively. The yield of distillate fractions increases more than 2 times from 28.0% to 60.9 61.4 wt. % (after deducting the mass of injected isopropyl alcohol). The increase in the yield of distillate fractions with the introduction of IPA is explained by the cleavage of bonds in the original macromolecules of OCM and the stabilization of the resulting radicals due to the donor activity of the solvent (IPA), which results in predominantly low molecular weight components. In the absence of donor additives or their lack, recombination reactions begin to dominate and as a result high-molecular fragments are formed.

1. It is recommended to have a dissolving ability, which is determined by the presence of highly polar components that reduce the EDA interaction between the macromolecules of the coal substance. Dissolving ability depends on the energy of cohesion, which is determined by the ratio of dispersion forces, constant dipole-dipole and hydrogen bonds. In accordance with this theory, coal products will dissolve in liquids that have similar values of the solubility parameters.

2. With the ability to stabilize the thermal decomposition products due to the transfer of hydrogen from saturated or easily hydrogenated components of the solvent, coal, its fragments and liquefaction products.

3. With precision for decomposition and the formation of coke, as well as to form a stable paste that does not impede its transport. A decrease in the viscosity of the pastes is observed with the introduction of various grades of coal, a number of inorganic components (Al_2O_3 , SiO_2 , CaCO_3 , etc., in a composition with organic additives).

Anthracene and shale oils, oil sand bitumens, oil fractions and residues, semicoking tar of petroleum pitch, as well as coal liquefaction products (own passer), which passed the preliminary hydrogenation in soft conditions for giving them donor-hydrogen properties.

Naturally, due to the difference in the chemical composition of paste-forming agents, the resulting hydrogenates will also differ in their composition. So in [27] studied the liquefaction of brown coal from the Borodino field of the Kansk-Achinsk basin under low hydrogen pressure when using petroleum products with a bale as a paste-forming agent. above 260 °C (oil paste-forming agent) and a mixture (70:30) of high-boiling coal distillates with m.p. above 400 425 °C and prehydrotreated coal fractions with m. bale. 300 400 °C (coal paste former). It has been shown that hydrogenation obtained on a coal paste generator contains 2 times more phenols and nitrogenous bases, and an increased content of sulfur, aromatic

hydrocarbons and asphaltenes is noted as compared to hydrogenation products obtained on an oil pasteforming agent.

Of great practical importance is the choice of the optimal composition of solvents, depending on the elemental and structural composition of coal of various degrees of metamorphism. So, for coals, mixtures of hydrogen donors and polar solvents are effective, which are not effective for brown coals (the donor-acceptor properties of solvents are more important) [26].

1.2 Catalysts for the processing of heavy hydrocarbon raw materials

Hydrogenation processes of heavy hydrocarbon feedstock (HHF) are carried out in the presence of domestic and foreign stationary catalysts based on compounds of Co, Mo, Ni, Fe, etc. [28–30]. In industry, (Al-Co-Mo and Al-Ni-Mo, TU-38-101194-77) catalysts are used, prototypes of broad porous catalysts synthesized at the Institute of Catalysis of the Siberian Branch of the Russian Academy of Sciences, and catalysts of the “Haldor Topsoe” company (Denmark) [31, 32]. It has been established that the best catalysts are substances with more or less acidic properties.

Liquid products of hydrogenation of HHF contains inaddition to heterocyclic compounds, a significant amount of aromatic hydrocarbons. If the removal of heterocyclic compounds and the production of motor fuels with improved environmental performance on existing industrial refining hydrotreating catalysts does not cause difficulties, then to reduce the content of aromatic hydrocarbons from 45-50% to 20% or less in diesel fuels, as required by promising standards adopted in many European countries, it is necessary to use new catalytic systems at the stage of hydro-refining of coal distillates [33, 34]. One of such catalysts is nickel-tungsten-sulphide (NTM-30), developed at the All-Russian Scientific Research Institute for Oil Refining (ARSRI OF) and allowing at low pressure to reach 92% desulfurization of raw materials and 75% hydrogenation of aromatic hydrocarbons compared to 75 and 35 % for existing industrial catalysts, accordingly. Despite the undoubtedly success of the application of heterogeneous catalysts, they have certain disadvantages associated with their deactivation, loss of mechanical strength, etc.

For the processing of high-molecular hydrocarbon feedstocks, catalysts introduced into the process in the form of fine particles evenly distributed in the volume of the feedstock are more efficient. Obviously, to ensure the stability of such a system, the size of the catalyst particles must be very small, i.e. approach the particle diameters in true or colloidal solutions.

Therefore, such catalytic systems can be considered as pseudohomogeneous systems. There are examples of the use of pseudohomogeneous catalysts (PHC) for hydrocracking the distillation of crude oil. For this purpose, molybdenum naphthenates soluble in raw materials, molybdenum alkyl phosphate and molybdenum sulfonate, an emulsion of an aqueous solution of paramolybdate of ammonium, etc. are used as starting compounds. The use of pseudohomogeneous catalysts allows reducing the temperature and pressure of the process, increasing the depth of raw material conversion and yield of the target product.

Figure 1 shows the formation of a catalyst globule from a drop of an aqueous solution of ammonium paramolybdate (PMA) in the process of heating and dispersing the raw material. Positive results of the application of PHC were used and confirmed at the SF-5 plant while developing the processes of hydrogenation processing of coal-oil paste, heavy oil residues and other types of raw materials into light distillate fractions and chemical products [35].

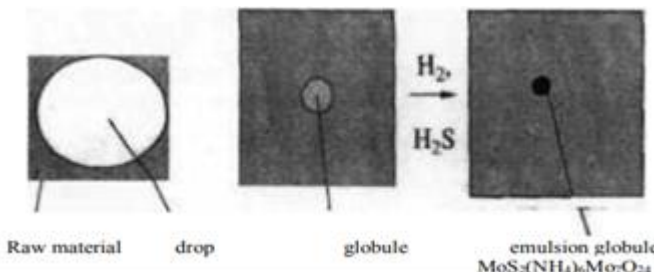


Figure 1. MoS₂ emulsified globule formation of Mo-containing catalyst when heated emulsion

Analysis of the scientific literature suggests that the majority of studies used the following catalytic systems: chlorides, sulfates, acetates, acetylacetates, carbonyls Fe (II, III), Zn, Al, Sn (II), Mo (V), and others. The highest degree of conversion is observed when using organometallic compounds Sn (II) and Pb(C₂H₅)₄. In the processes of coal hydrogenation, Fe (II, III), Mo (V), modified by sulfur showed the highest activity. Chlorides and sulfates of these elements are less active.

Thus, from the analysis of the scientific literature it follows that the processing of high-molecular-weight hydrocarbon feedstock into components of motor fuels and oils can be carried out using cat cracking processes in the presence of pseudo-homogeneous catalysts based on water-soluble compounds Mo, Ni, Si, etc. as well as hydrocracking under low hydrogen pressure.

1.3 Physico-chemical processes of cavitation in liquid media

Cavitation (from the Latin *cavitas* emptiness), the formation in the liquid droplet cavities filled with gas, steam or a mixture of them (the so-called cavitation bubbles, or cavities). Cavitation bubbles form in those places where the pressure in the liquid becomes below a certain critical value p_{cr} (in a real liquid p_{cr} is approximately equal to the saturated vapor pressure of this liquid at a given temperature) [36-38].

Cavitation in a liquid is understood to mean the formation of cavities or bubbles filled with steam and gas with a local decrease in the pressure in the liquid to a saturated vapor pressure. The ratio of gas and vapor in the cavity may be different (theoretically from zero to one). Depending on the concentration of steam or gas in the cavity, they are called steam or gas. It should be noted that lowering the pressure in the liquid to the pressure of saturated vapor is also possible during boiling or evacuating the liquid, but these processes spread throughout the entire volume of the liquid, unlike cavitation, which has a limited area. A cavitation cavity filled with steam and gas in various sources is called a cavity, bubble, bubble, sphere, etc.

When cavitation bubbles are destroyed, the energy of the fluid is concentrated in very small volumes. Thus, places of elevated temperature are formed and shock waves arise, which are sources of noise. When a cavern is destroyed, a lot of energy is released, which can cause major damage. Cavitation can destroy almost any substance [36-38]. The stable existence of vapor-gas bubbles is due to the fact that on the surface of the bubble there are uniformly distributed like charges due to ions in the liquid. The repulsion of these charges prevents the closure of the bubble.

When a cavitation bubble collapses, the $\cdot H$ and $\cdot OH$ radicals, low-energy ions and electrons formed in the gas phase during the splitting of the H_2O molecule and substances with high vapor pressure products of their interaction and partial recombinations, as well as metastable excited H_2O molecules pass into the solution.

The active particles arising in the system, after passing into solution, are solvated and react with solutes. At this stage, when indirect effects of acoustic oscillations take place, practically only chemically active gases — O_2 and H_2 — can influence the course of the process.

By the example of *n*-dekan and *n*-octane [39], the principal possibility of the effective course of the processes of chemical destruction of hydrocarbons by the type of thermal cracking under conditions of the action of pulsed heating and high pressure in the cavitation zone is shown. Search efficient processes of destruction (pyrolysis) of hydrocarbons, available for implementation on small-sized installations, have long been

conducted by numerous groups of researchers. One of the promising areas is the development of cavitation-type reactors, in which cavitation bubbles act as reactors with high internal temperature and pressure. The main condition for thermal cracking (thermolysis), as well as oxidation by molecular oxygen (auto-oxidation) of hydrocarbons in classical technologies, is to raise the temperature of the reagents to at least 400-600°C and pressure to 2-4 MPa in the entire volume being processed. This condition is not mandatory for cavitation-type reactors, since similar processes can take place inside and near collapsing bubbles, containing the reacting substrate in the gas phase. The bubble behaves like a reactor, in which periodically (tens of thousands of times per second) the temperature rises to a level far above what is necessary for the reaction. Achieved conditions last fractions of a microsecond. However, despite the short exposure time and a small amount of a substance reacting in a separate bubble, under certain conditions, the overall yield of the reaction products can be a noticeable value.

It is known that similar reactions of liquid-and gas-phase oxidation of hydrocarbons occurring in the classical high-temperature mode were implemented in a number of industrial processes [40, 41].

The limiting stage of the thermolysis reaction of saturated hydrocarbons (alkanes) is the cleavage of C – C or C – H bonds to form free radicals. With a sufficient depth of this transformation (up to 0.1-1%), the reaction as a whole can be significantly accelerated, because it proceeds via a chain mechanism. Moreover, the probability of disintegration of long hydrocarbon chains is significantly higher (2-5 times) than short ones, which guarantees the predominant disintegration of heavy fractions of oil and gas condensate. The average energy required to break a C-C bond is 346 kJ / mol, which is equivalent to the average energy of a photon emitted by a black body at a temperature of 36000°C. Obviously, obtaining such temperatures inside cavitation bubbles, if possible, requires special conditions and selection of cavitator operating modes.

Currently, there is no satisfactory model of a cavitation region that adequately describes its behavior and the behavior of a separate cavitation bubble belonging to it. The behavior of the cavitation region depends on many phenomena and factors: reproduction and coagulation (coalescence) of bubbles; their interaction; a change in the nature of bubble pulsations due to shock waves and sound radiation from neighboring bubbles; change in the average acoustic properties of the medium; microflows within the cavitation area and at the boundary of the bubble; cavitation germ distribution; gas containing.

In the course of its life cycle, cavitation bubbles lose their spherical shape to a greater or lesser extent, depending on the maximum radius,

frequency of the acoustic field, viscosity, and the presence of surfactants.

The greatest deformations are observed at the final stage of compression. The neighborhood of a solid wall or a closely spaced cavitation bubble has a particularly large effect. There are four types of compression, loss of stability and collapse of bubbles in an ultrasonic field near a solid surface. In the first type of collapsing cumulative jets are not observed. In the second and third types of collapse, a dynamic impulse is formed as a result of the action of pressure waves propagating from the part of the bubble adjacent to the surface, as well as the action of a cumulative jet formed when two annular jets merge. In the fourth type of collapse, a pressure wave propagating from a bubble separated from the surface by annular jets has a dynamic effect on the solid wall. At the confluence of these jets, a cumulative jet often arises from a solid surface through a cavitation bubble, which leads to a decrease in the dynamic impulse. With increasing viscosity of the fluid to mudflows weaken [43].

In addition to the annular and radial cumulative jets, cavitation bubbles form a series of small filamentous “processes” and “roughness”, the length of which increases with the compression of the bubbles.

To create the cavitation region, a certain part of the energy of the primary sound field is used. The ratio of the energy expended to the total energy of the primary field is called the coefficient of cavitation use of acoustic energy [44].

Thus, the cavitation region is a kind of power transformer, in which relatively slowly accumulated energy is released within a very short time, as a result of which the instantaneous power is many times greater than the average input by the radiator into the cavitation region.

The development and intensity of cavitation is greatly influenced by external conditions and fluid properties. During cavitation in degassed liquid, less air enters the cavitation bubbles than in the settled one, which leads to a decrease in the damping effect of the vapor – gas mixture in the bubble when it closes and the pressure in the shock wave increases. Fluid degassing leads to a decrease in the cavitation region with a simultaneous increase in the intensity of the shock wave created by the cavitation bubbles. As the temperature rises, the pressure inside the bubble, determined by the pressure of vapor and gas, increases, and the shock wave is attenuated, but this also leads to an increase in the cavitation region.

Erosion of a solid (surface destruction), surface cleaning, removal of burrs and microscopic irregularities, dispersion of solid particles and emulsification are mainly carried out by two characteristic manifestations of cavitation: shock waves and cumulative streams resulting from the collapse of cavitation bubbles.

On the surfaces of particles and solids there are stress concentrators in the form of microcracks, surface irregularities, and the like, on which cavitation nuclei are formed. Under the action of the sound-capillary effect and intense microflows, the liquid penetrates into the pores and cracks, where, when the cavitation bubbles collapse, a powerful shock wave arises, contributing to the destruction of materials. Cumulative trickles destroy the surface of a solid due to the kinetic energy of the liquid.

Thus, the technology of cavitation treatment for compounding oils and gasolines, obtaining bitumen, oxidizing high-viscosity oils, oxidizing tar, and destruction of high-viscosity oil are widely used in the oil and petrochemical industry.

From the review of the literature, it follows that the primary semi-coking oles have a number of unstable compounds with heteroatoms, phenols and aromatic compounds which are represented by highly substituted carbon with hydrogen from one to four rings. Primary tars are noticeably different from high-temperature coking tars due to the lack of high carbon content in them, and thus primary tars can be used as a source for the production of benzene, toluene, naphthalene and motor fuels.

Determination of the dynamic viscosity of the hydrogenate and the fraction up to 2700 °C was carried out on the SV-10 viscometer. The principle of operation of the SV-10 viscometer is based on the power that is spent on the excitation of the vibration of two thin plates with a purity of 30 Hz. Studies of the individual chemical composition of the fraction to 200 °C were carried out using the chromato-mass spectrometry method on the HP5890/5972SD instrument from the "Agilent" USA company, where helium gas was used as the carrier gas, the temperature in the column ranged from 50-150 °C to 4 minutes, the temperature from 150-300 °C rose within 4 minutes, the temperature in the evaporator 300 °C. Identification of chemicals was performed on the NIST-98 mass spectral base. The individual chemical composition of the fraction up to 200 °C was mainly represented by alkanes, cycloalkanes, phenols and polycyclic hydrocarbons. The chemical composition is represented by cycloalkanes and alkanes consisting of: decane 5.9%; cyclodecane 2.4%; methyl cyclodecane 0.5%; undecane 3.6%; dodecane 2.8%; tridecane 10.6%; 3-methyltetradecane 2.6%; 2methylheptadecane 1%; oxybis-hexadecane 13.1%; tetradecane 2.3%; 2-methyltetradecan 1.6%; pentadecane 3.1%.

Aromatic hydrocarbons were mainly represented by benzene and its derivatives, the quantitative composition being 32.1%. Phenol and its derivatives amounted to: phenol 4%, 2-methylphenol 3.1%, 3 methylphenol 7.1%.

Polycyclic hydrocarbons are mainly represented by naphthalene

1.2%, 2-methylnaphthalene 3.7% and a mixture of anthracene and phenanthrene in the amount of not more than 5%

Thus, the individual chemical composition of the fraction up to 200 °C of hydrogenate was determined, which was obtained by cavitation of a mixture of an organic mass of coal and a paste former.

We have established a general pattern of the influence of the catalyst and the preliminary cavitation treatment of the mixture, consisting of the organic mass of the coal and the pastor, moreover, it should be noted that in the individual chemical composition of the fraction up to 2000C there is an increase in the content of paraffin hydrocarbons and a decrease in aromatic and polycyclic hydrocarbons. Apparently, in the process of cavitation treatment, consisting of a mixture of an organic mass of coal and a paste-forming agent, two processes take place destruction and condensation. The individual chemical composition of the light fraction allows us to state that the destruction of paraffinic hydrocarbons prevails over the condensation processes.

1.4 Heavy oil residues

Heavy oil residues are formed in the processes of oil distillation in the form of fuel oil (fraction with a boiling point of more than 350 °C) and tar (fraction with a boiling point of more than 500 °C). In addition, the resinous products resulting from the purification of gasolines, kerosene, diesel and oil fractions of oil should be attributed to the heavy residues. The yield of heavy residues depends on the type of oil being processed and the technology for its refining, is presented in Table 5.

Table 5
Output of oil residues and other products in direct distillation processes

| Name product | The yield of the product in the calculation of the original oil% | | |
|-------------------|---|---------------------|----------|
| | Heavy residue | Targeted product | Total |
| Gasoline fraction | 0.8 1.5 | 11.2 17.5 | 12 18 |
| Kerosene fraction | 1.4 2.2 | 15.6 16.8 | 16 18 |
| Diesel fraction | 0.8 1.2 | 15.1 16.4 | 17 20 * |
| Oil fraction | 7 –12 | 6.8 10.4 | 22 24 ** |
| Tar | 19 30 | - | 19 30 |
| Total: | 29 36.3 | - | - |

*Note: * 1.1-2.0% of paraffins are extracted from the diesel fraction;*

*** 4.4-5.2% of petrolatum was isolated from the oil fraction;*

The data in Table 5 show that the yield of heavy residues is on average one third of the oil being processed. Heavy oil residues are used mainly for the production of petroleum bitumen. So the heavy residues can be recycled catalytic, thermal and hydrocracking to lighter fractions with the purpose of increasing the yield of gasoline and diesel fuels willow. However, heavy residues from cracking processes acquire a number of undesirable qualities. In particular, due to the processes of compaction of hydrocarbons during recycling, the physicomechanical properties of residues (elasticity, plasticity, fragility) are significantly deteriorated [45-49].

Resinous-asphaltenic substances are concentrated in heavy oil residues. Depending on the depth of selection of distillate fractions and the nature of oil, resinous asphaltene substances comprise from 40 to 60–70% of the heavy oil residue. The richest in tars and asphaltenes are young naphthenic-aromatic or aromatic base oils, especially resinous (up to 50%). These are oil from Kazakhstan, Central Asia, Russia and others. Old paraffinic oils of methane base, as a rule, contain much less tar from tenths (Markov oil) to 2-4% (dosorsks, surakhansk, bibiaybatsks). They do not contain asphaltenes at all. In other petroleum methane base their content does not exceed a few percent [50-51].

Deepening the selection of distillate fractions to 450-500 °C led to the fact that the compounds entering the tar have a minimum molecular weight equal to 400 u., and contain at least thirty carbon atoms in the molecule. Isolation of individual substances from residual fractions of oil is very difficult; therefore, the chemical characteristic of the composition of heavy oil residues is the quantitative content of group components in them. The division of tars (bitumen) into components was proposed as early as the beginning of the century by I. Richardson, and then improved by I. Markusson and is used with small changes these days. It consists in the separation of asphaltenes by precipitation with nalkanes (C₅ – C₈) from malten soluble in them. Maltenes are further divided into 5 components by adsorption chromatography on silica gel or alumina: paraffin-naphthenic, monoand bicyclo-aromatic compounds, toluene and alcohol-toluene tars. Paraffin-naphthenic compounds are sometimes separated by complexation with carbamide and thiocarbamide into n-alkanes, isoalkanes and polycycloalkanes (polycyclo-naphthenes).

The first three components are residual oils. These are viscous liquids from light yellow to dark brown in color with a density less than one, with a molecular weight of 400 600 a. eat.

Tars viscous inactive fluids or amorphous solids from dark brown to dark brown in color with a density of about one or slightly more. The molecular weight of the tars is on average from 700 to 1000 a... e m Tars are

unstable, isolated from oil or its heavy residues can turn into asphaltenes, i.e. no longer dissolve in the n-alkanes C₅ – C₈.

Asphaltenes amorphous solids dark brown or black. When heated, they do not melt, but transfer to a plastic state at a temperature of about 300 °C, at a higher temperature they decompose with the formation of gaseous and liquid substances and a solid residue coke. The density of asphaltenes is somewhat greater than one. Asphaltenes are very prone to association, so the molecular weight, depending on the method of determination, can fluctuate by several orders of magnitude (from 2,000 to 140,000 u.). At present, cryoscopy in naphthalene or osmometry of highly diluted solutions are generally accepted methods for determining the molecular weight of asphaltenes. The molecular weight of asphaltenes determined by these methods is about 2000 u. [52].

In the last 10-15 years, thanks to the use of a complex of methods for physico-chemical analysis, it has been possible to significantly expand the understanding of the principles of the chemical structure of substances that make up tars and bitumens. The combination of chromatographic and chromatography-mass spectroscopic methods of analysis isolated hydrocarbons from heavy oil residues (> 550 °C), identical in structure of the carbon skeleton to hydrocarbons entering the gas oil part of the oil. These are n-alkanes and isoalkanes with the number of carbon atoms from 30 to 40-45 and polycyclic compounds like steran (tetracyclic) and hopan (pentacyclic). Polycyclic compounds can be fully saturated (polycyclone naphthenes). In the molecules of such hydrocarbons, the polycyclic part has a number of methyl substituents and one a long, often branched, alkyl substituent (C₄ – C₁₂). In addition to evidence of the structure of individual, individually isolated hydrocarbons, studies were conducted on the characteristic structural parameters of compounds belonging to relatively narrow (chromatographic) fractions. On the basis of experimental data on structural parameters, an average statistical hypothetical formulas of the substances that make up this fraction were built by calculation (integral structural analysis) [45-47]. It is known that, despite the large variety of oils, even in tars and asphaltenes, fluctuations in the content of the main structural elements carbon and hydrogen are insignificant, and their atomic ratios are very close, as can be seen from tables 6 and 7.

Table 6
Physico-chemical characteristics of the tars of some oils

| Oil | M | ρ_{4}^{20} | Elementary composition, % | | | | | H:C (atomic) |
|-----------|-----|-----------------|---------------------------|------|-----|------|------|-----------------|
| | | | C | H | S | N | O | |
| Bavlynsks | 594 | 1,042 | 84.52 | 9.48 | 2.6 | 0.96 | 2.76 | 1,3 |

| | | | | | | | |
|---------------|------|-------|-------|-------|------|------|------|
| Romashinsky | 816 | 1,055 | 81.91 | 9.38 | - | 8.7 | 1.4 |
| Tuimazynsks | 725 | 1,042 | 84.10 | 9.80 | 4.00 | 2.1 | 1.4 |
| Bitkovsks | 501 | 1,021 | 84.30 | 10.36 | 2.79 | 2.55 | 1.4 |
| Sagaydaks | 769 | 1,033 | 86.40 | 10.01 | 1.80 | 2.1 | 1.4 |
| Radchenkovsks | 770 | 1,014 | 85.00 | 10.50 | 1.00 | 0.45 | 3.05 |
| Nebit-dags | 644 | - | 84.99 | 9.98 | 0.82 | 4.21 | 1.4 |
| Gyurgyansk | 585 | 1,024 | 86.12 | 10.09 | 1.40 | 0.94 | 1.4 |
| Soviets | 1055 | - | 80.82 | 10.48 | 1.41 | 1.24 | 6.05 |
| Samotlorsk | 1367 | - | 83.54 | 9.68 | 2.02 | 1.60 | 3.16 |

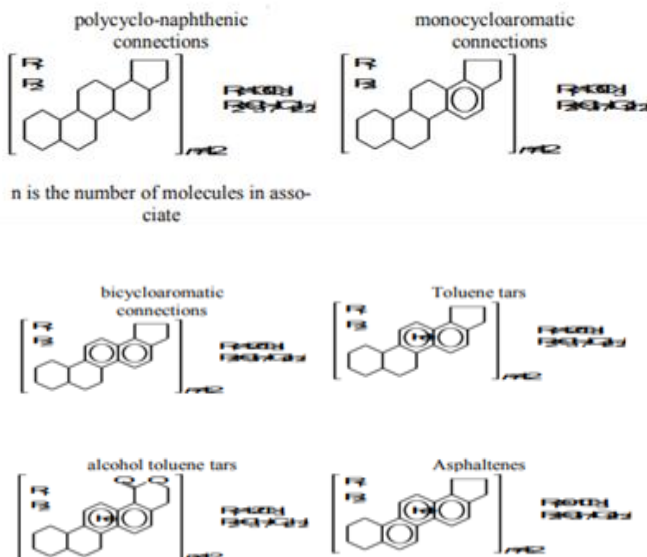
The results of the analysis confirm that the molecules of all components, except for nand isoalkanes, which are part of the heavy oil residues, are built according to a single principle. Molecules of both hydrocarbons and their hetero derivatives are hybrid compounds. The basis of such molecules is a polycyclic nucleus consisting of 4-6, mostly six-membered, rings. This polycyclic system may have several methyl and one long ($C_3 - C_{12}$) alkyl substituent. In the cyclic part of the molecule may include rings containing sulfur or nitrogen, oxygen functional groups, as a rule, are located on the periphery of the molecule.

Table 7
The elemental composition of the native asphaltenes of some oils

| Oil | Contents in an oil, % | Elementary composition, % | | | | | H:C (atomic) |
|-------------|-----------------------------|---------------------------|------|------|------|------|-----------------|
| | | C | H | S | N | O | |
| Bavlynsks | 2.0 | 83.50 | 7.76 | 3.78 | 1.15 | 3.81 | 1.19 |
| Romashinsky | 3.8 | 83.66 | 7.87 | 4.52 | 1.19 | 2.76 | 1.13 |
| Tuimazynsks | 3.9 | 84.40 | 7.87 | 4.45 | 1.24 | 2.04 | 1.13 |
| Bitkovskaya | 2.2 | 85.97 | 8.49 | 1.65 | 0 | 3.99 | 1.18 |
| Sagaydaks | 1.4 | 83.87 | 8.67 | 1.64 | 1.56 | 4.62 | 1.22 |
| Samotlorsk | 1.4 | 85.93 | 9.19 | 1.76 | 1.69 | 2.43 | 1.16 |

The difference in the structure of molecules depending on the type of component and oil features lies in the position and number of methyl substituents, the length and branching of the long alkyl substituent, the number of aromatic (heteroaromatic) cycles, and the presence, type and number of oxygen-containing functional groups.

The most probable average statistical structural formulas of the molecules of the components of heavy oil residues calculated by the method of integral structural analysis are presented below:



The tendency of molecules to associate increases with increasing degree of aromaticity and the number of heteroatoms, especially oxygencontaining functional groups. Therefore, polycyclo-naphthenic compounds and monocycloaromatic compounds in heavy oil residues are mainly at the molecular level and only 15–20% form associates of two molecules. The proportion of associated molecules of bicycloaromatic compounds is somewhat larger. Associates may include heterogeneous molecules. The association energy is rather high, and in the case of cryoscopic determination of the molecular weight in naphthalene, some of the molecules remain associated, so the molecular weight of these fractions ranges from 400 to 600 u. [53].

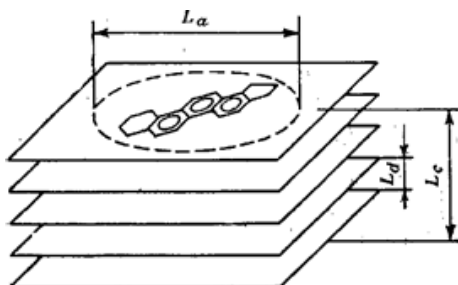
A characteristic difference in tars is the presence of heteroatoms in the molecule. Since sulfur and nitrogen atoms in tars are necessarily included in the cyclic aromatic structural unit of tin thiophene, pyrrole or pyridine, part of the aromatic cycles of the molecules will be heteroaromatic. Tar molecules contain two condensed aromatic (heteroaromatic) rings.

The alcohol-toluene tars, in turn, are characterized by the presence of peripheral oxygen-containing groups. Thanks to oxygen-containing groups, alcohol toluene tars are very prone to association, which probably explains their spontaneous conversion to asphaltenes, as mentioned earlier. The tars isolated compounds capable of complexing with a number of metals.

Asphaltenes differ sharply from the other components in that their molecules have three aromatic or heteroaromatic rings. Due to this, the molecules of asphaltenes have an almost flat spatial structure. Apparently, due to π -electron clouds and polar groups of heteroatoms, the molecules of asphaltenes form associates in the form of packs parallel to the arranged flat molecules.

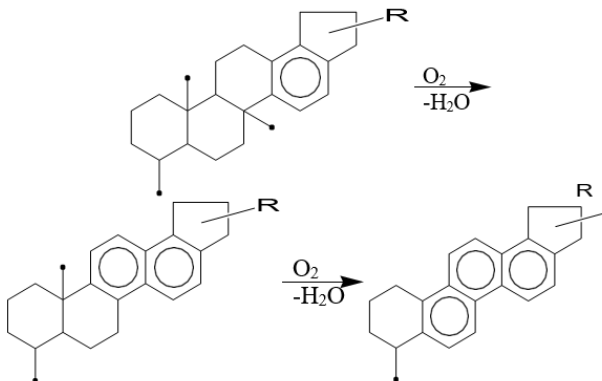
X-ray structural analysis revealed formations consisting of 4-5 parallel layers that are not ordered with respect to an axis perpendicular to these planes (Fig. 2).

The diameter of the layers (L_a) and the thickness of the pack (L_c) are comparable about 1.2–1.8 nm with the distance between the layers (L_d) 0.35–0.37 nm. Such a pseudospherical particle is an embryo of a solid phase of colloidal size. Due to the solvation shells, the particles of asphaltenes do not stick together with each other to form a coarse solid phase, even in oxidized bitumens with a high content of them. While dissolving oil residues and normal alkanes $C_5 – C_8$ the solvate shell of the asphaltene associates is destroyed, and they fall out in the form of a coarse powder. In aromatic hydrocarbons, asphaltenes remain at the level of associates even at elevated temperatures. Therefore, when a cryoscopic determination of their molecular weight in naphthalene is determined, the mass of the associate is about 2000 u. Recently it was proved that the true molecular weight of asphaltenes is 400-500 u., i.e. the same as the other components.



L_a – layer diameter; L_c – pack thickness; L_d – spacing between layers
Figure 2. The structure of asphaltene particles

Being in tars or bitumens, asphaltenes are chemically inactive and thermally stable. Asphaltenes are easily formed during the oxidation of tar by atmospheric oxygen at 180–280°C. Under these conditions, the predominant reaction is the oxidative dehydrogenation of oils and tars. A saturated ring condensed with an aromatic ring is subjected to oxidative dehydrogenation, and the cyclic system is increased by one aromatic ring:



If the number of aromatic cycles reaches three, then the molecules are collected in packs, forming particles of asphaltenes. The solvate shell of oils and tars protects them from further oxidation, and asphaltenes accumulate as the final oxidation product. The increase in the content of asphaltenes in the oxidized tar increases its viscosity, and it gradually turns into bitumen.

In addition to the considered type of asphaltenes in the fraction isolated from oil or its residues by n-alkanes, other substances with relatively low molecular weight may be found. These substances do not have three aromatic rings in a molecule, but they are characterized by a high content of heteroatoms and polar groups, for example, asphaltogenic acids. They do not have a layered block structure, but, apparently, contribute to its stabilization.

Asphaltenes isolated from petroleum have a relatively high reactivity. They are easily oxidized, halogenated, chloromethylated, react with phosphorus (III) chloride, condensed with formaldehyde, hydrogenated to tars and oils, etc. Based on these reactions, sorbents, ion exchangers and other products can be obtained, but so far these properties asphaltenes did not find industrial applications. But the formation of asphaltenes during the oxidation of heavy oil residues in order to produce bitumen is a large-tonnage industrial process. It consumes about 3-6% of all processed oil, which is commensurate with its consumption for the production of raw materials for organic chemistry. Bitumens are characterized by the following indicators: softening temperature, penetration (needle penetration under standard conditions), fragility temperature, ductility (stretching into a thread), etc. Depending on the combination of these indicators, bitumens are divided into road, construction, roofing and special. All of them are widely used in relevant sectors of the economy [54].

In the literature, there are no data on the effect of catalytic cavitation effect on the primary coal tar and HOR, thermodynamic and kinetic parameters of the process.

The paper discusses the data on the cavitation destruction and recovery of the organic mass of the primary coal tar, HOR in the presence of various water-soluble salts of Group VIII metals and nanocatalysts. This we explain the relevance of this work.

CHAPTER 2. CATALYSTS FOR THE HYDROGENIZATION OF SOLID HYDROCARBON RAW MATERIALS

Bergius' early work on the hydrogenation of coal and tar did not attach importance to the role of a catalyst in this process, which was one of the serious mistakes. At present, it has been proven that hydrogenation of high molecular weight organic compounds is a catalytic process [55]. A very large number of works are devoted to physicochemical studies of catalysts, the mechanism of catalytic action, the conditions of manifestation and the formation of catalysts, working hypotheses on the theory of catalysis, etc.

Numerous hydrogenating catalysts can be divided into two groups. The first group consists of catalysts operating at atmospheric pressure at low temperatures, easily poisoned in the presence of sulfur compounds and therefore not suitable for coal hydrogenation processes. The second group consists of catalysts operating at high pressures and temperatures and resistant to the effects of sulfur compounds. For this process, only molybdenum and tungsten catalysts are used. Recent studies have shown that iron catalysts can be successfully used for individual stages of the hydrogenation process.

The possibility or impossibility of using iron catalysts for the hydrogenation of coal in the liquid phase is determined by the chemical composition of coal.

The use of catalysts in the process of destructive hydrogenation of HHF allows the process to be carried out under milder conditions, to increase the conversion of the organic paste mass, the yield and quality of distilled products. Highly active catalysts that allow the process of coal liquefaction at relatively low hydrogen pressures (10-14 MPa) are catalysts based on molybdenum compounds. However, catalysts based on molybdenum are expensive and their regeneration is necessary, which complicates and increases the cost of the process technology and it is not economically feasible to use them in this industry. Scientists around the world are actively searching for cheap disposable catalysts.

In this connection, available iron-based catalytic systems, for example, iron-containing ores, ore concentrates of transition metals, are of considerable interest. Large-scale waste of the metallurgical industry can serve as promising catalysts. Their use makes it possible to eliminate the laborious and technically difficult stage of catalyst separation from the sludge residue of the process [56]. To carry out the hydrogenation of coal using carbon monoxide and water vapor, an industrial catalyst for the conversion of carbon monoxide (STK-1-1) and various iron-containing metallurgy was selected.

2.1. Physico-chemical properties of iron sulfides

Discussing the processes of hydrogenation of heavy hydrocarbon raw materials (coal, heavy oil residues, high-boiling oil fractions) using iron-sulfide compounds (pyrite, pyrrhotite) as catalysts, one cannot help but dwell on such a question as the physicochemical properties of sulfides.

Sulfur compounds, according to V.I. Vernadsky, make up 0.15 % of the weight of the crust. Their total number is more than 300. According to this indicator, sulfides take the second place after silicates. More than 40 chemical elements give compounds with sulfur, most of them are metals. According to the type of chemical bonds, sulfides belong to ionic compounds. Sulfur compounds, or sulfides, are divided into two large groups: simple sulfides and complex.

In the group of sulfides double sulfides are isolated, when two or three cations (solid solutions) participate in compounds with sulfur. For example, chalcopyrite CuFeS₂. Disulfide pyrite (pyrite) FeS₂, the most abundant mineral. Chemical composition: Fe-46.55 %, S-53.45 % As a rule, a chemical bond in iron sulphides arises due to the formation of various types of s x p x configurations of the valence electrons of the atoms of the components and various variants of their overlapping. When sp-orbitals are formed with sulfides, the high acceptor ability of sulfur atoms, which have the s₂p₄ configuration of electrons, tends to be extended to a stable inert gas configuration. According to Belov N.V., in contrast to oxides and chlorides, in which the "noble-gas form" of atoms is achieved due to Coulomb interactions, another principle is realized in sulfides during bond formation, namely after a certain amount of recoil sand p electrons cations formed around the 18electron shell krypton (4s₂4p₆3d₁₀) via a donor-acceptor mechanism in a cat of rum sulfur anion play easily. The chemical bond in iron sulfides (FeS and FeS₂) has a rather complex nature. In the sulfur ion S₂outer eight electrons of 3s₂3p₆ are weakly bound to the nucleus and when a bond is formed, the S₂ anion selects 4 donor pairs. If the same is not enough for metal cations stabilizing by the rule "18", if anions are combined into larger ones with an increased number of donor pairs, for example, with the formation of S₂₂ with six pairs of donor electrons, or the conversion into a metallic bond is the direct exchange of the missing number of electrons between approaching cations.

An example of the first case is pyrite, which exists in two crystalline modifications: marcasite is a rhombic lattice; pyrite is a cubic lattice. The sulfur atoms in FeS₂ are mated into an anionic dumbbell /: S: S: /, and already these anions S²⁻are overlapped by single iron cations of the "coordination number 6" type. The cation Fe²⁺ takes the place of Na⁺, aS²⁻the place of Cl⁻.

Each iron atom is located in the center of an octahedral void formed by six sulfur atoms, while the sulfur atom is surrounded by only three iron atoms.

Marcasite metastable pyrite, crystallizes in a less symmetrical rhombic cell, with lattice parameters. The difference between the structures of pyrite and marcasite is in the orthorhombic distortion of the latter and in the orientation of the group S_2 . The S-S distance in pyrite is 0.212 nm, and 0.221 nm in marcasite. The transition from marcasite to pyrite occurs at a temperature of 723K.

An example of the second case is the structure of pyrrhotite. In the literature, pyrrhotite is called iron sulfides with the general formula FeS_{1+x} . The two valence S-electrons, which succumbed to the sulfur atom, need Fe^{2+} cation with six electrons and need six pairs of additional ones and are accordingly located in the center of the octahedron. But each anion S^2 is able to provide only four pairs, and if it is impossible to organize a more complex anion S_2^{2-} in pyrrhotine octahedra.

Pyrrhotite is a compound of varying composition and changes its physicochemical properties depending on the sulfur content. The formula of the compound is usually written as FeS_{1+x} , where x is the excess sulfur in relation to the stoichiometric composition. With an increase in the sulfur content in FeS , iron vacancies arise, the interaction between which is repulsive. As shown by Goncharov, there are critical concentrations of vacancies that coincide with the phase boundaries in pyrrhotite. As soon as such a concentration of vacancies is reached, at which each hexagon of sulfur atoms is surrounded by only one row of iron atoms that have no vacancies, which corresponds to the composition at which $x = 0.09$, vacancies are redistributed along alternating planes.

The structure of all crystalline forms of pyrrhotite is not known in detail, but there is an assumption that they arise due to the ordering of vacancies. In the region of composition 53.2-53.5 at.% (39.4-39.8 wt.%) at normal temperature, the equilibrium phase is monotypic pyrrhotite, formed on the basis of the structure of the compound Fe_7S_8 (46.7 at.% or 60.4 wt.% iron and 53.3 at.%, or 39.6 wt.% sulfur). Monoclinic pyrrhotite phase is stable below 230°C. At a temperature of 300-320°C it is metastable and converted during firing in the hightemperature hexagonal pyrrhotite.

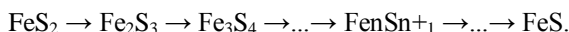
Pyrrhotite with its formula FeS_{1+x} has long attracted the attention of researchers, as the only sulfide with a deficiency of cations. In this regard, much attention was paid to the use of magnetic properties of pyrrhotite, which depend on the value of x. In the homogeneity region of FeS_{1+x} , the following structures can be distinguished: troilite, lowtemperature and high-temperature hexagonal, and monoclinic pyrrhotite.

The magnetic properties of the products of thermal decomposition

of pyrite were studied in [57]. To determine the phase composition of the sample products after exposure at appropriate temperatures, they were subjected to magnetic separation at field strengths up to 79.6 kAm⁻¹. The decomposition products of the following board, Fe5S6, Fe6S7 and Fe7S8, have been found to possess high magnetic susceptibility. The specific magnetic susceptibility of the products of thermal decomposition of pyrite, ranging from the composition of Fe5S6 to Fe8S9, increases from 565 to 1470x10⁻⁶ cm³g⁻¹ and decreases to 860x10⁻⁶ cm³g⁻¹ for Fe12S13, respectively. Further desulfurization leads to a decrease in the magnetic properties of up to 0.04 x 10 cm³g⁻¹ in pyrrhotite of the composition corresponding to the formula Fe21S22, i.e. The weakly magnetic pyrite gradually decreases to the ferromagnetic state as sulfur is removed, and with a further decrease in the sulfur content, it approaches troilite, and therefore the magnetic susceptibility sharply decreases.

Studies of the magnetic properties of the products of thermal decomposition of pyrite show that according to the technological classification by magnetic properties, the resulting pyrrhotite composition from FeS1,2 to FeS1,08 by the magnitude of the specific magnetic susceptibility can be attributed to strongly magnetic minerals.

Thermal dissociation of pyrite is a rather complicated process. It proceeds with the formation of a number of non-stoichiometric compounds pyrrhotite, the final product of which is iron monosulfide, troilite:



As noted above, one of the main features of the behavior of pyrite when heated in a neutral medium is the change in its magnetic properties. The acquisition of magnetic properties is associated with redistribution and the formation of disordered vacancies. The conclusion about the disorder of vacancies seems to us to be the most correct, since in the sample subjected to heating, the migration routes of iron, sulfur and vacancies are facilitated, the mobility of which also increases as a result of the partial removal of sulfur from the system. The resulting vacancies for sulfur open up the paths for additional Fe – Fe metallic bonds, as a result of which the magnetic properties sharply increase.

An example of the third case is the structure of ternary sulfide systems (solid solutions): copper-iron-sulfur, iron-nickel-sulfur. In ternary systems, the number of metal atoms exceeds the number of sulfur atoms. As a result, a number of unique structures arise, often with close metal-metal distances, indicating the presence of metal-metal bonds.

In the literature [58–60], contradictory data on the phase

composition and thermal decomposition of ternary solutions are observed, and as regards the magnetic properties of thermal decomposition products, there is no information in the literature.

Together in the IOSCC INT-SA of RK and CMI NC for IMP, targeted studies are carried out in the area of pyrite dissociation in order to obtain intermediate products and the development of catalytic additives from pyrite-containing polymetallic raw materials.

As noted above, the use of pyrite, pyrrhotite in the processes of destructive hydrogenation has been well studied in the works of scientists in Japan, the United States and the CIS countries. However, the use of iron sulfide solid solutions as catalysts for the destructive hydrogenation of coal, the demetallization of highly viscous oil, and the establishment of a relationship between the magnetic properties in the dissociation products of pyrite has not yet been studied.

2.2 Synthesis of iron sulfide solid solutions-catalysts for the hydrogenation of heavy hydrocarbons

Recently, interest has increased in the use of pyrite and pyrrhotite as catalysts for the destructive hydrogenation of heavy hydrocarbons. Despite the abundance of work in this direction, a number of key points are needed in theoretical discussion and practical refinement. The latter include, for example, the problem of the formation of non-stoichiometric iron sulfides and available x ferric position and behavior of the synthetic iron sulfide of ternary systems in the process of destructive hydrogenated coal and heavy oil. Previously our attention was focused mainly on the use of natural iron sulfide systems as catalytic additives in the processes of destructive hydrogenation of coal, heavy oil residues.

Pyrite (FeS_2), a natural iron disulfide, from the Akchatau deposit in the Republic of Kazakhstan, was used as a base object in the synthesis of iron sulfide solid solutions (ISSS). The bar chart and the Mössbauer spectrum are presented in Figure 3, which, in combination with the data of the results of phase and quantitative chemical analysis, confirm the monominearity of the base object.

Synthesis of solid solutions of the pyrrhotite series $\text{FeS}-\text{Fe}_7\text{S}_8$. Existing methods for analyzing iron sulfides are based on processes involving iron halides and ammonium polysulfides, sodium sulfides in aqueous solutions (hydrothermal synthesis), and gaseous iron, sulfur and hydrogen sulfide halides in a temperature gradient (gas synthesis) [61]. The most common method is a direct interaction of gland and sulfur in a vacuum. Such features of the above methods, such as high vacuum in the implementation of

gas transport and direct synthesis, participation in the reaction of gaseous components, imposing considerable vapor pressure, complicate their implementation on an aggregated scale. In all methods of synthesis, the problem of regulating the composition of the resulting sulfides remains unresolved.

The natural iron sulfides of the series $\text{FeS}_{1,14}\text{-FeS}$ (pyrrhotite) in pure monomineral form are rare. They are the main minerals of sulfide, copper-nickel deposits, where they are presented as mixtures of various modifications (monoclinic and hexagonal pyrrhotite and troilite), in thin mutual germination with the main minerals of copper, nickel and cobalt, which makes it difficult to use traditional methods to isolate them in pure form.

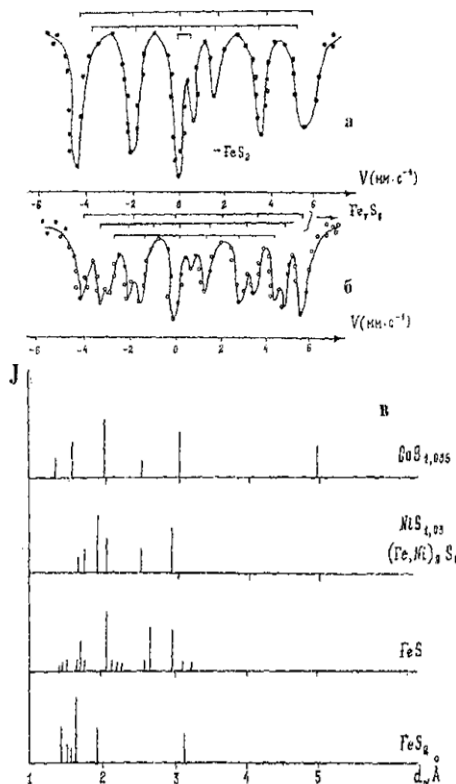


Figure 3. Mössbauer spectrum and X-ray diffraction pattern of iron sulfide solid solutions (ISSS) of HOR hydrogenation catalysts

The synthesis of iron sulfides of a number of pyrrhotites was carried out in the following sequence of operations. Monomineralic powdered pyrite, crushed to a particle size of 0.074 mm with a basic substance content of 99.1 % and powdered reduced iron of the "h" mark.

A weighed portion of 20 g was placed in a mixer and mixed in ethyl alcohol for 4 hours, then the resulting mixture was discharged and dried at room temperature.

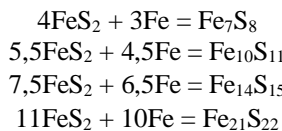
Pyrite and iron were mixed in a ratio of 1:0.35 and 1:0.42, i.e. on the basis of obtaining iron sulfides corresponding to the edges of the homogeneity region of FeS1+x . A weighed portion of 20 g (a mixture of pyrite and iron) was placed in a mixer and mixed in ethyl alcohol for 4 hours, then the mixture was unloaded and dried at room temperature, then the obtained products were placed in quartz ampoules, which were evacuated and sealed. Table 8 presents the conditions of the experiments, as well as the results of phase chemical analysis of the products of roasting.

Table 8
Synthesis of iron sulfides

| The ratio of Fe:Fe ₂ in the charge | Temperature, °C | Time, h. | The composition of the XPA and NGR |
|---|-----------------|----------|------------------------------------|
| 0.34: 1.0 | 500 | five | Fe0,875S(Fe7S8) |
| 0.36: 1.0 | 550 | five | Fe0,888S(Fe8S9) |
| 0.38: 1.0 | 600 | five | Fe0,909S(Fe10S11) |
| 0.40: 1.0 | 650 | five | Fe0,933S(Fe14S15) |
| 0.42: 1.0 | 650 | five | Fe0,955S(Fe21S22) |

Chemical phase analysis of these hardened butts shows the presence of iron sulfides of the general formula FeS1+x . According to X-ray phase analysis and NGR corresponds to the composition of Fe7S8, Fe8S9, Fe10S11, Fe14S15 и Fe21S22.

Based on the data of X-ray phase analysis and Mössbauer spectroscopy of the products of heat treatment of pyrite with iron, the following reactions should be considered:



Mössbauer spectroscopy (nuclear gamma resonance NGR) is an effective method of phase and structural analysis of this system.

NGR spectroscopy has been successfully used to study catalysts for the catalytic hydrogenation of coal.

Mössbauer spectra were obtained on a NGRS-4 spectrometer operating in a variable speed mode using an AI-1046 multi-channel analyzer. The source of γ -quanta was Co57 in the chromium matrix.

The graphic decomposition of the NGR spectra into the components of the sextuplet and their processing were carried out according to a Unified Electronic Computer System-1033 computer.

The appearance of the NGR spectra of the products of the interaction of FeS₂ with Fe indicates the complexity and multiplicity of structures, the presence in all samples of at least two states of iron ions. The shape of the spectra varies depending on the ratio of FeS₂: Fe and the treatment temperature of the charge.

The observed α -Fe characteristic lines and the central doublet related to FeS₂ in the spectrum of the calcine obtained at 500°C show that at this temperature the reaction of interaction of metallic iron with pyrite at their ratio (FeS₂:Fe) = 1:0.35 is not completed. A further increase in the process temperature to 550°C leads to a complete shift of equilibrium towards the formation of sulfides of the general formula FeS_{1-x} and FeS. A necessary condition for the completion of the reaction and obtaining sulfide of a given composition of FeS is reached at 650°C, as evidenced by one six-peak line with spectrum parameters (8 = 0.80 + 0.2 mm/s; 5 = 0, 8 + 0.05 mm/s).

For a mixture consisting of one part of FeS₂ and 0.35 parts of metallic iron (1:0.35), the temperature of 450°C is insufficient to complete the reaction. The broadened lines of the sextuplets can be suggested by the formation of the monoclinic modification FeS_{1,14} (Fe₇S₈) with an incomplete structure. The absence of the characteristic α -Fe line in the spectrum indicates the completion of the reaction of its interaction with pyrite. The change in the phase composition with increasing temperature from 500 to 650°C is due to the sulfidization of the previously formed FeS_{1+x} pyrite (residual) according to the total reaction:



Synthesis of solid solutions of a series of ternary sulfide systems FeS₂+Co,Ni. Synthesis of samples of ternary sulfide systems was carried out as follows: an initial sample of pyrite (FeS₂) weighing about 10 g was placed in a quartz ampule, sealed at one end, and metallic nickel or cobalt in powder form was placed (preliminary recovered in a stream of hydrogen). The ampoule was pumped to a pressure of 0.3-0.5 Torr and then sealed with an oxygen torch.

The ratio of $\text{FeS}_2:\text{M}$ varied from 1:0.14 to 1:0.20 for nickel and 1:0.06 to 1:0.14 for cobalt, respectively. The synthesis of ternary sulfide systems was carried out at a temperature of 450°C for 5 hours. The phase composition of the products of the interaction of pyrite with nickel or cobalt is presented in Table 9 (a, b).

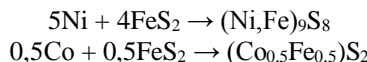
Table 9 (a)
**Phase composition of interaction of products pyrite
with nickel at 450 o C**

| The ratio of $\text{FeS}_2:\text{Ni}$ | XPA phase composition | | |
|---------------------------------------|-------------------------------------|----------------|--------------------|
| 1:0,14 | NiS | FeS_2 | FeS_{1+x} |
| 1:0,17 | $\text{NiS}_{1,03}$ | FeS_2 | FeS_{1+x} |
| 1:0,20 | $\text{NiS}_{1,03}$ | FeS_2 | FeS_{1+x} |
| 1:0,23 | $(\text{Fe},\text{Ni})_9\text{S}_8$ | FeS_2 | FeS_{1+x} |
| 1:0,26 | $(\text{Fe},\text{Ni})_9\text{S}_8$ | FeS_2 | FeS_{1+x} |

Table 9 (b)
**Phase composition of interaction of products pyrite
with cobalt at 450 o C**

| The ratio of $\text{FeS}_2:\text{Co}$ | XPA phase composition | | |
|---------------------------------------|-----------------------|----------------|--------------------|
| 1:0,06 | $\text{CoS}_{1,036}$ | FeS_2 | FeS_{1+x} |
| 1:0,08 | $\text{CoS}_{1,036}$ | FeS_2 | FeS_{1+x} |
| 1:0,10 | $\text{CoS}_{1,035}$ | FeS_2 | FeS_{1+x} |
| 1:0,12 | $\text{CoS}_{1,035}$ | FeS_2 | FeS_{1+x} |
| 1:0,14 | $\text{CoS}_{1,035}$ | FeS_2 | FeS_{1+x} |

From the data of X-ray phase analysis of the products of thermal processing of pyrite with nickel and pyrite with cobalt, the following reactions should be considered: [90-96]



Thus, the results of Mössbauer studies of the processes of interaction of pyrite with iron together with the data of X-ray phase analysis confirm the formation of nonstoichiometric sulfides.

2.3 Hydrogenation of coal in the presence of iron sulfide catalysts

The catalytic effect of iron compounds on the process of destructive hydrogenation of heavy hydrocarbon feedstock (HHF) has been known for a long time. At present, iron-containing compounds have found application as catalytic additives in the liquid-phase hydrogenation of coal and HOR. However, despite the low catalytic activity of iron compounds, the search for new iron-containing catalytic systems continues. Of great interest are various industrial waste. Recent studies have shown that the catalytic activity of iron compounds increases at the stage of the hydrogenation of coal, sulfiding agents of sulfur or hydrogen sulfide. In the H₂-H₂S-Fe system, the existence of several forms of iron has been established. For the process of destructive hydrogenation of HHF, pyrite and pyrrhotite are most important. Currently there is no single point of view in the literature explaining the high catalytic activity of iron sulfide. It is assumed that catalytic activity is manifested by the release of hydrogen sulfide and pyrrhotite [62]. To determine the activity of the selected additives and catalysts, we conducted a series of experiments. The results of the experiments are presented in table 10.

The data in Table 10 show that all catalytic systems used by us exhibit activity in different ways, but the sulfide-containing systems are the most favorable for hydrogenation of coal — pyrite, in their presence the conversion of OCM reaches 81.5%. In the absence of catalysts and the replacement of hydrogen by synthesis gas, the conversion increases by 13%. In the presence of catalysts, the use of synthesis gas leads to an increase in the conversion of the organic mass from 78.4 to 81.5, respectively.

Table 10

**Effect of various catalytic additives on the hydrogenation
of coal in reducing gases**

Conditions: T = 430°C; the ratio of coal: tetralin = 1:2; the amount of added catalyst is 5% for OCM; τ = 60 min

| Gas | Catalyst type | Coal conversion degree, wt. % |
|-------------------------|--|-------------------------------|
| H ₂ | Without catalyst | 58,1 |
| H ₂ :Co(1:1) | FeS ₂ + Co(CoS _{1,035}) | 81,5 |
| H ₂ :Co(1:1) | FeS ₂ +Ni(Fe,Ni) ₉ S ₈ | 78,4 |
| H ₂ :Co(1:1) | FeS ₂ +Fe(Fe ₇ S ₈) monoclinic | 78,9 |
| H ₂ :Co(1:1) | FeS ₂ +Fe(Fe ₇ S ₈) | 79,7 |
| Ar | CoS _{1,035} | 72,2 |
| Ar | (Fe,Ni) ₉ S ₈ | 76,8 |
| Ar | (Fe ₇ S ₈) monoclinic | 70,3 |
| Ar | Fe ₇ S ₈ | 77,3 |

The positive effect of waste from nonferrous metallurgy pyrite and pyrrhotite on the degree of conversion of highly viscous oil was shown. However, analysis of the literature shows that there is no data on the use of natural iron-sulphide solid solution as catalysts for the process of hydrogenation of coal and high-viscosity oils. The results of experiments on the hydrogenation of the Kenderlyk and Shubarkol deposits in the presence of natural iron-sulphide solutions and iron sulfides are shown in Table 11.

Table 11
The catalytic activity of natural iron sulfide solutions and iron sulfides on the transformation of OCM

Conditions: T = 425 °C; Ct 5% on OCM; R_{rab.} = 6,0 MPa; τ = 60 min in the atmosphere of an inert gas (Ar): P_{Ar} = 4.0 MPa.

| № cat.table №5 | OCM con- version,% | Liquid products yield | Products, % | | | |
|----------------------|-----------------------|-----------------------------|-------------|------------|----------|----------------|
| | | | Tetraline | Naphtalene | Decalyne | H ₂ |
| Kenderlyk coal | | | | | | |
| 1. | 72,7 | 59,9 | 55,8 | 38,9 | 3,7 | 1,6 |
| 2. | 81,9 | 68,9 | 59,7 | 35,3 | 3,5 | 1,5 |
| 3. | 82,4 | 66,8 | 65,3 | 30,6 | 2,8 | 1 |
| 4. | 84,4 | 68,4 | 62,3 | 32,0 | 4,3 | 1,4 |
| 5. | 67,5 | 54,7 | 59,2 | 33,7 | 5,6 | 1,5 |
| 6. | 81,1 | 65,7 | 58,6 | 35,5 | 4,4 | 1,6 |
| 7. | 88,3 | 71,6 | 65,0 | 30,7 | 2,8 | 1,5 |
| 8. | 77,6 | 62,9 | 56,8 | 38,5 | 3,1 | 1,6 |
| 9. | 75,2 | 61,0 | 59,1 | 34,5 | 4,9 | 1,5 |
| 10. | 88,6 | 71,8 | 60,3 | 34,4 | 3,8 | 1,5 |
| 11. | 83,9 | 68,1 | 54,0 | 40,1 | 4,3 | 1,6 |
| Shubarkol coal | | | | | | |
| 1 | 88,5 | 71,7 | 56,6 | 38,0 | 3,9 | 1,5 |
| 2 | 87,7 | 69,5 | 60,8 | 32,9 | 4,7 | 1,6 |
| 3 | 82,0 | 65,1 | 58,8 | 34,3 | 5,3 | 1,6 |
| 4 | 86,8 | 68,8 | 54,0 | 35,6 | 3,8 | 1,5 |
| 5 | 86,0 | 68,2 | 61,0 | 32,7 | 4,8 | 1,5 |
| 7 | 92,7 | 76,5 | 54,1 | 40,1 | 4,2 | 1,6 |
| 12 | 86,3 | 68,4 | 60,8 | 37,7 | 4,0 | 1,6 |

The activity of catalysts was evaluated by the degree of OCM conversion and the yield of liquid products and the conversion of tetralin to naphthalene. From the data presented in Table 11, it follows that the most

active catalysts are bentonite and a mixture of clinker with pyrite (1:1), while the degree of pre-rotation of the organic coal mass increases from 88.3% to 88.7%.

In the presence of a clinker catalyst, a mixture of pyrite and bentonite, there is a decrease in the degree of conversion of tetralin to naphthalene from 38.5 to 30.7%. Of all the tested catalysts, the lowest degree of conversion of OCM 67.5 is observed on the catalyst sample number 5. The yield of liquid products for the Kenderlyk coals changes from 37.2% (without catalyst) to 71.8%, and for the Shubarkol coals from 65.1 to 72.0%.

Tetralin is dehydrated into naphthalene, the Gibbs free energy is calculated using the isotherm equation, the data are given in Table 12. The Gibbs energy at 425°C was calculated according to the known relation:

$$rG = RT \ln K_p \quad (1)$$

Table 12

Thermodynamic parameters of the tetralin dehydrogenation reaction

| № of cat. from the table №5 | -rG, kJ/mol | K _p |
|-----------------------------|-------------|----------------|
| Kenderlyk coal | | |
| 1 | 43,7 | 18181,8 |
| 2 | 57,8 | 21301,5 |
| 3 | 58,3 | 22994,1 |
| 4 | 59,4 | 27964,3 |
| 5 | 59,4 | 28164,3 |
| 6 | 59,5 | 28216,4 |
| 7 | 57,1 | 18703,8 |
| 8 | 60,1 | 31487,4 |
| 9 | 59,8 | 29350,7 |
| 10 | 59,1 | 26326,7 |
| 11 | 61,3 | 39042,1 |
| Shubarkol coal | | |
| 1 | 60,2 | 32275,0 |
| 2 | 58,9 | 25433,0 |
| 3 | 59,2 | 27843,3 |
| 4 | 61,5 | 39800,0 |
| 5 | 58,9 | 25725,6 |
| 7 | 61,5 | 40173,9 |
| 12 | 58,9 | 25446,7 |

Thus, the thermodynamic calculations performed for the equilibrium compositions of the tetralin dehydrogenation reaction proceed favorably with the use of iron sulfide solid solutions and natural clays. Figure 4 shows the

line X-ray diffraction patterns of solid residues after the liquefaction of coal and high-viscosity oil. According to XFA and EM data, the general scheme for the transformation of an iron-sulfide catalyst can be represented as follows:



With an increase in the liquefaction time, a change in the size distribution of the magnetite particles is observed. At the beginning, a fraction with a size of 5-8 nm is formed, which then transforms into smaller and larger particles.

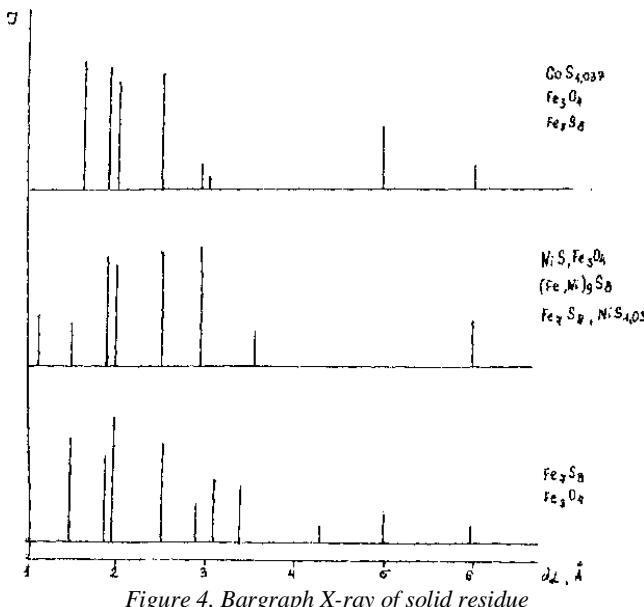


Figure 4. Bargraph X-ray of solid residue

Figure 5 (a, b) shows the Mössbauer spectra of the solid residues of coal hydrogenation in the presence of tetraline and the heavy oil fraction above 320°C. The resulting Mössbauer spectrum is decomposed into components, among which 3 phases have been identified.

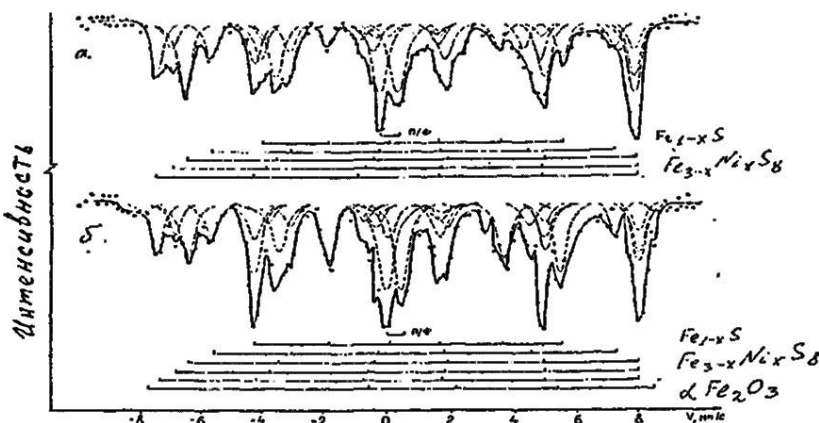


Figure 5. Mössbauer spectrum of solid residue:
a) passer – tetralin b) passer agent fraction above 320 °C

The first is the complex $\text{Fe}_{3-x}\text{Ni}_x\text{S}_8$ sulfide in sample a) and b) of table 13 is described by four sextuplets, of which one with the maximum Neff is assigned to the Fe^{3+} tetrahedral position and corresponds to hematite. Along with the complex iron sulfide in the Mössbauer spectrum, peaks of the pyrrhotine phase Fe_{1-x}S are distinguished. The isomeric shift indicates that iron is in the form of Fe^{2+} , and in composition it is close to troilite.

Table 13
Mössbauer phase parameter and the relative iron content associated with it

| Arr. | Phase | Position | I.S., mm / s | CR, mm / s | Effective magn.field on Fe^{57} , co. H _{eff} | Related Fe content, % |
|------|---------------------------|----------------------------|-----------------|---------------|---|-----------------------|
| A | Fe_{1-x}S | Fe^{2+}OKT | 0,84 | 0,04 | 306 | 16 |
| | | Fe^{3+}OKT | 0,33 | 0,05 | 490 | 20 |
| | Fe_{3-x} | $\text{FeOKT}(1)$ | 0,56 | 0,00 | 467 | 10 |
| | Ni_xS_8 | $\text{FeOKT}(2)$ | 0,75 | 0,00 | 456 | 27 |

| | | | | | | |
|------|--------|----------|--------------------|------------------|--|-------------------------|
| | | FeOKT(3) | 0,78 | - 0,10 | 403 | 13,5 |
| | II.Ф. | | 0,30 | 0,55 | 0,00 | 13,5 |
| Arr. | Phase | Position | I.S., mm / s | CR, mm / s | Effective magn.field on Fe57, co. Heff | Related Fe content,% |
| B | Fe1-xS | Fe2+OKT | 0,78 | 0,08 | 305 | 24 |
| | | Fe3+OKT | 0,36 | 0,01 | 485 | 17,5 |
| | Fe3-x | FeOKT(1) | 0,56 | 0,04 | 466 | 10 |
| | NixS8 | FeOKT(2) | 0,78 | 0,06 | 454 | 19,5 |
| | | FeOKT(3) | 0,80 | 0,03 | 398 | 11,5 |
| | Fe2O3 | Fe3+OKT | 0,51 | 0,09 | 515 | 3,0 |
| | P.F. | | 0,30 | 0,45 | 0,00 | 14,5 |

In addition to these two magnetically ordered phases, a doublet from the paramagnetic phase is observed in the Mössbauer spectrum. Its identification is difficult due to the strong overlap of the resonance lines. According to the Mössbauer data, the formation of complex $\text{Fe}_3\text{xNixS}_8$ iron sulphide is observed in the catalyst, where the nonstoichiometry parameter is defined in the range $0 < \text{X} < 0.145$. The obtained results are confirmed by the XFA data of the solid residue. The identified set of interplanar distances with $d = 2.9; 2.5; 1.9 \text{ \AA}$. They refer to the sulfide forms like $\text{NiS}, \text{NiS}_1\text{,03}$.

Table 14 presents the yield of liquid products, depending on the ratio of the added metal to pyrite (Fe, Co, Ni/FeS₂). The data in the table show that an increase in the ratio of cobalt to pyrite (91%) has a beneficial effect on the conversion of OCM. The dependence of the conversion of tetralin to naphthalene with an increase in the Co/FeS₂ ratio has an extreme character, and with an increase in the ratio of Ni/Fe/FeS₂, an increase in the conversion of tetralin to naphthalene is observed. The yield of liquid products varies from 65 to 70% when using Co, Ni. However, with an increase in the ratio of Fe/FeS, the output of liquid products decreases sharply.

Table 14
**The activity of the synthesized iron sulfide catalysts
 in the hydrogenation of coal**

Conditions: T=440 °C; R_{narAr} = 4.0 MPa, τ = 90 min, coal: tetralin ratio = 1: 2

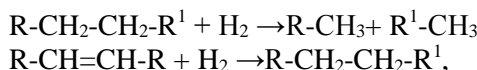
| The ratio of added metal to pyrite, M:FeS ₂ | Degree of conversion | | The total yield of liquid products,% of TSM |
|--|----------------------|------------|---|
| Nickel to pyrite | OCM,% | tetralin,% | |

| | | | |
|------------------|-------|------|------|
| 0.14: 1 | 84.5 | 26.0 | 65,8 |
| 0.17: 1 | 88.7 | 27.7 | 69.0 |
| 0.20: 1 | 90.2 | 30.1 | 70.1 |
| 0.23: 1 | 89.3 | 31.4 | 69.5 |
| 0.26: 1 | 87.3 | 33.5 | 67.9 |
| Cobalt to pyrite | | | |
| 0.06: 1 | 87.4 | 26.7 | 68.0 |
| 0.07: 1 | 88.5 | 33.6 | 68.9 |
| 0.10: 1 | 90.4 | 29.0 | 68.7 |
| 0.12: 1 | 91.1 | 33.6 | 70.7 |
| 0.14: 1 | 90.0 | 25.1 | 67.5 |
| Iron to pyrite | | | |
| 0.30: 1 | 92.1 | 27.1 | 71,6 |
| 0.36: 1 | 89.4 | 30.7 | 69.2 |
| 0.38: 1 | 87.0 | 31.3 | 68.0 |
| 0.40: 1 | 86.4 | 31.0 | 66.7 |
| 0.42: 1 | 80.11 | 30.7 | 62.5 |

It should be noted that the authors in [63–65] studied the effect of monoand bimetallic catalysts on the conversion of coal. Bimetallic catalysts (Fe – Co, Fe – Ni) showed the greatest activity in the process of hydrogenation of OCM, which is apparently due to the formation of a complex where Fe and Co are brought together within the same structure, which favors the formation of an alloy. Hydrogenation of OCM in the presence of alloy particles proceeds more efficiently than on metallic iron, cobalt, and pyrrhotite.

Thus, a high degree of conversion of OCM in the presence of iron sulfide catalysts seems to be related to the fact that hydrogenating centers are formed on the surface of the coal with increased nonstoichiometric formation of the complex $\text{Fe}_{3-x}\text{Ni}_x\text{S}_8$ and Fe_{1-x}S type sulfide complexes H_2S generated is adsorbed and provides transport of active hydrogen to the organic radicals of coal. To the catalytic reactions of the first group should be worn:

1. activation of hydrogen $\text{H}_2 \rightarrow 2\text{H}^*$ to free vacancies of iron;
2. catalytic cracking, thermal dissolution.



where R and R^1 – various hydrocarbon groups.

2.2 Polycyclic aromatic hydrocarbons are hydrogenated to form structures, including aromatic and hydrogenating rings;

2.3 Naphthenes are dehydrated to form aromatic hydrocarbons and hydrogen;

2.4 Oxygen-containing, sulfur-containing and nitrogen-containing compounds are reduced to the corresponding hydrocarbons and partially decomposed.

In order to present the mechanism of action of the LTCS and the mineral part of coal, one should refer to electronic representations in catalysis, according to which, as a result of lattice defects in the semiconductor and the presence of impurities, lattice sites with an excess of electrons or their lack of "holes" can form. It can be assumed that the chemisorbed radical or chemisorbed hydrogen, when interacting with the "hole," will give up their electrons and turn into a carbonium ion or proton:



It was noted above that nickel and cobalt contained in catalysts, increases the total splitting of OCM and blocks acid centers, and hydrogen sulfide formed during the hydrogenation of sulfur compounds that are contained in heavy oil, forms nickel and cobalt sulfides, and restores these centers. The formation of nickel and cobalt sulfides is confirmed by X-ray fluorescence analysis of solid residues of hydrogenation of coal.

Reactions of the second group, which take place in volume, can be attributed:

- 1) thermal dissolution of coal;
- 2) the transfer of proton from the solvent (tetralin) to coal with the transformation of tetralin into naphthalene.

The reaction of the first group is greatly influenced by the catalyst, and the second group by the nature and concentration of the solvent (pasteing agent). To assess the contribution of the solvent (tetralin, tar (HOR), fractions above 320 °C, high-viscosity oil) and dialyzer to the total conversion of coal during hydrogenation, experiments were carried out. The results obtained are presented in table 15.

Analysis of the results obtained in Table 15 shows that the nature of the solvent and the activity of the catalyst play a significant role in the process of coal liquefaction. As can be seen, the use of an active hydrogen donor (tetralin) increases the degree of conversion of OCM and the yield of liquid products in the presence of a catalyst 79.8 and 60.4%. Comparable results in comparison with the active hydrogen donor (tetralin) were obtained when

using the fraction above 320 °C as a passer, apparently, this is due to the high content of hydroaromatic compounds that can generate active hydrogen compared to other solvents.

Table 15

Hydrogenation of coal in the environment of various passers

Conditions: R_{rab} = 8,0 MPa; T = 723K; τ = 60 min; Kt (Fe₄Ni₅S₈), 5% for OCM. The ratio of coal: passer = 1: 2

| Ratio in catalyst Ni/FeS ₂ | Passer | Conversion degree of OCM, % | Liquid products yield on OCM, % |
|--|-----------------|-----------------------------------|---|
| 0,13 | Tetraline | 69,9 | 38,7 |
| 0,18 | | 74,8 | 55,0 |
| 0,23 | | 79,1 | 62,7 |
| 0,28 | | 79,8 | 63,3 |
| 0,33 | | 79,8 | 60,4 |
| Ratio in catalyst Ni/FeS ₂ | Passer | Conversion degree of OCM, % | Liquid products yield on OCM, % |
| 0,13 | | 47,1 | 26 |
| 0,18 | | 49,1 | 26,8 |
| 0,23 | Tar | 51,3 | 27,8 |
| 0,28 | | 50,6 | 29,2 |
| 0,33 | | 54,4 | 33,4 |
| 0,13 | | 55,3 | 32,4 |
| 0,18 | fractions above | 62,6 | 35,1 |
| 0,23 | 320оС | 64,8 | 36,0 |
| 0,28 | | 70,7 | 56,0 |
| 0,33 | | 73,4 | 58,7 |
| 0,13 | | 54,4 | 30,1 |
| 0,18 | | 55,3 | 30,0 |
| 0,23 | HVO | 57,4 | 31,3 |
| 0,28 | | 60,9 | 33,4 |
| 0,33 | | 62,8 | 35,0 |

Thus, the catalytic activity of heterogeneous catalysts is directly dependent on the properties of the solvent used — the hydrogen donor — the more actively the solvent gives a proton for the hydrogenation of coal, the more active the catalyst is to activate hydrogen and transfer hydrogen to the coal fragments and increase the rate of rupture C-C links in the latter.

2.4. Mathematical description of coal hydrogenation in the presence of heterogeneous catalysts

The method of multifactor planning is most convenient when there are not too many factors (no more than four) and for cases when it is possible to confine to straight and private dependencies. The method of selection of the approximating function is based on the least squares method applied to the equation of a straight line. However, it is known that the dependence of the product yield on a number of factors may be non-linear. In this regard, we believe that it is appropriate to consider experimental planning methods, which are based on nonlinear multiple correlation.

M.P. Malyshev used the formula of M.M. Protodyakonov as applied to the planning of a chemical experiment [66]. Work on this technique on chemical objects showed that the description of the matrix data by the equation of M.M. Protodyakonov can be considered prematurely correct. It is very important that the formula M.M. Protodyakonov (senior) has an advantage over the regression equation. In the equation M.M. Protodyakonov private dependencies are combined as a product, and in the regression equation as a sum. Consequently, at zero value of any of the factors, in the first case, the generalized function turns into zero, and in the second, it retains a certain value due to non-zero characteristics of the other factors. For example, if the duration of the process is zero, then using the Protodyakonov formula, we get a zero product yield, and the regression equation gives a non-zero, which is absurd.

The hydrogenations of coal from the Shubarkol deposit in the presence of synthesized heterogeneous catalysts — iron sulfide solid solutions — was investigated using multivariate planning.

Factors in these experiments, the intervals of variation by level are shown in Table 16.

Table 16
Levels of factors under study

| Factors | Levels | | | |
|---|--------|--------|--------|--------|
| | 1 | 2 | 3 | 4 |
| X ₁ – temperature, K | 663 | 683 | 703 | 723 |
| X ₂ – fraction ration to coal above 320 ⁰ C | 0,5:1 | 1:1 | 1,5:1 | 2:1 |
| X ₃ – the ratio of metal to pyrite Ni:FeS ₂ | | | | |
| Co: FeS ₂ | 0,17:1 | 0,20:1 | 0,23:1 | 0,26:1 |
| Fe: FeS ₂ | 0,08:1 | 0,10:1 | 0,12:1 | 0,14:1 |
| | 0,36:1 | 0,38:1 | 0,40:1 | 0,42:1 |

| X ₄ – duration, min | 45 | 60 | 75 | 90 |
|--|-----|-----|-----|-----|
| X ₅ – the amount of catalyst, % | | | | |
| Fe ₄ Ni ₅ S ₈ | | | | |
| Fe ₇ S ₈ | 0,0 | 2,0 | 4,0 | 6,0 |
| Co _{0,5} Fe _{0,5} S ₂ | 0,0 | 2,0 | 4,0 | 6,0 |
| | 0,0 | 2,0 | 4,0 | 6,0 |

Table 16 shows the results on the response functions of the performed experiment. The response function was taken to be the degree of conversion of OCM, where Y₁ is the degree of conversion of OCM (Fe₄Ni₅S₈ catalyst); Y₂ the degree of conversion of OCM (Co_{0,5}Fe_{0,5}S₂ catalyst); Y₃ the degree of conversion of OCM (catalyst Fe₇S₈). According to the results obtained (Table 17), all calculations are given in terms of the average value of the response Y₁ function.

Table 17
The response functions of the five-factor experiment at four levels

| № p/p | Response function | | |
|---------------|-------------------|----------------|----------------|
| | Y ₁ | Y ₂ | Y ₃ |
| 1 | 59,2 | 50,3 | 62,4 |
| 2 | 68,5 | 60,1 | 70,1 |
| 3 | 75,7 | 72,3 | 75,4 |
| 4 | 67,2 | 70,1 | 70,4 |
| 5 | 65,4 | 66,1 | 58,5 |
| 6 | 66,7 | 59,5 | 67,4 |
| 7 | 73,3 | 77,1 | 70,5 |
| 8 | 75,2 | 68,4 | 69,6 |
| 9 | 68,6 | 63,4 | 67,7 |
| 10 | 74,8 | 76,3 | 71,4 |
| 11 | 60,5 | 62,4 | 60,6 |
| 12 | 71,7 | 73,6 | 68,9 |
| 13 | 70,4 | 76,1 | 74,7 |
| 14 | 79,4 | 72,3 | 73,3 |
| 15 | 66,7 | 67,5 | 70,4 |
| 16 | 70,5 | 76,4 | 67,1 |
| Average value | 69,61 | 68,24 | 68,65 |

Figure 6 shows the corresponding approximation curves and scatter plots. Since for Kt.(Fe₄Ni₅S₈) all functions are significant. All functions will be included in the general expression, and the Protodyakonov equation will be represented by the formula (2 and 3)

$$y_{ln} = \frac{(-0,0036+0,14X_1-0,0001X_1^2)(6,07+106,2X_2-37,74X_2^2)(6,53+285,9X_3)}{69,6^4(0,52+2,15X_4-0,016X_4^2)^{-1}(1,96+19,84X_5+1,33X_5^2)^{-1}} \quad (2)$$

For the $\text{Co}_{0,5}\text{Fe}_{0,5}\text{S}_2$ catalyst, the Protodyakonov equation will be represented by the formula

$$y_{ln} = \frac{(-0,109+0,099X_1)(9,601+511,58X_3)(0,14+2,12X_4+0,016X_4^2)}{(6,82+97,11X_2-32,89X_2^2)^{-1}(1,66+18,45X_5-1,17X_5^2)^{-1}68,2^4} \quad (3)$$

Table 18 and 19 present the experimental and calculated values of the partial functions of $\text{Kt}(\text{Fe}_4\text{Ni}_5\text{S}_8)$.

*Table 18
The experimental values of the partial functions of cat. $\text{Fe}_4\text{Ni}_5\text{S}_8$*

| Function | Lvels | | | | Average value, y_{cp} |
|----------|-------|------|------|------|-------------------------|
| | 1 | 2 | 3 | 4 | |
| y_1 | 65,9 | 72,4 | 69,1 | 71,2 | 69,6 |
| y_2 | 64,2 | 68,1 | 74,7 | 71,4 | 69,4 |
| y_3 | 70,9 | 68,7 | 71,6 | 67,3 | 69,6 |
| y_4 | 68,9 | 70,2 | 71,1 | 68,1 | 69,6 |
| y_5 | 67,6 | 70,2 | 68,9 | 71,8 | 69,6 |

*Table 19
The calculated values of the private functions of cat. $(\text{Fe}_4\text{Ni}_5\text{S}_8)$*

| Function | Lvels | | | | Average value, y_{cp} |
|------------------------------------|-------|-------|-------|-------|----------------------------|
| | 1 | 2 | 3 | 4 | |
| $y_1=0,11-0,1003X_1$ | 66,61 | 68,61 | 70,62 | 72,63 | 69,8 |
| $y_2=6,07+106,2X_2-$ $37,74X_2$ | 49,70 | 74,53 | 80,46 | 67,50 | 68,0 |
| $y_3=6,53+285,85X_3$ | 55,12 | 63,70 | 72,30 | 80,90 | 68,0 |
| $y_2=0,52+2,15X_4-$ $0,016X_4$ | 64,90 | 71,90 | 71,80 | 64,40 | 68,30 |
| $y_2=63,53+1,69X_5-$ $0,025X_5$ | 65,20 | 66,81 | 69,90 | 72,80 | 68,70 |

For the catalyst (Fe_7S_8) , the Protodyakonov equation will be represented by formula (3).

$$y_{3n} = \frac{(0,17+0,099X_1)(6,77+102,2X_3)(0,91+102,2X_3)}{(0,43+2,16X_4-0,016X_4^2)^{-1}(2,54+19,35X_5-1,29X_5^2)^{-1}68,6^4} \quad (4)$$

Mathematical processing of the factor experiment, especially the cyclical interpretation, is of great importance, since it gives a three-

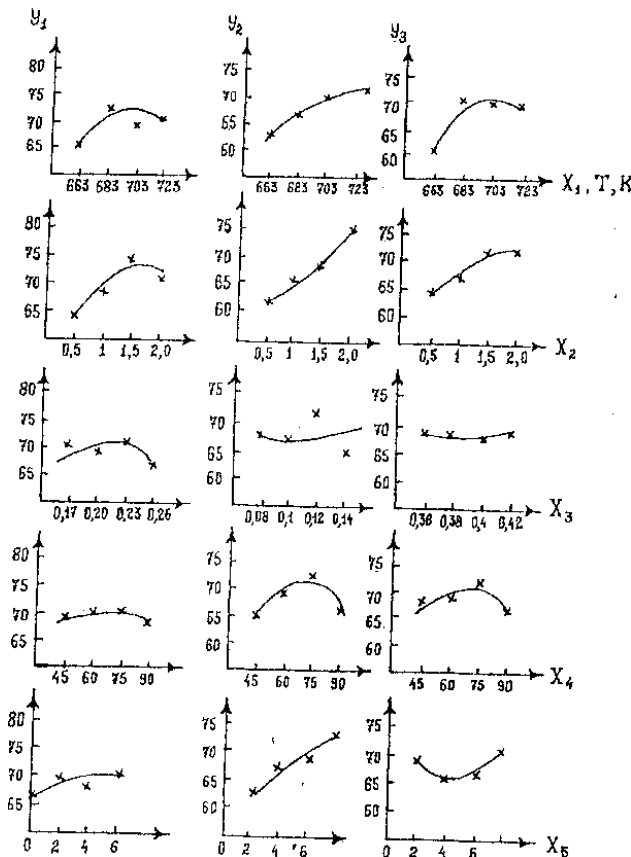


Figure 6. The change in the function of the degree of conversion of coal with a change in the composition of the catalyst

dimensional idea of the effect on the ratio of pastor to coal, temperature, amount of catalyst, duration and the ability to compare these factors on the conversion of the organic mass of coal.

Analysis of the results obtained in the mathematical processing of the experiment (Table 18 and Figure 6) showed the following:

1) For the function U_1 ($Kt Fe_4Ni_5S_8$) all factors are significant. Factor X_1 has an optimum in the range of 72.0-72.4%.

X_2 affects the function of U_1 unambiguously, the greater the ratio of the pastor, the higher the degree of conversion of OCM.

X_3 the influence of this factor on the function of U_1 is ambiguous, the higher the ratio of nickel to pyrite in solid solution, an increase in the degree of conversion of OCM is observed, and a further increase above 0.23 leads to a sharp decrease in the degree of conversion of WMD, apparently due to the non-stoichiometric pyrrhotite in the catalytic system.

X_4 an increase in contact time passes through the optimum in the range of 70.2-72.2%.

X_5 is a direct relationship, which confirms the high activity of the analyzer.

2) For the function U_2 ($Kt Co_{0.5}Fe_{0.5}S_2$) all factors are significant. X_1 and X_2 for these factors there is a direct dependence, the higher the temperature and the ratio of the pastogenizer to coal, the higher the value of the function U_2 .

X_3 the influence of the ratio of cobalt to pyrite in solid solution has an optimum in the range of 70.0-72.8%.

X_4 an increase in the time of the hydrogenation of coal leads to an increase in U_2 ,

X_5 is a straight-line relationship, an increase in the amount of added catalyst leads to an increase in the degree of conversion of OCM.

3) For the function U_3 ($Kt Fe_7S_8$) all factors are significant. X_1 has an extremum in the range of 70.5%.

X_2 an increase in the ratio of pastor to coal leads to an increase in the degree of conversion of OCM.

X_3 a direct relationship, the smaller the ratio of iron to pyrite in solid solution, the higher the value of U_3 . Apparently, this is due to an increase in the ratio of sulfur to iron in pyrrhotite.

X_4 with an increase in the contact time of the hydrogenation of coal, the degree of conversion of OCM decreases.

X_5 a factor in which the function has an extremum at 66.5%.

So, according to the results [67-69] of mathematical planning for activity in the process of hydrogenation of coal, a number of catalysts are arranged in the following sequence:



2.5. Optimization of the process of hydrogenation of coal deposits of Karazhar

The use of tetralin as a hydrogen donor on an industrial scale is almost impossible due to its high cost. Researchers, both abroad and in the CIS countries, are searching for an alternative hydrogen donor. Such donors or solvents can be heavy oil residues (HOR) or highviscosity oils (HVO).

The Republic of Kazakhstan has unique reserves of highviscosity oil, HVO is characterized by a high content of asphalt-resin substances, heavy metals vanadium or nickel, increased viscosity and differs from ordinary oils in total sulfur content above 3% and the absence of light fractions. In this regard, HVO requires hydrogenation treatment in the presence of catalysts.

During the hydrogenation of coal, the HVO of the Karazhambas deposit was used as a passer. When optimizing the process of hydrogenation of coal with high-viscosity oil in the presence of pyrite catalyst FeS_2 , the influence of the following factors was studied:

1. additive to the catalyst (g);
2. duration (min);
3. amount of catalyst FeS_2 (g);
4. the ratio of coal and HVO;
5. temperature (K).

Since the dependence of the yield of liquid products from coal on the above factors is nonlinear, we used the method of mathematical planning of an experiment, based on nonlinear multiple correlation. Variable factors ranged on 4 levels. The experiment planning matrix is given in table 20.

Table 20
Matrix of 5-factor experiment at 4 levels

| № | Levels | | | | | $\bar{Y}_{\text{эксп.}}$, % | $Y_{\text{п.}}$, % |
|---|--------|--------|--------|-------|-------|------------------------------|---------------------|
| | X 1 | X 1 | X 2 | X_4 | X_5 | | |
| 1 | 1 | 1 | 1 | 1 | 1 | 9,20 | 16,01 |
| 2 | 2 | 2 | 2 | 2 | 1 | 15,82 | 27,36 |
| 3 | 3 | 3 | 3 | 3 | 1 | 57,43 | 47,69 |
| 4 | 4 | 4 | 4 | 4 | 1 | 73,60 | 77,41 |
| 5 | 1 | 2 | 3 | 4 | 2 | 56,22 | 51,07 |
| 6 | 2 | 1 | 4 | 3 | 2 | 54,14 | 56,38 |
| 7 | 3 | 4 | 1 | 2 | 2 | 25,90 | 27,40 |
| 8 | 4 | 3 | 2 | 1 | 2 | 32,65 | 33,09 |
| 9 | 1 | 3 | 4 | 2 | 3 | 51,36 | 51,59 |

| | | | | | | | |
|----|---|---|---|---|---|-------|-------|
| 10 | 2 | 4 | 3 | 1 | 3 | 34,91 | 32,36 |
| 11 | 3 | 1 | 2 | 4 | 3 | 69,78 | 68,13 |
| 12 | 4 | 2 | 1 | 3 | 3 | 67,87 | 47,78 |
| 13 | 1 | 4 | 2 | 3 | 4 | 41,14 | 35,82 |
| 14 | 2 | 3 | 1 | 4 | 4 | 31,79 | 34,09 |
| 15 | 3 | 2 | 4 | 1 | 4 | 50,86 | 37,35 |
| 16 | 4 | 1 | 3 | 2 | 4 | 56,42 | 57,65 |

The structure of the matrix is such that during the conduct of all experiments, each level of any factor occurs once with each level of all factors. To do this, each level of each factor is set in the experiment as many times as the accepted levels. To simplify the graphic design of the results, a uniform increase is assumed (Table 21)

Table 21
Experiment planning matrix

| Factors | Levels | | | |
|--|---------|---------|---------|---------|
| | 1 | 2 | 3 | 4 |
| X ₁ – additive to the catalyst, % | 0 | 1 | 2 | 3 |
| X ₂ – duration, min | 0 | 30 | 60 | 90 |
| X ₃ – the amount of catalyst, % | 0 | 2 | 4 | 6 |
| X ₄ – HVO:Y ratio | 0,5:1,0 | 1,0:1,0 | 2,0:1,0 | 3,0:1,0 |
| X ₅ – temperature, K | 593 | 623 | 648 | 673 |

The factor experiment was carried out according to the matrix, where each row corresponds to the conditions of the experiment. The results were evaluated by function: the conversion of the organic mass of coal (Y_{exp} , %). In the column Y_{exp} (Table 20) presents the results of all experiments, and for Y_p for the remaining functions are given immediately using a generalized equation. The values of the private functions, respectively, of each factor X₁, X₂, etc. are shown in table 22.

Sampling for levels is carried out from experimental data (Table 19). To obtain the value of Y at the first level, it is enough to add the results of the first four experiments and divide the sum by four. The sampling principle for the remaining functions remains the same, but here the same levels are arranged in a spread, so the corresponding experiment results are scattered along the same lines. The data of table 22 are plotted (Fig. 7).

Table 22

Experimental values of private functions

| Function | Levels | | | | Average value Y_{cp} |
|----------|--------|-------|-------|-------|---------------------------|
| | 1 | 2 | 3 | 4 | |
| Y_1 | 39,48 | 34,17 | 50,99 | 57,38 | 45,51 |
| Y_2 | 47,14 | 47,69 | 43,31 | 43,89 | 45,51 |
| Y_3 | 33,69 | 39,85 | 50,99 | 57,49 | 45,51 |
| Y_4 | 31,91 | 37,13 | 55,15 | 57,85 | 45,51 |
| Y_5 | 39,01 | 42,23 | 55,98 | 44,80 | 45,51 |

Empirical formulas are selected to describe each curve by the least squares method (LSM). Selection and calculation using the OLS method was carried out on a 1VM-386 computer. The calculated values of all private dependencies and the dependencies themselves are listed in Table 22. Each of the functions was passed for significance using the nonlinear multiple correlation coefficient and significance for the 5% level:

$$R = \sqrt{1 - \frac{(N-1) \sum (Y_s - Y)^2}{(N-K-1) \sum_{i=1}^n (Y_s - Y_{-p})^2}} \quad (5)$$

$$t_r = \frac{Rx\sqrt{N-K-1}}{1-R^2} > 2 \quad (6)$$

where, N is the number of points described; K is the number of active factors; Y_s is an experimental result; Y_t theoretical (calculated) result; Y_{cp} the average experimental value.

In analyzing the importance of private dependence $N = 4$, $K = 1$, because only the value of one factor is taken into account. Data for the Y_s was taken from table 20, and for Y_t from table 23.

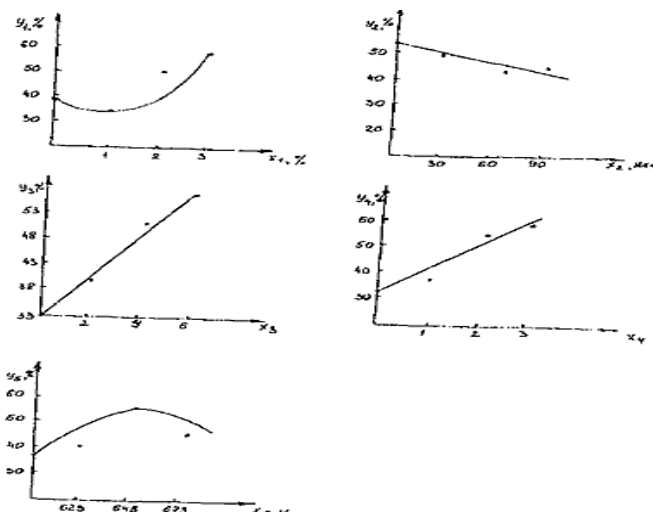


Figure 7. Point plots and partial dependences of coal hydrogenation on: X_1 catalyst additives; X_2 duration, min; X_3 the amount of catalyst, %; X_4 the ratio of HVO:Y; X_5 temperature, K

Calculated values of private functions for Y_{KCN}

| Function | Levels | | | | Average value $Y_{\text{cp.}}$ |
|-------------------------------|--------|-------|-------|-------|--------------------------------|
| | 1 | 2 | 3 | 4 | |
| $Y_1=37,85-1,72X_1+2,93X_1^2$ | 37,85 | 39,06 | 46,18 | 59,06 | 45,51 |
| $Y_2=47,63-0,047X_2$ | 47,63 | 46,22 | 44,80 | 43,39 | 45,51 |
| $Y_3=33,12+4,12X_3$ | 33,12 | 41,38 | 49,64 | 57,90 | 45,51 |
| $Y_4=41,14+15,9X_4$ | 30,12 | 41,14 | 52,16 | 58,69 | 45,51 |
| $Y_5=56,0-2,4X_5-375X_5^2$ | 39,03 | 44,0 | 56,60 | 44,00 | 45,51 |

In selecting private dependencies, the method of successive approximation was used. At the beginning of the point was approximated by a straight line equation. If this model turns out to be adequate (with significant correlation coefficients), then it is left; if the model is inadequate, they will go over to models of higher orders. The result of the calculation of the nonlinear multiplicative correlation coefficient and its significance are presented in Table 24.

Table 24

**Nonlinear Multiple Correlation Coefficient R and the significance of tr
— for particular functions in coal hydrogenation**

| Function | R | t _r | Significance |
|----------------|------|----------------|--------------|
| Y ₁ | 0,87 | 5,22 | significant |
| Y ₂ | 0,71 | 2,03 | significant |
| Y ₃ | 0,96 | 16,70 | significant |
| Y ₄ | 0,81 | 3,31 | significant |
| Y ₅ | 0,98 | 38,93 | significant |

These results of table 24 testify to the reliability of the obtained equations on the basis of private dependencies. Having determined the dependence of private functions, they made up a generalized equation for each optimization parameter:

$$y_n = \frac{\sum_{i=1}^k y_i}{y^{k-1}_{-p}} \quad (7)$$

where Y_n is a generalized function, Y_i is particular functions, P is the product of all considered values of generalized functions, k is the number of factors of private functions.

When optimizing the process of coal hydrogenation, the generalized equation is:

$$Y_n = (45?51)^{-4} \times Y_1 \times Y_2 \times Y_3 \times Y_4 \times Y_5 \quad (8)$$

The generalized equation for each response function was tested for significance by comparing the calculated results for the generalized equation with experimental data. The results of the calculations for U_p are given in Table 20. Further, the correlation coefficients R were found for N-16 and K = 5. Consequently, each of the five arguments in carrying out the process of hydrogenation of coal and HVO using synthesis gas influences and determines the value of one or several optimization parameters characterizing the process. Since the conversion of the organic mass of coal increases with an increase in the amount of catalyst and catalytic additive, an increase in the process temperature above

648K leads to a slight decrease in the conversion of the organic mass of coal. The positive effect of an increase in the HVO to coal ratio on the conversion of OCM should be noted.

Thus, we have found the optimal conditions for the hydrogenification of coal and HVO. Optimal conditions for the process:

X₁ additive to the catalyst 3-5%,
X₂ the duration of 70-90 minutes
X₃ the amount of catalyst (FeS₂) 5-6%, X₄ the ratio of HVO: coal - 3:1,
X₅ temperature 648-673 K.

The experiment implemented under these conditions gives a good agreement with the theoretically calculated conversion of the organic mass of coal. Experimental data confirm the adequacy of the mathematical model of the process and it can be used to regulate the technological regime and predict the correction of the yield in liquid products and the creation of an integrated coal hydrogenation unit and testing.

Hydrogenation of coal under optimal conditions:

- the degree of conversion of OCM, % 75.2;

- product yield, % of TSM:

gas 17.2

H₂O 1.0

- liquid products, %: 70.2 including:

up to 473 K 20.1

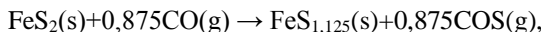
above 573 K 12.7

2.6. Thermochemical and thermodynamic calculation of ironcontaining catalysts

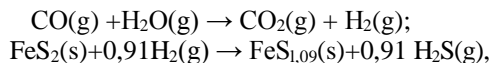
Pyrrhotite of composition FeS_{1,143} is obtained from pyrite by treatment with synthesis gas with an initial gas pressure of 4.0 MPa, a process duration of 120 minutes in a rotating autoclave with a volume of 0.5 l. The results of X-ray phase analysis showed that the compound obtained corresponds to the pyrrhotite of composition FeS_{1,143}, which is the product of the following reaction:



The pyrrhotite of composition FeS_{1,125} is obtained from pyrite by treatment with CO, with an initial gas pressure of 4.0 MPa, the duration of the process is 120 min:



The pyrrhotite of composition FeSi_{1,09} was obtained from pyrite by treatment with CO/H₂O, with an initial gas pressure of 4.0 MPa, and a process time of 120 minutes:



X-ray phase analysis showed that the compounds obtained correspond to the pyrrhotines $\text{FeS}_{1,125}$ and $\text{FeS}_{1,09}$.

3 DEVELOPMENT OF AN EXPERIMENTAL TECHNIQUE AND ANALYSIS OF THE RECEIVED PRODUCTS

3.1 Source materials and methods for the study of coal tar

Coal tar obtained at the enterprise of "Sary-Arka Speccoke" LLP and heavy oil residue (HOR) waste of the Petrochemical Plant in Pavlodar was used as a raw material. The yield of coal tar in the production of coke is 6.6% of dry coal and the yield of HOR is 30-35% of the original oil.

The process of coal semi-coking is carried out at a temperature of 500-550°C, the hardened semi-coke is heated to 700 °C, however, the volatile substances that form practically do not pass into the furnace through the heating zone to 700-750 °C and therefore undergo a minor degree of secondary pyrolysis. Therefore, the released tar must be of the same quality as the primary semi-coking tars. We have found that increasing the yield of volatile substances in the special coke of the plant of "Sary-Arka Speccock" LLP to the optimum value (7-8%) improved mechanical strength and physicochemical properties. Increasing the volatile matter yield from 3.0 to 7.0% not only increases the output of coke by 2.5%, but also improved the extraction of primary coal tar vapors in the process of coal semi-coking.

Coal tar obtained from the coals of the Shubarkol mine belongs to the primary tars, i.e. for tars not subjected to secondary thermal processes. Unlike high-temperature coking tars, it is characterized by a high content of oxygen-containing compounds, mainly phenols and unsaturated compounds. Semi-coking tar contains almost no aromatic unsubstituted compounds. Hydrogen in the tar compound is mainly included in the composition of the aliphatic groups (substituents) of aromatic and unsaturated compounds. The tar consists of a large number of compounds, with components present in small quantities.

The technical characteristics of coal tar are given in Table 25. The tar under study is characterized by low density (about 1042 kg/m³), high water content (about 10%), lack of crystallization fractions, lower yield of residue (pitch), high content of phenols.

Indicators of technical analysis are defined in accordance with TC 14-7-100-89 "Coal tar for processing".

The fractional composition of the tar was determined by the method given in [70]. Due to the close values of the tar and water density, the dehydration of the tar is practically impossible to settle, which makes the tar fractionation process difficult.

To separate water from the tar, toluene was added in an amount of 10% of the tar before distillation, and after azeotropic toluene mixture was

distilled off with water, fractionation was performed, and the temperature was measured both in the vapor and in the liquid phase. Fractionation was stopped when the temperature in the liquid reached 390-400 °C to avoid a significant change in the primary tar due to thermal reactions in the cube. The limits for the selection of fractions are taken by analogy with the distillation of the high-temperature coking tar. For fractional distillation, fractions boiling in the range: up to 230 °C; 230-270 °C; 270-300 °C; more than 300 °C; pitch residue.

Table 25

**Technical characteristics of the primary coal tar
“Sary-Arka Speccoke” LLP**

| Indicator | Primary coal tar |
|--|------------------|
| Volume fraction of water, % | 10.4 |
| Density at 20 °C, kg / m ³ | 1042 |
| up to 180 °C | 3 |
| 180-230 °C | 7.2 |
| 230-270 °C | 15.1 |
| 270-300 °C | 17.1 |
| final temperature 300 °C | 6.2 |
| total distillate, % | 48.9 |
| End boiling point, ° C | |
| in pairs | 315 |
| in liquid | 390 |
| Pitch yield, % | 50 |
| Indicator | Primary coal tar |
| Mass fraction of substances of unsoluble in toluene, % | 3.8 |
| Mass fraction of substances unsoluble in quinoline, % | Missing |
| Ash content, % | 0.1 |
| Phenol content, % | > 20 |
| Naphthalene content, % | Traces |

Determination of phenol content. One of the limiting factors of industrial use of the studied tars is the presence of phenols in it, whose content reaches 25%.

The total content of phenols in the resin and fractions was determined by extraction with an aqueous solution of alkali by incrementing the volume of the alkaline layer in the Cattwinkel burette (TU 2457170-

00190437-02), representing a graduated burette with two balls at the ends.

The bottom ball of the burette is filled with 10% NaOH solution, saturated with sodium chloride to the bottom division of the burette. Then 10-20 ml of benzene is poured and the level of the alkaline layer is measured.

The tar (2-5 g) or fractions dissolved in 10-20 ml of benzene is transferred to a Cattwinkel burette, shaken for 5 minutes and allowed to stand for 1 hour.

The concentration of phenols in the sample is calculated by the formula:

$$C_{\phi} = \frac{V \cdot 1,04 \cdot 100}{m} \quad (9)$$

where V is the increment of the volume of the alkaline layer (ml); 1.04 is the average density of phenols (g/cm³); m is the mass of the fraction, (g) taken for analysis.

According to the results of the analysis, it was established that the total content of phenols in the tar is about 25%.

Physico-chemical methods of analysis of tar, HOR and their fractions. The study of coal tar by chromatography-mass spectrometry (CMS).

Sample preparation: 1 g of the sample was dissolved in 20 ml of acetone and dried with sodium sulfate. 1 ml of the solution was diluted to 10 ml and 10 µl of an internal standard of *o*-picoline and flurantene with a concentration of 40 g/l was added. The concentration of standards in the tar was 8 g/kg. The analysis of the sample was performed by the gas CMS method on an HP 5890/5972 MSD instrument manufactured by "Agilent" (USA). Substance identification was carried out using the NIST98 mass spectral database.

Chromatography conditions:

Column: DB-5, 30 m X 0.25 mm X 0.5 µm Gas: helium, 0.8 ml / min

Thermostat: 50°C 4 min

50-150°C 10°C/min

150-300°C 20°C/min 300°C 4 min

Evaporator: 250°C Evaporator: 200°C

The results of the analyzes of the tar are given in table 26. The concentration of substances was determined semi-quantitatively relative to fluoranthene. The HP 1050 instrument with a diode matrix confirmed the

content of polyaromatic hydrocarbons by the HPLC method.

Table 26

Tar composition

| Exit time, min. | Name of identified substances | Concentration in substances, g / l |
|-----------------------|-----------------------------------|---------------------------------------|
| 1 | 2 | 3 |
| 7.65 | Phenol | 23.73 |
| 8.44 | 2,3-dimethylcyclopent-2-en-one | 0.97 |
| 8.65 | 2-methylphenol | 14.31 |
| 8.94 | 3-methylphenol | 36.91 |
| 9.30 | 2,6-dimethylphenol | 2.15 |
| 9.41 | 2,2,6,6-tetramethyl-4piperidinone | 0.89 |
| 9.61 | 2-ethylphenol | 2.96 |
| 9.74 | 2,4-dimethylphenol | 17.19 |
| 9.95 | 3-ethylphenol | 23.77 |
| 10.04 | 3,5-dimethylphenol | 2.05 |
| 10.18 | Azulene | 7.63 |
| 10.25 | 1,2-dihydroxybenzene | 6.41 |
| 10.30 | 2,4,6-trimethylphenol | 0.65 |
| 10.43 | 4-propylphenol | 1.21 |
| 10.49 | 2-ethyl-6-methylphenol | 5.37 |
| 10.59 | 4-ethyl-3-methylphenol | 4.74 |
| 10.62 | 3-ethyl-5-methylphenol | 1.54 |
| 10.77 | Propylphenol | 7.89 |
| Exit time, min. | Name of identified substances | Concentration in substances, g / l |
| 10.81 | 4-methyl-1,2dihydroxybenzene | 5.30 |
| 10.85 | 3,4,5-trimethylphenol | 3.47 |
| 10.89 | 2,3,6-trimethylphenol | 2.89 |
| 11.06 | 3-methyl-1,2dihydroxybenzene | 11.11 |
| 11.16 | 1 methylnaphthalene | 2.51 |
| 11.30 | 2-methylnaphthalene | 5.05 |
| 11.40 | 6-methyl-2H-1benzopyran-2-one | 0.87 |

| | | |
|-------|---|------|
| 11.46 | 2,3-dihydro-1H-inden-5-ol | 4.67 |
| 11.49 | 2,3-dihydroxytoluene | 2.57 |
| 11.55 | 4-hydroxy-phenylethanol | 1.95 |
| 11.66 | 3,5-dihydroxytoluene | 1.55 |
| 11.76 | 4-ethyl-1,3dihydroxybenzene | 6.92 |
| 11.82 | Tetradecane | 7.79 |
| 11.94 | 1,2,3,4-tetrahydro-1,1,6trimethylnaphthalene | 1.24 |
| 12.00 | 1,3-dimethylnaphthalene | 3.34 |
| 12.12 | 1,4-dimethylnaphthalene | 3.03 |
| 12.15 | 2,6-dimethylnaphthalene | 1.37 |
| 12.26 | 1,2-dimethylnaphthalene | 2.64 |
| 12.34 | 2-methylpentylbenzene | 2.17 |
| 12.45 | 1-pentadecene | 1.46 |
| 12.50 | Pentadecane | 4.26 |
| 12.69 | 1-naphthol | 3.09 |
| 12.75 | 2-naphthol | 2.64 |
| 12.79 | 2,3-dihydro-3,3,5,6tetramethyl-1H-inden-1-one | 2.53 |
| 13.08 | 9-eicozen | 4.01 |
| 13.13 | Hexadecane | 4.82 |
| 13.25 | 1,4,6-trimethylnaphthalene | 4.34 |
| 13.35 | 2-methyl-1-naphthol | 3.68 |
| 13.41 | 4-methyl-1-naphthol | 4.15 |
| 13.54 | 7-methyl-1-naphthol | 4.22 |
| 13.67 | Unsaturated hydrocarbon | 1.76 |
| 13.72 | Tridecan | 8.88 |
| 13.82 | 1,6-dimethyl-4-isopropylnaphthalene | 3.16 |
| 13.97 | 1,2-dihydro-2,5,8-trimethylnaphthalene | 2.63 |

| Exit time, min. | Name of identified substances | Concentration in substances, g / l |
|-----------------|---------------------------------------|------------------------------------|
| 14.09 | 3-methyl-2-isopropylbenzofuran | 1.75 |
| 14.14 | 1,4-dihydro-2,5,8trimethylnaphthalene | 2.32 |
| 14.23 | 1-tetradecene | 3.00 |
| 14.27 | Octadecane | 8.46 |
| 14.43 | Phenanthrene | 0.75 |
| 14.48 | Anthracene | 1.40 |
| 14.69 | not identified | 1.16 |
| 14.76 | 1-hexadecene | 2.41 |
| 14.80 | Hexadecane | 7.90 |
| 14.89 | 1-tridetsen | 0.49 |
| 15.12 | 1-methylphenanthrene | 1.46 |
| 15.19 | 2-methyl anthracene | 2.05 |
| 15.30 | Eykasan | 10.66 |
| 15.39 | Cyclohexadecane | 0.90 |
| 15.49 | not identified | 0.55 |
| 15.78 | Genekasan | 14.34 |
| 15.92 | Fluoranten (standard) | 8.00 |
| 16.21 | 1-docosen | 1.19 |
| 16.24 | Heptadecane | 8.96 |
| 16.59 | 2,4,5,7-tetramethylphenanthrene | 3.79 |
| 16.68 | Octadecane | 12.54 |
| 17.02 | Benzyl butyl phthalate | 0.99 |
| 17.10 | Saturated hydrocarbon | 8.71 |
| 17.52 | Cyclopentadecane | 8.88 |
| 17.97 | Saturated hydrocarbon | 4.30 |
| 18.47 | Hexatricante | 2.97 |
| 19.02 | Dotrikantan | 1.82 |
| 19.66 | Saturated hydrocarbon | 1.25 |
| 20.41 | Saturated hydrocarbon | 0.89 |
| 20.48 | not identified | 0.52 |
| Total | | 410.8 |

As a result of studying the component composition of the tar by the gas CMS method, compounds of the following classes were identified: phenols and cresols, naphthols, hydrocarbons with molecular masses of 200-

300, polyaromatic hydrocarbons (naphthalenes, anthracenes and phenanthrene).

Electron-microscopic analysis of the liquid phase of the primary coal tar after catalytic-cavitation treatment was performed on a JSM (JOEL) 5910 (LV) instrument.

3.2 The method of catalytic cavitation treatment of primary coal tar and hexane

The cavitator used in the processing of petroleum and petroleum products, coal tar and other raw materials is shown in Figure 8.

Cavitator parameters:

The parameters of the pump OGP 5 25 4.0 / 25:

| | |
|--------------------|--------------------------|
| Liquid consumption | 4.0 m ³ /hour |
|--------------------|--------------------------|

| | |
|-----------------------|------|
| Operating temperature | 70°C |
|-----------------------|------|

| | |
|------------------------|---------|
| The outlet pressure is | 25 atm. |
|------------------------|---------|

VCPHG model-4.0/0.1-D:

| | |
|--------------------|--------------------------|
| Liquid consumption | 4,0 m ³ /hour |
|--------------------|--------------------------|

| | |
|-----------------------|-------|
| Operating temperature | 250°C |
|-----------------------|-------|

| | |
|--------------------|---------|
| Operating pressure | 30 atm. |
|--------------------|---------|

This device creates an axial region of low pressure, sufficient to break the continuity of the liquid and the appearance of the paragas phase at a temperature of 25 °C. On the axial line, a zone of almost 100% boiling of a liquid is created with the appearance of vapor-gas bubbles and cavities of maximum geometry. This, in the subsequent, outside the design of the device, in the region of atmospheric pressure causes vapor-gas bubbles to collapse, creating powerful cavitation zones without destroying the vortex cavitator. This device allows cavitation processing of various liquids with a maximum flow rate of 4 m³/hour, at a pressure of 25 atm. But as viscosity increases, the flow through the vortex cavitator will fall.

A sample of coal tar with a volume of 150 ml was subjected to rotary pulsation cavitation at a stirring speed of "3".

The exposure time was 1 and 5 minutes, after which the kinematic viscosity of the coal tar was measured at temperatures of 313, 333, 353 K. To optimize the experiment, the method of mathematical planning was used. After that, samples were taken for analysis in order to determine the elemental and functional compositions of the original and deconstructed coal tar samples.



Figure 8. Appearance of the assembled cavitator

3.3 Method of viscosimetric measurements

While the viscometric method of the study measured the expiration time of the object. For this, a 100 cm^3 coal tar was poured into a clean dry viscometer VZ-4 ($K = 0.94$), the viscometer was installed vertically and the flow time was measured at temperatures of 313, 333, 353 K. After each measurement, the viscometer was washed 2-3 times with the following in order by sample. After completion of the measurements, the viscometer was removed from the thermostat and poured the test object. The average value of the expiration time of the solvent was reproduced with an accuracy of 0.2-0.3 s. In this study, the viscosity of the initial tar was determined after the catalytic-cavitation treatment (Fig. 9).

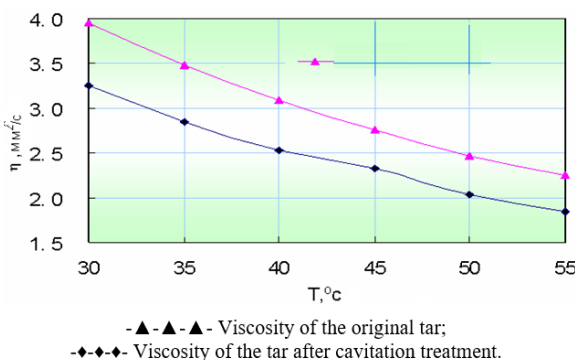


Figure 9. Influence of cavitation treatment on resin viscosity

As a result of the cavitation effect, it was possible to reduce the viscosity of the tar by almost an order of magnitude.

3.4 Method of pycnometric measurements

Each pycnometer must have a carefully established water number, i.e., the mass of water in the volume of the pycnometer at the temperature of determination, which according to the standard should be equal to 20 °C. The water number is determined as follows. The pycnometer is thoroughly washed with a chromium mixture, alcohol and distilled water, dried with well-purified air and weighed on an analytical balance with an accuracy of 0.0002 g. Then the pycnometer is filled. Then the pycnometer is placed in a thermostat (or bath) at a temperature of 20 °C and kept for about 30 minutes.

When the water level in the pycnometer neck stops changing, excess water is taken, the neck is wiped inside, the stopper is closed, the pycnometer is carefully wiped outside (best of all with a linen cloth that does not give flakes capable of changing the weight of the pycnometer) and weighed precisely to 0.0002 g. In the case of pycnometers with a label, excess water (above the label) is collected with a pipette or filter paper rolled up into a tube. In a water thermostat (or bath) pyknometers are strengthened on a test float or attached to the wall of a thermostat (or bath) with a wire. The water level is measured at the upper edge of the meniscus.

The discrepancy between parallel tests shall not exceed 0.004. In determining very viscous petroleum products, proceed as follows. A dry and clean pycnometer with a label, the water number of which is known, is half filled with petroleum products, taking care not to cover the walls of the pycnometer. Very viscous products are preheated to 5060 °C. When determining the density of oil products that are solid at room temperature, the pyknometer is filled to about half with small pieces of product. Then (in both cases) the pycnometer with the product is placed in a thermostat with a temperature of 80-100 °C to remove air and completely melt the product. Then the picnic meter with coal tar is filled with distilled water and kept in a thermostat until the water level ceases to change. Excess water is drawn off with a pipette or a strip of filter paper rolled into a tube, then wipe the inside of the neck. The water level is set on the upper edge of the meniscus, after which, having carefully wiped out the pycnometer outside, weigh it with an accuracy of 0.0002 g

3.5 Equipment and methods for the hydrogenation of coal and a mixture of model organic compounds

Experiments on the hydrogenation of coal and a mixture of organic compounds (anthracene, phenanthrene, benzothiophene) were performed in a reactor (volume 0.05 l), (Fig. 10).

A mixture of coal and HOR (1:2 ratio, coal 10g HOR 20g). Organic substances (2 g) and solvent 0.5 g (tetralin) were loaded into an autoclave, then the calculated amount of Fe_2O_3 nanocatalyst was added to the mixture, based on 1% of the organic mass of the mixture. The autoclave was closed. They flushed with argon or hydrogen and gave an excess (initial) gas pressure of 6.0 MPa (heated to the required temperature of 400-420°C at a rate of 100°C/min and held for a specified time (60 min). After cooling the autoclave to room temperature, gaseous products were measured with a GMB-400 gas meter.



Figure 10. High Pressure Reactor

3.6 Method of elemental analysis

The amount of carbon and hydrogen was determined by burning in a stream of oxygen, followed by trapping water and carbon dioxide, and calculating the amount of carbon and hydrogen. Sulfur was determined (State standard 1437-56) by burning a sample with chamotte clay, followed by trapping the resulting sulfurous and sulfuric anhydrides with hydrogen peroxide solution.

3.7 Methods of processing experimental data

3.7.1 Calculation of structural and chemical indicators of primary coal tar

Currently, a new unified classification system of combustible minerals has been developed, built on the basis of the interrelation of structural and chemical indicators (δ , η , B) and technological properties [71]. This system allows using structural and chemical indicators to characterize combustible minerals (gas, oil, coal, shale), intended for energy purposes, as well as for thermal and thermochemical processing processes.

As the main parameters for the characteristics of combustible minerals are the following structural and chemical indicators:

n_{at} is the total number of atoms; n_{cb} is the total number of bonds;

δ is a parameter characterizing the degree of metamorphism;

B is a parameter characterizing the degree of reduction of organic matter of combustible minerals.

The total number of atoms of all basic elements (C, H, N, O, S) in a unit mass (100 g) n_{at} is calculated:

$$n_{at} = \sum_{i=1}^5 n_i = \sum_{i=1}^5 \frac{A_i}{m_i} = \frac{A_c}{12} + A_H + \frac{A_o}{16} + \frac{A_N}{14} + \frac{A_s}{32}, \quad (10)$$

where

n_i is the number of gram moles of the i-th element; A_i the percentage of the i-th element (in 100 g); m_i is the atomic mass of the i-th element;

A_C —percentage of carbon (in 100 g);

A_H the percentage of hydrogen (in 100 g); A_O is the percentage of oxygen (in 100 g); A_N is the percentage of nitrogen (in 100 g); A_S is the percentage of sulfur (in 100 g).

The total number of bonds in the organic matter of combustible minerals (n_{cb}) is calculated:

$$n_{cb} = \frac{1}{2} \sum_{i=1}^5 \omega_i^\sigma \cdot n_i = \frac{1}{2} (4 \cdot n_c + n_H + 3n_N + 2n_O + 2n_S) = \frac{A_c}{6} + \frac{A_H}{2} + \frac{3A_N}{28} + \frac{A_O}{16} + \frac{A_S}{32} \quad (11)$$

where ω_i^σ is the number of σ bonds of the i-th element in the valence state [72].

The parameter characterizing the degree of metamorphism (nonsaturation) of the fuel molecule (δ) takes into account the contribution of

all elements to the composition of the organic mass and is calculated from the elemental composition:

$$\delta = 2(n_{ce} - n_{am}) = \frac{A_c}{6} - A_H + \frac{A_N}{14}, \quad (12)$$

Values for δ solid fuels are within:

$$-12,5(\text{methane}) \leq \delta \leq 16,67(\text{graphite}).$$

o characterize the degree of unsaturation of the organic matter of combustible minerals, the indicator η also serves:

$$\eta = \frac{n_{am}}{n_C} = 1 + 12 \left(\frac{A_H}{A_C} \right) + \frac{6}{7} \left(\frac{A_N}{A_C} \right) + \frac{3}{4} \left(\frac{A_O}{A_C} \right) + \frac{3}{8} \left(\frac{A_S}{A_C} \right), \quad (13)$$

where n_C is the number of gram moles of carbon (in 100 g);

A_N - the percentage of hydrogen (in 100 g);

A_C is the percentage of carbon (in 100 g);

A_N - percentage of nitrogen (in 100 g);

A_O is the percentage of oxygen (in 100 g);

A_S - percentage of sulfur (in 100 g).

The values of this indicator vary within the following limits:

$$1 \leq \eta \leq 5 \quad (14)$$

The maximum value of this indicator is 5 and corresponds to methane; the minimum value of this indicator is typical for graphite. By chemical determination, the more hydrogen in the composition of a substance, the more it is restored, and the content of N, O and S heteroatoms reduces the reduction.

The parameter of coal recovery (B) is a structural indicator, used as a technological parameter. To characterize the restoration of combustible minerals, such indicators as n_C/n_H , the degree of aromaticity, as well as H^{daf} are traditionally used. The more the structure of hydrogen contains, the more it is restored.

The rate of recovery is calculated:

$$B = \frac{50(n_H - 2n_O - 3n_N - 2n_S)}{n_C + 1}. \quad (15)$$

The values of B varies within the following limits:

$$0(\text{graphite}) \leq B \leq 100(\text{methane}). \quad (16)$$

With an increase in the degree of metamorphism (a decrease in the

number of hydrogen and heteroatoms), the value of B approaches zero.

3.7.2 Calculation of the heat of combustion and enthalpy of formation

The enthalpy of formation of the organic mass of HHF, being one of the important thermodynamic functions, can be used to assess its reactivity in various processes and determined in various ways [73].

It should be noted that the determination of the enthalpy of HHF in the framework of the structure-property model is associated with some difficulties. First, the HHF generally consists of a set of compounds that differ in structure and molecular weight, and second, both the structure and molecular weight of these compounds varies over a wide range.

The calculation of the heat of combustion is carried out by several methods:

1. Method of Mendeleev:

To calculate the upper heat of combustion Mendeleev D.I. proposed a formula without nitrogen:

$$Q_{\text{M}}^e = \frac{4,184[81C + 300H - 26(O - S)]}{10}, \quad (17)$$

Mathematically, he proposed to calculate the lower calorific value by the following equation:

$$Q_{\text{M}}^n = \frac{4,184[81C + 247,88H - 26(O - S)]}{10}, \quad (18)$$

2. Method proposed by the Institute of Combustible Minerals (ICM):

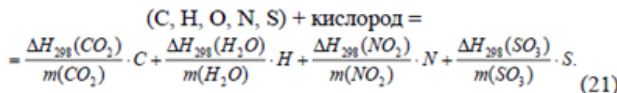
To calculate the net calorific value of the HHF in the ICM, the following equation was proposed:

$$Q_{\text{exp}} = \frac{4,184(80,860C + 239,548H - 20,741O + 15,225N - 63,650S)}{10}, \quad (19)$$

The dependence of the lower heat of combustion Q_i^{dof} on the parameter δ has the following form:

$$Q_i^{\text{dof}} = -18,50\delta^2 + 421,71\delta + 996,7 \quad (R = 0,896) \quad (20)$$

Calculation of the enthalpy of formation of HHF by the method of ICM. To calculate the enthalpy of formation of HHF use the reaction of complete combustion 100g:



According to the data, we have:

$$\Delta H_{298}(CO_2)/m(CO_2) = -393,50/12,011 = -32,76 \text{ кДж/с(С)}, \quad (22)$$

$$\Delta H_{298}(H_2O, \text{ж})/m(H_2O) = -285,84/2,0156141,81 \text{ кДж/с(Н)}, \quad (23)$$

$$\Delta H_{298}(H_2O, \text{ж})/m(H_2O) = -241,84/2,0156 = 199,98 \text{ кДж/с(Н)}, \quad (24)$$

$$\Delta H_{298}(NO_2)/m(NO_2) = 33,85/14,0067 = 2,42 \text{ кДж/с(Н)}, \quad (25)$$

$$\Delta H_{298}(SO_3)/m(SO_3) = -395,26/32,064 = -12,33 \text{ кДж/с(С)}. \quad (26)$$

Having taken $\Delta H_{\text{реакции}} = -Q_i^{\text{dof}}$, according to the law of Hess, we have:

$$-Q_i^{\text{dof}} = \sum \Delta H_{298}(\text{combustion products}) - \Delta H_{298}^{\text{dof}}. \quad (27)$$

Therefore, for the enthalpy of formation it has:

$$\Delta H_{298}^{\text{dof}} = \sum \Delta H_{298}(\text{combustion products}) + Q_i^{\text{dof}}. \quad (28)$$

Hence, for the case when in the products of complete combustion

water is in the liquid phase:

$$\Delta H_{298}^{daf} (H_2O, \text{ж}) = -32,76C - 141,81H + 2,42N - 12,33S + Q_i^{daf}, \quad (29)$$

and in the gas phase:

$$\Delta H_{298}^{daf} (H_2O, \text{г}) = -32,76C - 119,98H + 2,42N - 12,33S + Q_i^{daf}, \quad (30)$$

If there are no experimental data on the heat of combustion Q_i^{daf} , you can use the calculation formulas (16) and (17)

The dependency equations are as follows:

$$\Delta H_{298}^{daf} (H_2O, \text{г}) = -4,188\delta^2 + 114,04\delta - 764,39 \quad (R^2 = 0,973), \quad (31)$$

$$\Delta H_{298}^{daf} (H_2O, \text{ж}) = -3,165\delta^2 + 105,9\delta - 886,75 \quad (R^2 = 0,985). \quad (32)$$

It should be noted that the value of enthalpy by equations (31) and (32) with the maximum value $\delta = 16.667$ for "graphite" should be zero. With the accuracy of calculation for "graphite", from equation (31) we get -27.05, and from (24) -0.91 kJ/100g.

3.7.3 Calculation of thermodynamic parameters

In evaluating various chemical reactions involving HOR, thermodynamic calculations used data on the enthalpy of individual organic compounds. In this case, an assumption was made when considering the organic mass of HHF, which was considered as a mixture of a number of individual compounds [74]. Contributions to the enthalpy of intermolecular interactions for each of the components are taken into account in the initial data taken for the solid state of molecular crystals. Possible deviations from the additivity principle are insignificant.

The enthalpy of formation $\Delta H_{f,c}$ (kJ/mol) of a certain fragment of HOR with a specific molecular mass M must satisfy the formula:

$$\Delta H_{f,c} = \sum_k m_k \Delta H_{f,k} \quad (33)$$

where m_k is the number of moles of the k th component; $\Delta H_{f,c}$ is the standard enthalpy of its formation, kJ/mol.

The following conditions must be met:

The number of moles of mk should correspond to the total molecular weight:

$$M = \sum_k m_k n_k \quad (34)$$

where M_k is the molecular weight of the k-th component.

2. The atomic balance condition must be observed:

$$n_i = \sum_k m_k n_{ki}, \quad (35)$$

where n_i is the number of atoms of the i-th chemical element ($i = 1$ (C), 2 (H), 3 (O), 4 (N), 5 (S)) in the selected fragment of the HOR; $n_{k,i}$ is the same in the k-th molecular component that models its structure.

The molecular mass of the fragment will be:

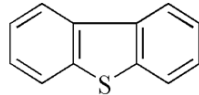
$$M = \sum_i \alpha_i n_i, \quad (36)$$

where α_i is the atomic mass of the i-th element. And the empirical formula of the fragment will be expressed in the form:

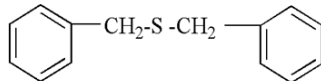
where α_i is the atomic mass of the i-th element. And the empirical formula of the fragment will be expressed in the form:

$$C_{n1}H_{n2}O_{n3}N_{n4}S_{n5}, \quad (37)$$

For thiophene sulfur in aromatic heterocycles S_{ar} and sulfur sulfide in the composition of aliphatic sulfides S_{al} , dibenzothiophene (I) and dibenzyl sulfide (II) are used as molecular models:



I



II

The total number of moles of the forms (I) and (II) describing the

sulfur-containing part will be n₅. These forms are related by:

$$\omega = \frac{S_{ar}}{S_{ar} + S_{al}}, \quad (38)$$

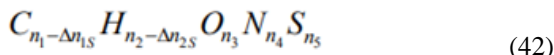
$$\omega = 0,0193 C^{daf} - 0,849 \quad (39)$$

The number of moles of the forms (I) and (II) involved in the construction of a fragment of the organic mass of HHF will be:

$$m_I = \omega n_5, \quad (40)$$

$$m_{II} = (1 - \omega) n_5 \quad (41)$$

It will be spent on Δn₁, s = 12m_I + 14 m_{II} grams-atoms of carbon and Δn₂, s = 8m_I + 14 m_{II} grams-atoms of hydrogen, then the empirical formula will look like:



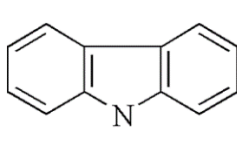
Nitrogen is present in the form of pyrrole-like compounds (NH) and pyridine-like structures (N_{py}), which are described by the relationship:

$$\chi = 0,8368 - 0,3535 x + 26,844 x^2 - 322,625 x^3 + 888,5x^4 \quad (43)$$

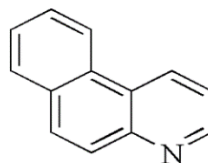
where x = (Cdaf-79,5) / 100. For nitrogen, model compounds are carbazole (III) and benzoquinoline (IV), for which the number of moles will be determined:

$$m_{III} = \chi n_4, \quad (44)$$

$$m_{IV} = (1 - \chi) n_4. \quad (45)$$



III



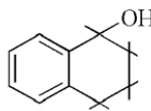
IV

This will consume $\Delta n_{1,N} = 12m_{III} + 13m_{IV}$ grams of carbon atoms and $\Delta n_{2,N} = 9(m_{III} + m_{IV})$ grams of hydrogen atoms, then the empirical formula of the oxygen-containing part of the fragment will look like:

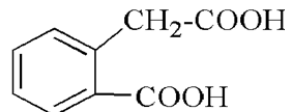
$$C_qH_pO_{n_3}, \quad (46)$$

where $q = n_1\Delta n_{1,S} - \Delta n_{1,N}$; $p = n_2\Delta n_{2,S} - \Delta n_{2,N}$.

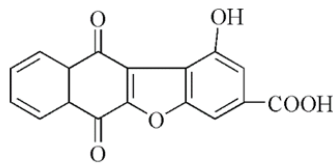
Oxygen is present in the form of individual oxygen-containing compounds tetralol-1 (V) and acetoxybenzoic acid (VI) and the conditional (model) compound $C_{17}H_8O_6$:



V



VI



VII

For model compounds (I) (VI), the values of the standard enthalpy of formation $\Delta H_{f,k}$ are taken from literature data, and for compound (VII), the value $\Delta H_{f,k}$ is estimated by an additive method.

For these model compounds $\Delta H_{f,k}$ (kJ/mol):

| (I) | (II) | (III) | (IV) | (V) | (VI) | (VII) |
|-------|------|-------|-------|--------|--------|--------|
| 120,0 | 99,0 | 125,1 | 149,7 | -241,4 | -815,6 | -908,3 |

Based on this technique, the authors of [75] developed a program for calculating thermodynamic indices using a personal computer, which was used in this work. The elemental analysis data of HOR and the concentration of functional groups were used as the initial data.

CHAPTER 4. CATALYTIC PROCESSES. HYDRAULIC EXPOSURE TO HEAVY OIL AND HEAVY HYDROCARBON RAW MATERIALS

Heavy petroleum and petroleum bitumens differ from ordinary petroleum by a higher content of metals (vanadium, nickel, iron, molybdenum, copper, sodium) of sulfur, nitrogen and asphaltenes.

In 1974, the Karazhambas heavy oil field was discovered on the Buzachi peninsula of the Republic of Kazakhstan [72]. Karazhambas is a multilayer deposit, oil deposits are found in six layers of the lower cretaceous (A₁, A₂, B, C, D, D) and two horizons (Y-1, Y-2).

High-tar oil, high-sulfur oil, is characterized by a low yield of light fractions. The physico-chemical characteristics of the Jurassic oil (interval 362-376 m well №108) and neocomian (interval 251-258 m Well №101) horizons are p₄-0.9431 and 0.9395 respectively; M-409 and 309; kinematic viscosity at 20 °C 539 and 920 mm²/s, at 50 °C 117 and 150 mm²/s; flash point 108 and 60 °C, pourings minus 17 and minus 26 °C; the paraffin content is 1.40 and 1.49%; its melting point is 42 and 59 °C; the sulfur content is 2.51 and 2.15%; nitrogen 0.88 and 0.55; sulfuric acid resins 64 and 60; asphaltenes 4.1 and 6.5; coking ability 7.20 and 7.44;

As can be seen from these data, oil is characterized by a low content of the distillate part (Well №108). Karazhambas oil is the most viscous among the known oils of Western Kazakhstan, the elemental composition of oil (well No. 108) is as follows (%): C 84, 09; H 12, 5; No. 2, 14; O 0, 88; S0, 39. A high sulfur content is noted in other samples; 1.75% (well №135); 2, 03 (well №122). The yield of fractions boiling to 200°C is low; 3.5% (well №135); 2.03 (well №122); 6.5 (well №101).

Karazhambas oil can be used as sulfur-containing fuel oil and for the production of road binders. Direct processing by known methods is constrained not only by the high content of sulfur and nitrogen compounds, but also due to the presence of vanadium and nickel. The presence of these metals promotes the formation of low-melting slags during combustion. Vanadium and nickel adversely affect the selectivity and activity of cracking catalysts, cause corrosion of equipment.

4.1. Catalytic methods for removing metals from crude oil

Due to the significant increase in the share of sulfur and high-sulfur oils in the total amount of processed oils, hydrogenation anionic processing methods have been widely developed [73-73-75]. Hydrogenation processing is one of the best methods for removing the most undesirable components

from petroleum and petroleum products: sulfurous, nitrogenous, metal-containing compounds, much of asphaltenes and resins by hydrogenating them under hydrogen pressure with the participation of catalysts. When hydrofining is achieved the most deep cleaning of crude oil from metals to trace content (less than 5 g/t). At the same time, in addition to reducing the sulfur content to less than 0.3-0.5% by weight, the content of nitrogen, tar, asphaltenes and coking properties of the raw materials are reduced. Hydro-exaggerated products are the highest quality raw material for hydrocracking and cracking fluid [73-75]. Almost all modern designed and operating catalytic cracking units are equipped with a hydrotreating unit for raw materials with an increasingly heavy fractional composition. However, the possibility of demetallization of oil residues in hydrofining processes is limited. This is due to the fact that the deposition of metals on the catalyst gradually leads to its irreversible deactivation [73-75]. It was established that if the total amount of metals in the feedstock is less than 25 g / t, the process can be carried out with high technical and economic indicators and in a reactor with a stationary layer of a catalyst of one type, characterized by high hydro-desalting activity and low metal intensity. When the content of metals is more than 25 g/t, it is necessary to use two types of catalysts, and the first of them should have a high capacity and low hydrodesulfurizing activity. Another catalyst must be highly active in the hydrodesulfurization reaction. In practice, this is reflected in the fact that the process is carried out in two or even three reactors, and in the first reactor hydrodemetallization and hydrodeasphalting are carried out on a cheap catalyst with a large pore volume, hydrodesulfurization in the second, and hydrocracking in the third if necessary [76]. In the works [76-77], the course of the reaction of hydrodemetallization of the residue of atmospheric distillation of petroleum and the relationship of the reaction with the cracking of asphaltenes was studied. A good correlation was obtained between the degrees of asphaltene removal from cracking and metals during demetallization. As the process temperature increases, the rates of vanadium removal from asphaltenes significantly increase, while the size of molecules also decreases. The nickel content in the asphaltene fraction, hydrotreating products does not decrease until the size of the molecules significantly decreases. Thus, the hydrodemetallization of petroleum residues proceeds in close relationship with the reduction of asphaltenes molecules. It was concluded that the cracking of asphaltenes promotes their demetallization, but demetallization does not have a large effect on their cracking. When asphaltenes are cracked, smaller molecules of maltenes are formed, the demetallization of which proceeds significantly faster [76]. It is established that the contribution of diffusion to the vanadium removal reaction is greater than that in the nickel

removal reaction, which is confirmed by the optimal value of the catalyst pores for these reactions. The selectivity of vanadium removal compared to nickel removal selectivity continuously decreases with decreasing pore diameter of the catalyst. During the processing of heavy oils and its fractions, in which the combination of metals and asphaltenes is concentrated, the components contained in its composition primarily react with the active sites of the catalysts, causing their poisoning. In world practice, before undergoing deep refining, heavy oils are demetallized.

Moreover, the degree of demetallization of hydrocarbon raw materials in known processes does not exceed 50-69%, and at the same time a small yield of light products is provided. Researchers of the Institute of Oil and Gas of Atyrau University of the Republic of Kazakhstan proposed a process of hydrodemetallization of the oil residue with dilution of the wood fraction of the pyrolysis resin in a reactor with a two-stage catalyst layer under hydrogen pressure. As catalysts at the first stage, an alum-nickel-cobalt-molybdenum catalyst and an industrial catalyst AP-64 were tested. When combining the two catalysts, 80% demetallization of the raw material and 94% conversion of the fraction with a boiling point above 350 °C occur. One of the methods for the demetallization of HOR is their combined hydrogenation with coal [77].

In co-hydrogenation of coal with an oil fraction with a boiling point above 300 °C, the bulk of the metals, including nickel and vanadium, pass into the solid residue. In [77], the effect of coal additives on the nickel and va-nadium content in the liquid tar hydrogenation product was studied. The authors proposed a mechanism for demetalization of tar together with coal, which consists in the fact that organic-mineral components of coal have a catalytic effect on the destruction of highmolecular compounds of tar, promoting, on the one hand, their more intensive transformation into liquid and gaseous products, and on the other, compaction products that bind metals to tar.

In the literature, there is currently no information on methods for studying the mechanism of the reaction of demetallization. Presumably, the catalyst adsorbs, for example, vanadylporphyrin in unchanged form, then the porphyrin ring is opened and nevanadyl compounds are formed. Many researchers have noted the increased resistance of nickelcontaining complexes. This is explained by the nature of the complex bonds of nickel and molecules of asphaltenes and resins, as well as by the peculiarities of the location of the nickel atom in the structure of porphyrin. The high depth of vanadium removal is presumably due to the fact that the heteroatom of oxygen projecting from the vanadylporphyrin plane is strongly bound to the catalyst surface and facilitates the detachment of the vanadium atom [78].

**4.2. Chemical composition of catalytic hydrogenation products
(coal, high-viscosity oil, petroleum bitumen)**

Hydrogenates obtained from the liquefaction of coal, highviscosity oil, petroleum bitumen, are a complex mixture of hydrocarbons. Information about the individual and group hydrocarbon composition of the products under study can provide additional information on understanding the structure of coal, heavy oils and the mechanism of the reaction in the process of catalytic hydrogenation of HHF. The group hydrocarbon composition of the hydrotreated product obtained from the coal of the Shubarkol deposit after distillation is given in table 27.

Table 27

**Characteristics of the liquid products obtained
during the hydrogenation of coal from the Shubarkol deposit**

| Indicators | Hydrogenate | Coal distillate with T _{кип} , °C | | |
|--|-------------|--|-----------|--------|
| | | до 200 | 200 – 350 | >350 |
| The content of the fraction in the hydrogenate | | 16,34 | 28,6 | 36,8 |
| Density, g / cm 3 | 0,8942 | 0,78913 | 0,8854 | 0,9665 |
| Group carbohydrate about native composition,% | | | | |
| olefins | 7,89 | 9,52 | 9,3 | 5,4 |
| aromatic | 34,22 | 20,0 | 22,4 | 35,7 |
| paraffins + naphthenes | 57,89 | 70,5 | 68,3 | 58,9 |

As can be seen from the data of table 27, the content of aromatichydrocarbons is rather high and this fraction can serve as a source for the production of individual aromatic hydrocarbons. In addition, it can be used to obtain individual paraffinic hydrocarbons. The low content of olefins of 1.8 and 2.7 wt.% suggests that this fraction is little affected by the processes of oxidation and stability during long-term storage.

Table 28 shows the results of the study of the fraction to 200 °C, obtained by hydrogenation of Shubarkol coal and heavy oil residue.

In the studied samples, hydrocarbons from C₇ to C₈ (21.2%) are also contained in the highest concentrations. This is typical for both paraffin-naphthenic and aromatic hydrocarbons. Among parafinonaphthenic hydrocarbons, along with alkanes with normal pentane and octane and 2-methylpentane, which are dominant in the medium, the content of

methylcyclo- and ethylcyclohexane and pentane is high.

Table 29 shows the results of the study of the individual hydrocarbon composition of the distribution of aromatic hydrocarbons in a fraction with a boiling point of up to 200 °C.

Data on the group composition of the fraction with a boiling temperature of 180–350 °C, obtained by hydrogenation of a heavy oil residue and coal, are given in Table 30.

Table 28
**The composition of paraffin and naphthenic hydrocarbons
 in a fraction with a boiling point of up to 200 °C**

| Hydrocarbons | Content, mass., % |
|--|-------------------|
| C ₅ – C ₇ (from n pentane to 2,2 dimethylbutane) | 0,29 |
| C ₅ – C ₇ (from cyclopentane to 3 methylcyclohexane) | 9,18 |
| C ₇ – C ₈ (from 1,3 dimethylcyclopentane to 2 methylpentane) | 21,2 |
| C ₈ – C ₉ – (from 1,3,5 trimethylcyclohexane) | 17,1 |
| C ₉ – C ₉ (from 4 methyloctane before n nonane) | 12,52 |
| C ₉ – C ₁₀ (from 1,2,3 trimethylcyclohexane to n decane) | 17,2 |

Table 29
**Distribution of aromatic hydrocarbons of different rows
 in the fraction with b.p. up to 200°C**

| Hydrocarbons | Content, mass. % | |
|--|------------------|-----------------|
| | HO R | HOR coal=1:2 |
| Benzene | 0,33 | 3,93 |
| Toluene | 2,30 | 7,00 |
| Ethylbenzene | 0,90 | 1,80 |
| P-xylene + m-xylene | 2,33 | 3,70 |
| O-xylene | 1,30 | 1,90 |
| Isopropyl benzene | 0,32 | 1,90 |
| Hpropylbenzene | 0,30 | 0,10 |
| 1methyl 3-ethylbenzene, 1-methyl 4-ethylbenzene | 0,96 | 1,84 |
| 1,3,5-trimethylbenzene | 0,56 | 1,20 |
| 1,2,4-trimethylbenzene | 0,61 | 1,40 |

Note HOR is a fraction with a boiling point above 350 °C.

Table 30

Group hydrocarbon composition of the fraction with b.p. 180–350°C

| Hydrocarbon class | Hydrocarbons content, mass. % | |
|------------------------|-------------------------------|----------|
| | HOR | coal+tar |
| Paraffins + naphthenes | 52,5 | 50,2 |
| Olefins | 1,8 | 2,7 |
| Aromatic | 45,2 | 47,2 |

4.3 Influence of the nature of catalysts on the chemical composition of liquid products

One of the main ways to improve the efficiency of hydrofining processes in coal and oil distillate fractions is to improve the porous structure of catalysts. It has been established that the presence of wide pores with a radius of more than 100 nm in the structure of bentonite clay reduces diffusion complications and contributes to its fuller utilization [79].

In southern Kazakhstan there are large reserves of bentonite clay (not less than 10 million tons). The most studied and of industrial interest are the bentonitic deposits of the Shymkent region: Kyngraksks, Darbazinsks, Dzerzhinsks, Chardarinsks.

The activity of catalysts from bentonite clays was compared with the activity of an industrial catalyst BAS-2 of the Gorky refinery.

As can be seen from table 31, Narynkol activated clay has, along with high activity, the greatest surface and exchange capacity, which allows a greater degree of replacement of cations by H⁺ ions and active metal ions.

A fraction of coal oil with a boiling point of 180–350 °C (4.0 MPa, 300–450 °C; bulk feed rate 1.0 h⁻¹; catalyst — activated bentonite clay) was subjected to cracking.

Table 31

Comparative characteristics of bentonite clay catalysts

| Name of bentonite clay | Bulk weight | Activity, % | Surface m ² / accordi ng to BET | Total pore volume, cm ³ | Average pore size, nm | Volumetric cationic capacity, EMC / 1000 |
|--------------------------------|-------------|-------------|--|------------------------------------|-----------------------|--|
| Kangarskaya without activation | 0,695 | Not active | | | | |
| Monrakskaya without activation | 0,680 | Not active | | | | |

| | | | | | | |
|-----------------------------|-------|------|-----|------|-----|-------|
| Narynkol without activation | 0,780 | 11,0 | | | | |
| Kyngar activated | 0,670 | 32,0 | 170 | 0,35 | 7,2 | 62,6 |
| Monraksky activated | 0,650 | 35,0 | 200 | 0,24 | 1,4 | 104,0 |
| Narynkol activated | 0,640 | 37,0 | 230 | 0,42 | 6,6 | 110,5 |
| Industrial catalyst | BAS-2 | 35,0 | 180 | 0,22 | 2,5 | 54,6 |

The data given in table 32 shows that, in the composition of the gaseous products, there is a significant amount of hydrogen and g increases in temperature from 300 to 450 °C and the amount of hydrogen decreases in the gas phase from 68.0 to 15.0%.

Table 32

The effect of temperature on the composition of gaseous products (up to C5 inclusive) obtained by cracking the coal oil fraction

| The composition of the gas.productsabout.,% | Experiment temperature, °C | | | |
|--|----------------------------|------|------|------|
| | 300 | 350 | 400 | 450 |
| H ₂ | 2,1 | 38,1 | 25,1 | 14,5 |
| CH ₄ | 4,3 | 1,6 | 0,5 | 0,5 |
| C ₂ H ₆ | 4,0 | 8,4 | 10,5 | 12,0 |
| C ₂ H ₄ | 8,8 | 15,0 | 17,7 | 19,0 |
| C ₃ H ₈ | 1,7 | 5,3 | 6,7 | 8,0 |
| C ₃ H ₆ | 13, 1 | 18,0 | 21,5 | 23,0 |
| iC ₄ | 0,5 | 0,5 | 0,7 | 1,0 |
| nC ₄ | 0,2 5 | 0,7 | 0,9 | 1,5 |
| α – butylene | 4,3 | 8,7 | 11,9 | 15,0 |
| β – butylene | 0,6 | 1,2 | 1,3 | 2,0 |

Perhaps with increasing temperature, the catalyst accelerates the dehydrogenation reactions and dehydrocyclization of paraffinic hydrocarbons, and the decrease in the content of naphthenic hydrocarbons within 300-450°C is probably due to the fact that in addition to the cyclization reaction, the dehydrogenation reaction of naphthenic compounds also takes place.

Based on the above, taking into account the obtained data of the

group composition of hydrogenation and the individual composition of gaseous products depending on temperature, it can be said that the cracking of liquid products using bentonite clay as a catalyst leads to the formation, in addition to aromatic and unsaturated hydrocarbons in the hydrogenated product, also limiting and unsaturated components in the gas. Apparently, the decrease in the amount of hydrogen with increasing temperature from 300 to 450°C is associated with the consumption of hydrogen for the reaction of the catalytic hydrogenation of aromatic and olefinic hydrocarbons, which are part of the gaseous products and hydrogenation.

In hydrogenating of HHF (coal, HVO, bitumen), iron sulfides, non-ferrous metallurgy wastes, sulfide-containing solid solutions, red mud, natural clays were used as catalysts. It has been established that the catalysts containing iron sulfides and activated natural bentonite clays have the highest activity.

Table 33 presents the effect of iron sulfide catalysts, bentonite, red mud and clinker in the atmosphere of synthesis gas, argonan is the individual hydrocarbon composition of the gasoline fraction of synthetic oil.

Table 33

Influence of the nature of the catalyst on the individual hydrocarbon composition of the gasoline fraction of synthetic oil

| Hydrocarbon name | Comparison of composition c | | | | | |
|------------------|-----------------------------|------|--------|------|------|------|
| | B1 | | B 1 | | B1 | |
| 1 | 2 | 1 | 2 | 1 | 2 | 1 |
| Parafini c | | | | | | |
| i-butane | - | 0,07 | - | 0,48 | 0,06 | - |
| n-butane | 0,26 | 1,03 | - | 1,37 | 0,08 | 0,26 |
| 2-butane | 0,18 | - | - | 0,48 | 0,07 | - |
| n-pentane | 4,12 | 2,46 | 7,81 | 6,44 | 9,39 | 7,84 |
| 2-m-pentane | 1,62 | 2,0 | 4,38 | 2,68 | 4,75 | - |
| ns 6 | 2,91 | 2,83 | 7,3 | 3,75 | 9,21 | 6,4 |
| 2-hexane | 0,21 | 0,5 | 0,55 | 0,55 | 2,49 | 2,04 |
| 3-hexane | 0,67 | 1,38 | 2,06 | 1,23 | - | 2,74 |
| 3-ethylpentane | 0,51 | 0,90 | 0,65 | 1,01 | 0,66 | 0,90 |
| ns 7 | 2,52 | 3,46 | 4,44 | 3,13 | 4,42 | 3,97 |
| 2,3,4-trip | 0,05 | 0,07 | 0,08 | 0,18 | 0,21 | 0,23 |
| 2,3,3-trip | - | 0,17 | - | 0,07 | - | - |
| 2,3-MEP | - | 0,63 | 0,48 | 0,11 | 1,14 | - |
| 3,4-dMG | 0,98 | 2,79 | 2,39 | 1,72 | 2,76 | 2,44 |
| 4-MGP | 0,15 | 0,63 | 0,45 | 0,37 | 0,62 | 0,45 |

| | | | | | | |
|-------------------|------|------|------|------|------|------|
| 2-MGP | - | 1,16 | - | 0,04 | - | - |
| 2,2,4,4-tetraMP | 0,33 | 0,13 | 1,11 | 0,71 | 1,31 | 0,85 |
| 3-EG | - | 0,07 | - | 0,09 | - | 0,17 |
| n-octane | 1,54 | 3,0 | 2,52 | 1,98 | 4,12 | 2,10 |
| 2,2-dMGp | 0,28 | 0,67 | 0,25 | 0,60 | 1,52 | 0,45 |
| 2,3,5-triMG | - | - | - | 0,07 | 0,43 | 0,11 |
| 2,2,4-triMG | - | 0,33 | - | 0,04 | - | 0,11 |
| 2,2,3-triMG | 0,18 | 0,33 | - | 0,31 | - | 0,57 |
| 2,2,3,4-tetraMP | 0,21 | - | - | 0,24 | - | 0,62 |
| 2,2di-M-3-EP | 0,18 | 0,76 | - | 0,48 | - | 0,45 |
| 2,3,3Three-MG | 0,1 | 0,73 | - | 0,53 | - | 0,51 |
| 2,4-dMHp | 0,28 | - | - | 0,46 | - | - |
| 3,3-dMHp | 0,64 | - | 0,26 | 0,7 | 0,23 | - |
| 3M-3EG | - | 1,26 | 0,5 | 0,73 | 0,58 | 0,74 |
| Парафиновые | | | | | | |
| 2,4-diM-3EP | - | 0,17 | 1,0 | 0,13 | - | - |
| 2,3,4-TriMGII | 0,64 | 1,46 | 0,93 | 0,77 | 1,11 | 0,96 |
| 3,3,4-TriMG | 0,31 | 0,2 | 0,4 | 0,24 | 0,12 | 0,11 |
| 3M-3EG-2 | 0,15 | 0,27 | 0,08 | 0,2 | 0,14 | - |
| 3.4dM-Gp-1 | 0,41 | 0,2 | 0,65 | 0,88 | 0,23 | 0,62 |
| 2,3,4-TriMG-1 | 0,26 | 0,5 | 0,13 | 0,2 | 0,1 | 0,1 |
| 2,3,3,4-tetraMP | 0,19 | 0,85 | 0,33 | 0,55 | 0,12 | - |
| 2,3-dMGp | - | 0,47 | 0,35 | 0,31 | 0,15 | 0,21 |
| 4 moctane | - | 1,66 | 0,91 | 0,95 | 0,28 | 0,96 |
| 2-Moktan | 0,07 | - | - | 0,13 | - | - |
| 2,2,3,3-TetraMP | 0,09 | 0,17 | - | 0,04 | - | 0,96 |
| n-nonane | 0,24 | 0,86 | 0,4 | 0,57 | 0,46 | 0,51 |
| 2-methyl-4-Egp | - | 0,43 | - | 0,17 | 0,04 | 0,28 |
| 2,4,5-triGP | - | - | 0,1 | 0,24 | 0,04 | 0,23 |
| 2,3,5-triMGpI | 0,13 | 0,27 | - | 0,15 | 0,2 | 0,20 |
| 2,3,5-triMGpII | 0,18 | - | 0,05 | 0,17 | 0,23 | 0,51 |
| 2,3,6-triMGp | 0,12 | - | 0,33 | 0,09 | - | 0,28 |
| 2,2,3-triMGp | 0,1 | 0,5 | - | 0,09 | - | 0,17 |
| 2 Methyl isoPrGp | - | 0,23 | - | 0,17 | - | 0,79 |
| 4 Methyl isoPrGp | - | 0,17 | - | 0,07 | - | 0,40 |
| 3Metil-5-EGP | - | 0,22 | - | 0,11 | - | 0,17 |
| 2,4-Dim-3-isoPrP | - | 0,67 | - | 0,33 | - | 0,17 |
| 2,2,3,3,4-pentaMp | - | 0,66 | - | 0,46 | - | 0,57 |
| 3M-3EGP | 0,64 | 1,86 | 0,88 | 1,32 | 0,28 | 0,46 |
| 4M-4EGP | 0,36 | 0,80 | 0,43 | 0,71 | 0,21 | 0,45 |
| 2,3-Dimoctane | 0,36 | 0,96 | - | 0,4 | 0,11 | - |
| 2,3,3,4-TetraMg | 0,21 | 0,7 | - | 0,48 | 0,1 | - |

| | | | | | | |
|-----------------------|------|------|------|------|------|------|
| 2-Mnonan | 0,1 | 0,57 | 0,48 | 0,43 | - | - |
| 2,2,3,3,4-PentaMp | - | 0,43 | - | 0,15 | 0,1 | - |
| 2M-3,3DiEP | 0,54 | 0,3 | 0,08 | 0,15 | 0,11 | - |
| 3-Mnonan | - | 0,2 | 0,35 | 0,07 | 0,23 | - |
| n-decane | 0,85 | 1,86 | 0,4 | 1,12 | 0,22 | 0,96 |
| 2,3,7-3Moctane | 0,11 | 0,13 | - | 0,6 | - | 0,28 |
| 2,5-Dimnonan | 0,12 | 0,4 | - | 0,35 | - | - |
| 2,8-DIMNonan | - | 0,53 | - | 0,15 | - | - |
| 2,7-Dimnonan | - | 0,27 | - | - | 0,09 | - |
| Циклопарафиновые | | | | | | |
| Cepentan | 0,13 | - | - | 0,11 | - | 5,1 |
| MCPentan | 2,01 | 1,5 | 3,02 | 2,29 | 1,79 | 2,96 |
| 1,3-dimtz trans | 0,64 | 0,60 | 0,86 | 0,71 | 1,17 | 0,68 |
| 1,2-DIMCP trans | 0,46 | 0,76 | 1,51 | 0,79 | 1,1 | - |
| Vinyl Center | - | 0,07 | - | 0,13 | 0,19 | 0,11 |
| 1,2-DIMCP | 0,21 | 0,37 | 0,28 | 0,44 | 1,59 | 0,4 |
| 1,1,3-TriMTSP | - | - | - | 0,11 | 0,1 | - |
| MTF | 0,93 | 1,4 | 1,71 | 1,5 | 1,0 | 1,7 |
| EDS | - | 0,23 | - | 0,22 | - | 0,5 |
| 1,2,4-TriMTSP | 0,23 | 0,56 | 0,28 | 0,4 | 1,51 | 1,58 |
| 1,3-EMCP | 0,21 | 0,23 | 0,5 | 0,24 | 0,23 | 0,57 |
| CGP | 0,44 | 0,83 | 0,65 | 0,73 | 0,52 | 0,96 |
| 1,3-EMCP | 0,51 | 1,23 | 0,86 | 0,95 | 0,34 | 0,85 |
| Bis-1,4CG | - | 0,3 | 0,27 | 0,2 | 0,62 | 0,28 |
| MECP | 0,39 | 0,73 | - | 0,07 | - | - |
| ECG | 0,49 | 0,86 | 0,83 | 0,55 | 0,68 | - |
| 1M-3n-butylCP-cis | - | 0,23 | 0,63 | 0,14 | 0,45 | - |
| 1M-3n-butylCP-trans | - | 0,2 | 0,38 | 0,15 | 0,2 | 0,17 |
| Diene | | | | | | |
| Octadien-2,6 | 0,49 | 1,53 | 1,11 | 1,06 | 1,49 | - |
| Hexadiene-1,5 | - | 0,33 | - | 0,4 | - | 2,44 |
| Cyclodienes | | | | | | |
| Cptadiene-1,3 | - | 0,27 | 0,08 | 0,2 | - | 0,74 |
| Cptadiene-1,3-cis | - | 0,07 | 0,5 | 0,29 | - | - |
| Cptadiene | - | - | - | 0,4 | - | 0,51 |
| Olefinic | | | | | | |
| Butene | 1,67 | 0,27 | 2,14 | 2,98 | 4,13 | 3,68 |
| 3-Mbutene-1 | - | - | 0,25 | 0,6 | - | - |
| 2-MethylButene-2 | - | 0,23 | - | 0,6 | 0,16 | 0,91 |
| 3-Methylpenten trans | 0,18 | 0,47 | 0,65 | 0,48 | 0,34 | 1,01 |
| 3-Methylhexene-1 | 0,54 | 0,9 | 1,26 | 1,04 | 2,25 | 1,86 |
| 2,3-DimethylPenthen-1 | - | 0,07 | - | 0,09 | 0,14 | 0,06 |

| | | | | | | |
|-------------------------|------|------|------|------|------|------|
| 5-Methyl Hexene-1 | - | 0,2 | - | 0,09 | 0,34 | - |
| Olefinic | | | | | | |
| 4Mhexene-2 | 0,08 | 0,33 | 0,08 | 0,24 | 0,85 | 0,4 |
| 2Mhexen-1 | 0,46 | 0,06 | 0,53 | 0,46 | 1,78 | 1,76 |
| 2-Methyl Hexene-1 | 0,54 | 0,17 | 0,13 | 0,15 | 0,62 | - |
| 3-Methylhexene-2 | - | - | 0,78 | 0,62 | - | 0,74 |
| Hepten-2 | - | 0,67 | 0,4 | 0,11 | - | - |
| 2,4,4-trimpenten-1 | 0,18 | 0,6 | 0,83 | 0,57 | 1,6 | 0,28 |
| 2,3-Dimpenten-2 | - | 0,13 | - | 0,07 | 0,1 | 0,57 |
| 3,4-Dimethylhexene-3 | 0,18 | 0,6 | 0,45 | 0,57 | 0,55 | 0,79 |
| Nonen-1 | 0,08 | 0,3 | - | 0,2 | 0,03 | 0,23 |
| Nonen-4-trance | - | 0,27 | - | 0,15 | 0,03 | 0,17 |
| Nonen-4-cis | - | 0,57 | - | 0,4 | 0,07 | - |
| Nonen-3 trans | 0,21 | 0,28 | - | 0,33 | 0,07 | - |
| Nonen-3-cis | 0,23 | - | 0,13 | 0,18 | 0,03 | - |
| Mezitelen | - | 0,57 | - | 0,26 | - | - |
| Decen-5-cis | - | 0,13 | - | 0,11 | - | - |
| Decen-4-trans | - | 0,2 | - | 0,07 | - | - |
| Decen-1 | 0,11 | 0,23 | - | 0,14 | - | - |
| Decen-2-trans | - | 0,37 | 0,30 | 0,11 | 0,19 | - |
| Cycloparaffin | | | | | | |
| Cyclopenten | - | - | - | 0,4 | - | - |
| 3-methyl-cyclo-pentene | 0,33 | 0,53 | 0,98 | 0,64 | 0,88 | 0,74 |
| Cyclopenten | - | - | 0,2 | 0,07 | 0,11 | 0,34 |
| Cyclononen-trans | 0,39 | 0,37 | - | 0,31 | 0,07 | 0,51 |
| Cyclononen-cis | 0,3 | - | - | 0,15 | - | - |
| Vinyl Cyclohexene | 0,28 | 0,63 | 0,28 | 0,48 | 0,14 | 0,34 |
| Aromatic | | | | | | |
| Benzene | 0,46 | 0,5 | 10,1 | 2,71 | 8,3 | 3,9 |
| Toluene | 1,6 | 2,06 | 2,8 | 2,1 | 2,23 | 2,1 |
| Ethylbenzene | 0,49 | 0,90 | 0,43 | 0,82 | 0,81 | 0,62 |
| p-xylene | 0,42 | 1,06 | 0,8 | 0,76 | 0,12 | 1,4 |
| m-xylene | 1,48 | 2,47 | 2,59 | 2,26 | 0,43 | 0,22 |
| o-xylene | 0,44 | 1,56 | 1,28 | 1,3 | 0,37 | 0,34 |
| Cumene | 1,25 | 2,92 | 1,11 | 1,72 | 0,6 | 1,7 |
| nPropyl Benzene | 0,18 | 0,37 | - | 0,29 | 0,28 | 0,62 |
| 1-Methyl-2-Ethylbenzene | 0,18 | 0,67 | - | 0,33 | 0,12 | - |
| 1,2,4-Trimethylbenzene | 1,34 | 2,43 | 1,06 | 1,59 | 0,27 | 1,02 |

Note: B1 fraction up to 200 °C, obtained by hydrogenation of HVO in the CO/H₂ medium, pyrite catalyst; B2 fraction up to 200 °C with

hydrogenation of OB in a CO/H₂ medium, catalyst — activated bentonite; BZ fraction up to 200C with hydrogenation of coal in argon, catalyst activated bentonite; B4 fraction up to 200 °C with hydrogenation of coal in argon, pyrite catalyst; B5 fraction up to 200 °C with hydrogenation of coal, catalyst red sludge; B6 fraction up to 200 °C with hydrogenation of OB in argon, catalyst activated bentonite.

Thus, identified: 65 saturated hydrocarbons, 25 unsaturated; 18 cycloparaffin; 6 cycloolefin; 11 aromatic. Normal hydrocarbons are represented by pentane, hexane, octane. The presence in the fraction up to 200 °C of a large number of branched saturated hydrocarbons cycloparaffinic, cycloolefinic and aromatic hydrocarbons indicates a high octane number. Comparison of the composition of gasoline obtained by hydrogenation of HHF (coal, HVO, OB) showed a difference in the qualitative and quantitative composition. So, in straight-run gasoline (BZ), the maximum amount of aromatic hydrocarbons is 20.1% by volume when using activated bentonite, and the minimum yield of aromatic hydrocarbons is 5.63% in B4 catalyst pyrite.

As can be seen, the use of iron sulfide catalysts (solid solutions) in the hydrogenation of HHF leads to a significant increase in cycloparaffin and cycloolefinic hydrocarbons and a decrease in aromatic hydrocarbons, which is connected, apparently, with a decrease in the nonstoichiometry of iron sulfide catalysts.

4.4. Paramagnetic properties of coal, products of their catalytic pyrogenation

The method of electron paramagnetic resonance (EPR) has shown high informativity in studying the structure of natural organic compounds, in particular, coal. The EPR spectra of natural highmolecular compounds are characterized by structurelessness due to the presence of various types of paramagnetic titers (PMT). While working with coal substances, three basic characteristics of the EPR spectra, the g-factor, the width of the lines (AN) and the concentration of paramagnetic centers are usually used. The EPR spectra of coal and their catalytic hydrogenation products (hydrogenate) were recorded as the first derivative of the absorption lines on the RE-1306 radio spectrometer. The concentration of PMT in coal and liquefaction products was determined by comparison with a standard sample, which was used as 2,2,6,6-tetramethyl-piperidine -NOXID. Table 34 shows the results of the determination of PMT and (DN) and the initial coal and high-viscosity oil.

Table 34

Paramagnetic characteristics of coal and high-viscosity oil

| Sample | (PMT) $\times 10^{17}$ spin/g | ΔH_{Er} | H/C |
|--------------------|-------------------------------|------------------------|------|
| Kenderlyk coal | 219 | 0,77 | 0,7 |
| Shubarkol coal | 21,4 | 0,56 | 0,81 |
| High viscosity oil | 1,1 | 0,43 | - |

The data of table 34 show a clear dependence of the concentration of PMT on the atomic ratio H/C; as well as the difference in the petrographic composition of the above men, and are in accordance with the results of other researchers. The increase in the concentration of PMT in the Kenderlyk coal, as compared to the Shubarkol coal, is apparently due to both the increase in the number of carbon networks, and the orderliness in the system of macromolecules, as well as the convergence of carbon networks to each other, which leads to an increase in the collective electron interaction effect of unpaired. A relatively high concentration of fusin in the Kenderlyk coals above 10% also results in a strong EPR signal (Fig. 11.12).

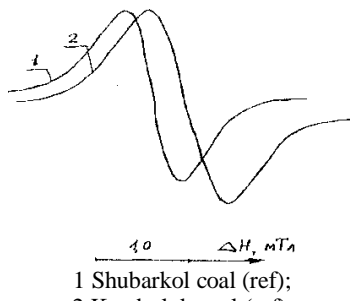


Figure 11. EPR spectra of coal samples

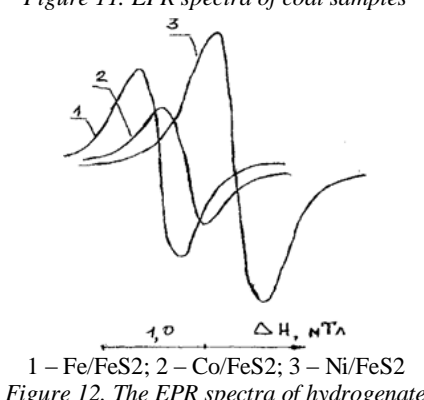


Figure 12. The EPR spectra of hydrogenate

Aust and Van Krevelen [59] believe that the increase in the number of free radicals in coal with a degree of metamorphism is associated with the formation of ringed systems that stabilize unpaired electrons, the source of which the authors consider the broken bonds of the border atoms of the condensed carbon. It was found in [60] that the concentrations of PMT do not reflect the true picture of coal liquefaction, since, parallel with the formation of PMT, radical redistribution reactions occur due to their interaction with hydrogen, OCM, solvent molecules, liquefaction products, and also recombination, reducing the concentration of the observed radicals. In addition, when interacting with a solvent (naphthalene), an increase in PMT concentrations was observed. This is explained by the fact that the structure of the conjugated bonds of naphthalene is capable of delocalizing the unpaired electron, which leads to the formation of stable naphthyl radicals.

The effect of the amount of added iron, nickel, cobalt on iron sulfide (an iron-containing solid solution) in the process of catalytic hydrogenation of a heavy hydrocarbon feedstock on the PMT concentration was studied. Figures 13-15 show the curves of changes in the concentration of PMT from the amount of heavy metals added (Fe, Co, Ni) to iron sulfide. Increasing the amount of heavy metals added (nickel 1.7%, cobalt 0.8%) leads to an increase in the concentration of PMT. With a further increase in the amount of cobalt and nickel, the concentration of PMT decreases. A similar dependence is observed with an increase in the added iron of 0.9%, and then the concentration of the PMT approaches a linear value. The dependence of the concentration of PMT on the amount of heavy metals added shows that the concentration of fixed PMT is the lowest for nickel and cobalt 2.0×10^{17} and 3.0×10^{17} spin/g and the highest for iron 8.0×10^{17} spin/g. It can be assumed that the nonlinear nature of the curves seems to be associated with an increase in the concentration of naphthalene formed during the dehydrogenation of tetralin.

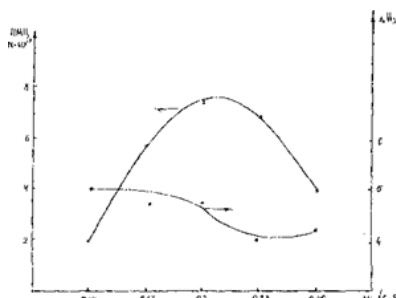


Figure 13. Changes in the concentration of PMT in hydrogenated and line widths (ΔH) from nickel to pyrite ratio

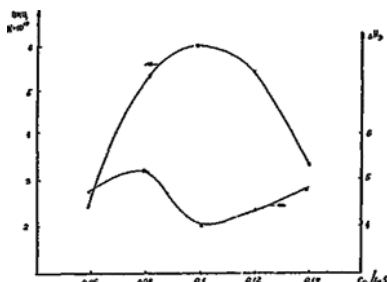


Figure 14. Changes in the concentration of PMT in hydrogenated and line widths (ΔH) from the ratio of cobalt to pyrite

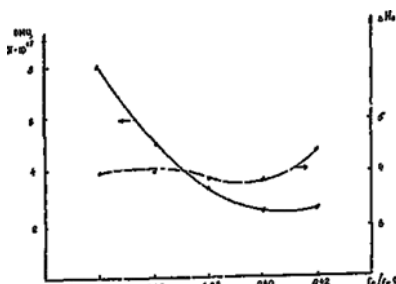


Figure 15. Changes in the concentration of PMC in hydrogenated and line widths (ΔH) from the ratio of iron to pyrite

The noted high activity of solid sulfide-containing solutions in high coal conversion and liquid product yield, a decrease in the concentration of PMT in the hydrogenation product is associated with the formation of active pyrite, pyrrhotite and cobalt sulfide and nickel. According to [60], pyrrhotite — an active catalyst for the direct hydrogenation of aromatic hydrocarbons, H₂S, as is known [61], can catalyze the process of liquefaction due to participation in the transfer of hydrogen from the expander donor to coal and coal radicals. It is possible that catalysis in the presence of synthetic samples of sulfide-containing solid solutions is due to the combination of the actions of pyrite and hydrogen sulfide.

Figure 16 shows the catalytic hydrogenation of phenanthrene in the presence of iron sulfide solid solutions. With an increase in the Ni/FeS₂ ratio, an extreme dependence of the yield of 9,10 dihydronaphthalene and tetrahydronaphthalene is observed, which, apparently, is associated with a decrease in nonstoichiometry and an increase in the effect of nickel sulfide as a catalyst for phenanthrene hydrogenation. This confirms the nonlinear character of the change in the concentration of PMC with an increase in the

Ni/FeS₂ ratio.

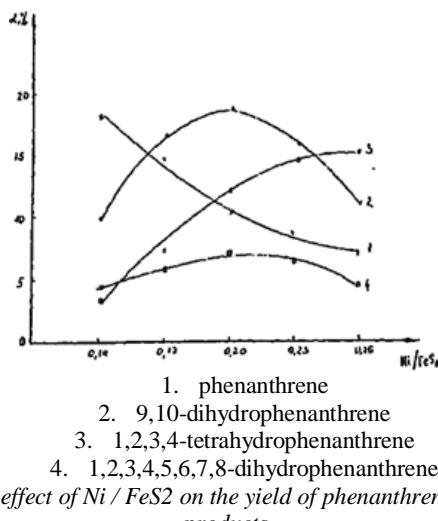


Figure 16. The effect of Ni / FeS₂ on the yield of phenanthrene hydrogenation products

Thus, the use of solid solutions in the process of hydrogenation of TUS is more efficient than the use of monoand bimetallic catalysts (Co, Ni, pyrite, pyrrhotite).

CHAPTER 5. KINETICS OF CATALYTIC HYDROGENIZATION OF HEAVY HYDROCARBON RAW MATERIALS AND HIGH- VELOCITY OIL

One of the most important stages of preparing the process for implementation is the development of reliable methods for the technological calculation of the reactor, which requires data on the rate constants of the main reactions, activation energy and other parameters that determine the macrokinetics of the process. Considering that the feedstock (coal, heavy oil, oil residue, petroleum) is a complex system, both chemically and physically, and all the main and side reactions occur on the surface of poly-dispersed catalysts under increasing deactivation, the study problems of the kinetics of processes in the pyrogenization of heavy hydrocarbon feedstock (HHF) is based on two levels of theoretical concepts. At the first level, the heterogeneity of the process is not taken into account, i.e. formal approaches of homogeneous catalysis are used. At the second level, macrokinetic methods of heterogeneous catalysis are used, taking into account the pattern of processes occurring on the grain or in the pores of the catalyst. The study of the kinetics of hydrogenation processing of coal is complicated by the interdependence of a variety of factors, including the difference in the compositions and properties of the used raw materials. The activation energy calculated by various authors varies in a rather wide range from 63.6 to 192 kJ/mol, and the order of the kinetic equations is defined as the first, and in some works as the second [62].

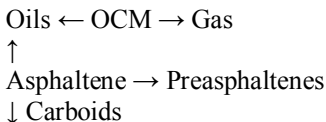
In one of the first publications it was assumed that the transformation of coal proceeds according to the scheme:



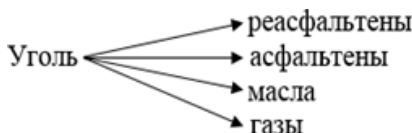
Studies in recent years have shown that the process of hydrogenation of the organic mass of coal (OMC) is carried out by a more complex mechanism and consists not only of sequential reactions.

Identification of kinetic patterns are of significant importance in the development of the scientific foundations of the process and issues of its directional implementation.

Mathematical modeling of the kinetics of liquefaction of brown coal under isothermal conditions was carried out. In [63], a scheme for the transformation of OCM during hydrogenation was proposed, taking into account inverse processes:



A number of studies [64–67] are devoted to studying the conversion of coal at short contact times. So in [67], the kinetics of coal liquefaction at a temperature of 400–450°C, a pressure of 13.8 MPa, and a contact time of 8 minutes were investigated. For kinetic calculations, the following scheme was proposed, taking into account parallel and concurrent transformations:



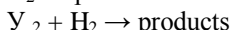
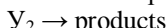
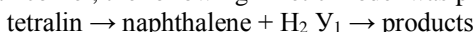
The experimental results obtained with a small contact time are markedly different from the data obtained earlier, with prolonged experiments. The nature of the change in the concentration of preasphaltenes suggests that the reaction of formation of this component has an order higher than the first. Foster and his collaborators [68] conducted a series of experiments to study the kinetics of coal liquefaction and proposed a scheme for the transformation of OMC in which all reactions were prescribed a second order.

Interesting results were obtained in [69], where the authors believe that, in contact with hot solvent, coal instantly breaks up into smaller fragments, which produce oils, or form preasphaltenes or asphaltenes. The latter reactions make it possible to explain the fact that in the presence of a weak hydrogen donor solvent, the oil concentration reaches a minimum in the second and third minute of the reaction and all reactions are of the first order.

Based on the data obtained for the study of kinetics in a short time, the authors [69] concluded that the stabilization of fragments of a coal substance primarily occurs as a result of disproportionation.

In recent years, a number of researchers [70, 71] have observed some inconsistency of data on the kinetics of coal liquefaction. They introduced the concept of “instantaneous” decay of the original substance with the subsequent transformation into more stable intermediate and final products. The introduction of the concept of “instantaneous” suggested that the process of liquefaction proceeds in two stages: instantaneous dissolution of coal with the formation of various products and further slow disintegration of heavy

products. Attempts to reflect the nature of coal in the study of kinetics were undertaken in the work of Gosh [72]. He believes that coal consists of three parts: Y_1 , Y_2 , Y_3 , having different properties: Y_1 undergoes "instantaneous" transformation by thermal decomposition with the formation of gases; U_2 forms products due to the disproportionation reaction in the coal itself; U_3 adds hydrogen given by the donor. Based on the experiments with the Vectorian corner, the following kinetic model was proposed:



In the process of catalytic hydrogenation of coal, solid products are formed, and a number of authors began to introduce the concept of the maximum degree of conversion of OCM [73–75]. However, a number of researchers took into account the incomplete transformation of coal, introducing reverse reactions [76]:



All reactions have the first order. The calculations carried out according to this scheme led, at first glance, to a somewhat contradictory fact of a large value of reverse reactions. Apparently, the authors believe that under the conditions of hydrogen deficiency, necessary for stabilization of coal fragments, oils act as such. In accordance with this, one can also explain the fact that the rate of direct and reverse reactions of the transformation of coal into preasphaltenes is higher than the rates of reactions.

Thus, the analysis of literature data on the kinetics of the hydrogenation of coal showed that the transformations of OCM are in a complex relationship with numerous factors. From relatively simple sequential and parallel kinetic schemes, researchers are moving to more complex ones, including reversible transformations in sequential and parallel schemes [77-80], in order to explain the mechanism of the transformation of OCM into liquid products.

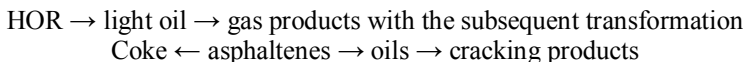
The increased content of nitrogenous and oxygen-containing compounds, unstable unsaturated hydrocarbons and impurities of sulfur compounds in the products of liquefaction with a boiling point of 180–360°C and 360–520°C causes certain difficulties in hydrogenation processing to obtain components of motor fuels. The authors [77-80] have developed kinetic models for the hydrocracking of coal distillates. The kinetic description of the hydrocracking fraction of the liquid-phase hydrogenation with a boiling point of up to 180–360 °C can be represented as follows:

Raw material → gasoline → gas

The scheme for the second raw material (fraction with a boiling point of 360–520 °C) is complicated by the fact that along with gasoline, a component of diesel fuel (DF) is formed.

Raw material → DF → gasoline → gas

Heavy oil residues (HOR), high-viscosity oils (HVO), oil bitumens (OB), as already noted above, include a wide range of components with different reactivity. Analysis of the literature data [81–86] shows the entire complexity of studying the kinetics (HOR, HVO, OB), which is determined by the difference in the rates of conversion in sulfur-containing compounds. A review of the kinetic models of the hydrogenation of heavy oils and oil residues was proposed in [81]:



The values of the rate constants range from 0.02 to 3.59 min⁻¹ at temperatures from 648 to 693K. The apparent activation energy is from

85 to 200 kJ/mol. The authors believe that the activation energy of 168 kJ/mol can be attributed to the reaction of the formation of as-falenes into coke, and 201 kJ/mol to the cracking reaction. High values of activation energy were obtained for the reaction of the formation of asphaltenes in oils and oils in asphaltenes: 224 ± 15 and 284 ± 28 kJ/mol, respectively.

The presented kinetic models in the review [82] show the entire complexity of the processes (condensation, polycondensation, cracking reactions).

Thus, an analysis of the literature on the kinetics of the hydrogenation of coal, heavy oil residues and high viscosity oils shows that their industrial realization requires an experimental determination of the kinetic parameters for each type of raw material.

5.1. Macrokinetics of the process of coal hydrogenation

Due to the complexity of the chemical structure of coal, the multiplicity of the resulting liquid products, a large number of various kinetic schemes of the process of hydrogenation of coal are created, which makes it difficult to interpret the results and the uncertainty of calculating the kinetic parameters. The number of complex reactions occurring in the condensed

phase and heterogeneous processes is such that the description of the kinetics of each individual reaction is impossible. Therefore, in a theoretical analysis of the process of coal hydrogenation, it is considered as a certain first-order, unified reaction and for its description some averaged kinetic equations are used depending on the temperature of formation of liquid and gaseous products.

Analysis of the literature data proves that information on the kinetics of coal hydrogenation is mainly represented in hydrogen and a catalyst based on molybdenum and cobalt, and the kinetics of pyrolysis of coal in synthesis-gas and iron sulfide systems is negligible.

Figure 17 shows the kinetic dependences of the conversion of the organic mass of coal into liquid and gaseous products. Analysis of the curves shows that with an increase in the duration of the experiment and the temperature of the process, the conversion of OCM increases from 55.3 to 82.0 mass. % however, at temperatures above 698 K, the yield of gaseous products increases.

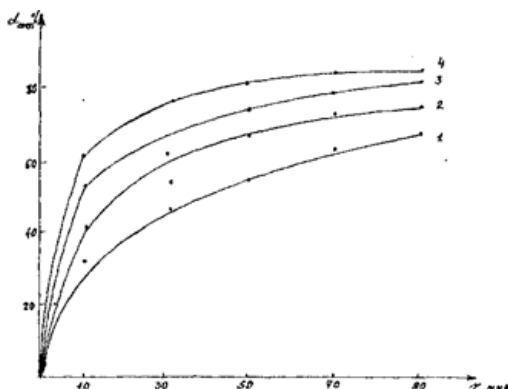
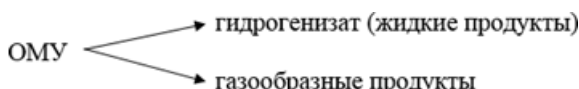


Figure 17. The dependence of the conversion of WMD (a) on the contact time at temperatures: 1 648K; 2 673K; 3 698K; 4 723K

Analysis of the kinetics of the coal liquefaction processes allowed us to propose the following scheme for the transformation of the organic mass of coal in the process of its catalytic hydrogenation in the presence of an iron sulfide catalyst in a synthesis-gas atmosphere:



Taking into account the effect of braking the reaction due to coke formation on the active centers of the catalyst (pyrite), the transformation of OCM is satisfactorily described by the equation of the first order:

After integration, the equations obtained:

$$\frac{dy}{d\tau} = \frac{\alpha(1-y)}{1-\beta(1-y)} \quad (47)$$

$$x\tau = \ln \frac{1}{1-y} - \beta y \quad (48)$$

where u is the transformation of OCM, per unit mass of the catalyst, α is a constant proportional to the rate of transformation of OCM; β inhibition coefficient, taking into account the neoplasm.

The values of α and β were determined graphically. The linear dependence of the $\frac{1}{\tau} \ln \frac{1}{1-y}$ values on y/τ is observed and the value of β remains equal to 1, and α increases with increasing temperature of the experiment. From the data obtained for the four temperatures, the apparent activation energy was calculated. Instead of reaction rate constants, proportional values of α were taken, which is possible due to the constancy of the drag coefficients in the temperature range studied. The results of the experiments were processed using the equation. From the graphs, where the values $\frac{1}{\tau} \ln \frac{1}{1-y}$ were plotted along the ordinate axis, and the axis values were taken along the abscissa axis y/τ (Fig. 18), the axis value was found as segments cut off by straight lines drawn through experimental points.

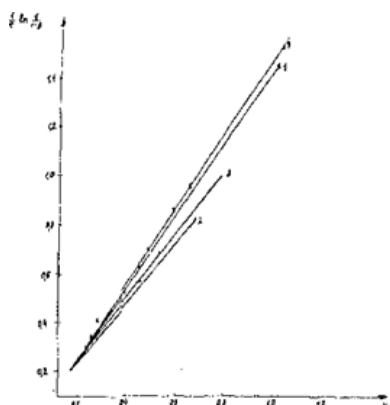


Figure 18. Dependence $1/\tau \ln(1/(1-y))$ on y/τ for hydrogenation of coal in the environment of synthesis gas at temperatures: 1 648K; 2 673K; 3 698K; 4 723K

The calculated rate constants (α) and the activation energy of catalytic hydrogenation of coal in a synthesis gas medium in the temperature range from 648 to 723 K are presented in table 35.

Table 35
Macrokinetic total rate constants for the hydrogenation of coal,
 $E = 57.1 \text{ kJ/mol}$

| Temperature, K | 648 | 673 | 698 | 723 |
|--------------------------|-------|-------|-------|-------|
| Speed constant, α | 0,084 | 0,173 | 0,264 | 0,221 |

The values of the activation energy E were obtained by approximation of the well-known Arrhenius equation of the linear function $\ln\alpha = f(1/T)$ (Fig. 19). From the data of table 35, it follows that the apparent energy of activation of Karazhar coal in the temperature range 648–723 K is 57.1 kJ/mol, which is typical of heterogeneous catalytic hydrocracking processes of heavy hydrocarbon feedstock [87].

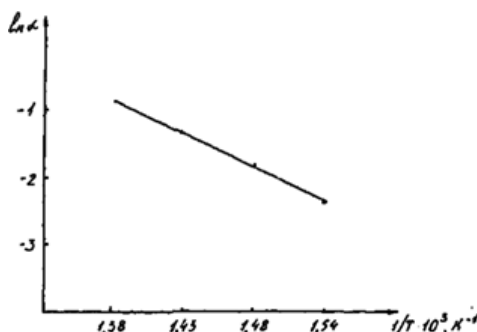


Figure 19. The dependence of the rate constant from the inverse temperature

It is known from literature that the transformation of OCM proceeds in two main directions: by thermolysis with saturation of organic fragments with hydrogen and by transformation into products of coke formation. According to the data obtained above, the transformation of OCM is due to the ratio of the rates of reaction of hydrogenolysis and coke formation.

Thus, the hydrogenation of coal from the Karazhar field in the middle of synthesis gas in the presence of tetralin and an iron-sulfide catalyst makes it possible to achieve a high value of the conversion of OCM (82.0 mass%). The adopted kinetic model of the process of coal hydrogenation makes it possible to study the laws governing the transformation of OCM into

liquid and gaseous products and can be used to optimize the process of coal hydrogenation.

We believe that the high catalytic activity of the iron-sulfide catalyst may be due to the increased nonstoichiometry of the pyrrhotines formed during the process. The defects that causes the nonstoichiometric properties of iron-sulfide compounds are the centers of activated chemisorption of the formed H₂S [88], which ensures the transport of active hydrogen to organic coal fragments.

5.2. Investigation of the kinetics of thermal destruction of coal Kenlelyk and Shubarkol deposits

Thermal destruction of coal includes the process of breaking donor-acceptor and valence bonds with the release of moisture, the formation and release of gaseous and volatile, liquid and solid products, as well as the polycondensation of the products of destruction with the formation of coke and then coke and release of an additional amount of gaseous products [89].

The processes of thermal decomposition of coal and polymers are widely presented in [91, 92]. There are various methodological approaches to the study of thermal degradation through the use of derivatographs. However, all known methods for studying the thermal destruction of coal do not reflect the different sides of this complex process, and gravimetry does not take into account the formation of nonvolatile heavy products, changes in the solid residue itself.

A qualitative analysis of changes in temperature (T), mass (TG), rate of change in mass (DTG), and changes in heat content (DTA) shows that in different temperature ranges the destruction of coal occurs at different rates.

The problem of calculating kinetic parameters on the basis of changing various indicators (mass, heat, gas composition, etc.) under non-isothermal heating conditions has been the subject of many papers [91]. The main difficulty lies not in the choice of the method, but in the determination of the individual stages of the process, which at least can be considered conditionally homogeneous with fixed parameters K₀, E and p.

In the literature [92], at least three stages are distinguished on the DTG curves of coal in the main decomposition area: processes involving the release of moisture (100–120 °C), degradation of the coal substance (400–440 °C), the formation of the structure of coke (680–700 °C).

In the case of a symmetric DTG curve, the Reich and Levy method used for polymers by Slokimsky and many other authors for coals is used to calculate the effective activation energy for the destruction of the organic activation mass (OCM):

$$\Gamma = \frac{nRT^2(dC/dT)_{\max}}{C_{\text{nep}}} \quad (49)$$

where R is the universal gas constant, T_m is the temperature where the maximum speed is reached, $(dC/dT)_{\max}$ is the rate of destruction at the maximum of the interval, referred to the value of the mass loss of the interval in this temperature range, S_{pur} is the fraction of undecomposed material.

In [92], V.P. Malyshев showed that the use of DTG curve for direct processing as a formally kinetic speed of the process seems to be mathematically incorrect.

It is known that the heating rate is recorded by a derivative-graph in the form of a DTG curve at a variable temperature for some time, therefore this curve is a complete (and not particular) derivative of the sample mass (M) in two variables:

$$\frac{dM}{dt} = \frac{\partial M}{\partial t} + \frac{\partial M}{\partial T} \frac{\partial T}{\partial t} \quad (50)$$

and the law of the masses for the reaction rate (in this case, heterogeneous) is only valid with respect to the partial derivative:

$$\frac{\partial M}{\partial t} = k_0 S C^n \exp(-E/RT) \quad (51)$$

where k_0 is the preexponential factor, E is the effective activation energy, R is the gas constant, T is the absolute temperature; S is the surface area of the response; C is the concentration of the gaseous reactant; n is the order of the process.

For kinetic analysis, it is necessary first to find the general expression for the dependence of the sample mass on temperature and duration in order to determine the partial derivative. The analytic form of this generic expression is not yet known and is the subject of intense search [92].

For more information on the effect of catalysts on the process of thermal decomposition of coal in the temperature range of intense decomposition of coal, we studied the kinetics of the process on a derivatograph of the system of F. Paulik, D. Paulik and L. Erdei in argon.

According to [92], let's submit the degree of reaction (α) of the kinetics of thermal destruction of a model mixture of coal or a mixture of coal with a catalyst (the amount of catalyst added to coal 10% on the initial organic mass of coal) by an exponential equation of the form:

$$\alpha = 1 - \exp[-Ar^m \exp - \frac{3}{T}] \quad (52)$$

Where A, B are constant.

After double logarithmization we get:

$$\ln[-\ln(1-\alpha)] = \ln A + m \ln - \frac{3}{T} \quad (53)$$

From the derivatograms we find α , T and τ , and then by the least squares method we find the parameters A, B, m. Differentiate:

$$\frac{\partial \alpha}{\partial \tau} = Am^{m-1} \exp[-\frac{3}{T} - Ar^m \exp - \frac{3}{T}] \quad (54)$$

Appeal τ and α

$$\tau = [-\frac{\ln(1-\alpha)}{A} \exp \frac{3}{T}] \quad (55)$$

and substitute

$$\frac{\partial \alpha}{\partial \tau} = Am[-\frac{\ln(1-\alpha)}{A}]^{m-1/m} \exp[\frac{(m-1)3}{T} - \frac{3}{T} + \ln(1-\alpha)] \quad (56)$$

we obtain the equation of the rate of thermal destruction, which allows us to find the activation energy (E) and the preexponential factor (K_0).

From the analysis of derivatographic data, it follows that the nature of thermal transformations of coal and model mixtures in an inert medium is determined by the presence of a catalytic additive that, when heated, maximally accelerates the rate of destruction of OCM. The main load in the mass loss is observed in the temperature range 340-440°C. In the future, all calculations and comparisons were carried out in this temperature region, since it corresponds to the interval of the most effective and important from a technological point of view for the processes of hydrogenation of coal, heavy oil residues, and highly viscous oils.

During the formation of organic-mineral structures in the model mixture in the process of thermal destruction, a decrease in the activation energy and a preexponential factor is observed. From the studied range of catalytic additives, the sulfides of iron had the greatest influence on the reduction of the activation energy and the preexponential factor — composition 6 for Kenderlyk coal and composition 7, 9, 8 Shubarkol coal.

When combining two catalytic additives with a ratio of (1:1) pyrite + bentonite, an increase in the activation energy is observed. The authors of [93] showed that the combination of iron and molybdenum salts leads to a sharp narrowing of the maximum of the main decomposition, an increase in the activation energy and a pre-exponential factor. The observed change in the process of destruction of model mixtures of coal with catalytic additives indicates the chemical interaction of structural fragments of OCM with metal ions and the change in the electronic structure of OCM fragments.

Iron-sulphide catalytic additives showed high catalytic activity, and the kinetic parameters E and K_0 were obtained for only three samples. The maximum loss of pyrites is shifted to higher temperatures 500-600°C. However, since we study the thermal destruction of coal at a temperature range of 340-440°C, then the kinetic data were obtained in this temperature range. The magnitude of the activation energy (E) and (K_0) are presented in table 36.

Table 36
**Pyrolysis of coal Shubarkol and Kenderlyk deposits
with inorganic additives**

| № | Sample | decomposition rate, °C | Temperature of thermal effects | | E, кДж/моль | K_0 |
|----|-------------------------------------|------------------------|--------------------------------|--------------------------|-------------|--------------------|
| | | | Endo | exo | | |
| 1 | 2 | 3 | 4 | 5 | 6 | 7 |
| 12 | Kenderlyk coal | 105 | 150 400 470 550 | 350 425 505 720 | 172,2 | $1,39 \times 10^6$ |
| 11 | Kenderl. coal+pyrite+ clinker | 95 | 150 390 450 545 | 360 420 500 | 132,5 | $1,08 \times 10^6$ |
| 8 | Kenderl. coal+bauxite | 100 | 150 300 400 530 | 270 370 430 760 | 156,3 | $1,27 \times 10^6$ |
| 9 | Kenderl. coal+bentonite | 90 | 150 400 530 800 | 325 420 655 | 163,6 | $1,33 \times 10^6$ |

CHEMICAL TECHNOLOGY IN PRODUCTION

| | | | | | | |
|----|---|-----|---------------------------------|---------------------------------|--------|--------------------|
| 7 | Kenderl. coal+pyrite | 90 | 160 340 400 460 575 | 360 425 505 | 154,9 | $1,26 \times 10^6$ |
| 6 | Kenderl. coal+Kt.№3 | 70 | 160 340 400 460 575 | 310 370 425 520 | 91,2 | $7,4 \times 10^6$ |
| 5 | Kenderl. coal+ clinker | 105 | 165 330 380 560 | 283 400 430 500 750 | 217,9 | $2,2 \times 10^6$ |
| 10 | Kenderl. coal+смесь+pyrit e+bentonite | 120 | 120 400 460 | 370 425 490 | 191,6 | $1,6 \times 10^6$ |
| 2 | Kenderl. coal+Kt.№2 | 90 | 120 400 460 | 370 425 490 | 123,8 | $1,0 \times 10^5$ |
| 4 | Kenderl. coal+pyrite+ bentonite | 70 | 120 415 475 535 | 350 405 435 500 690 | 72,0 | $5,9 \times 10^5$ |
| 3 | Kenderl. coal+Kt.№3 | 70 | | | 82,3 | $6,7 \times 10^5$ |
| 1 | Kenderl. coal+Kt.№1 | 90 | 140 195 390 540 | 360 220 430 | 125,5 | $1,02 \times 10^6$ |
| 12 | Shubark. coal | 80 | 140 405 545 | 275 420 | 103,51 | $8,4 \times 10^5$ |
| 4 | Shubark. coal+Kt.№4 | 70 | 140 540 | 270 690 775 | 99,9 | $8,1 \times 10^5$ |

| | | | | | | |
|---|----------------------------|-----|---|--|-------|-------------------|
| 7 | Shubark. coal+pyrite+Co | 70 | 140 250 410 565 | 330 395 430 630 740 | 77,2 | $6,3 \times 10^5$ |
| 8 | Shubark. coal +bauxite | 70 | 140 300 340 620 | 280 430 | 99,6 | $8,1 \times 10^5$ |
| 9 | Shubark. coal+bentonite | 75 | 145 360 | 290 440 | 101,1 | $8,1 \times 10^5$ |
| 3 | Shubark. coal+Kt.Nº3 | 70 | 145 350 | 95 270 440 | 108,6 | $8,8 \times 10^5$ |
| 2 | Kt.Nº12 | 90 | 105 285 500 680 | 225 445 540 610 | 263,0 | $2,1 \times 10^6$ |
| 1 | Kt.Nº12+Kt.Nº9 | 390 | 390 500 570 780 | 460 520 590 | 36,3 | $3,0 \times 10^5$ |
| 3 | Kt.Nº12+Kt.Nº5 | 10 | 120 150 305 505 570 670 930 | 140 190 445 530 600 720 | 36,3 | $3,0 \times 10^5$ |

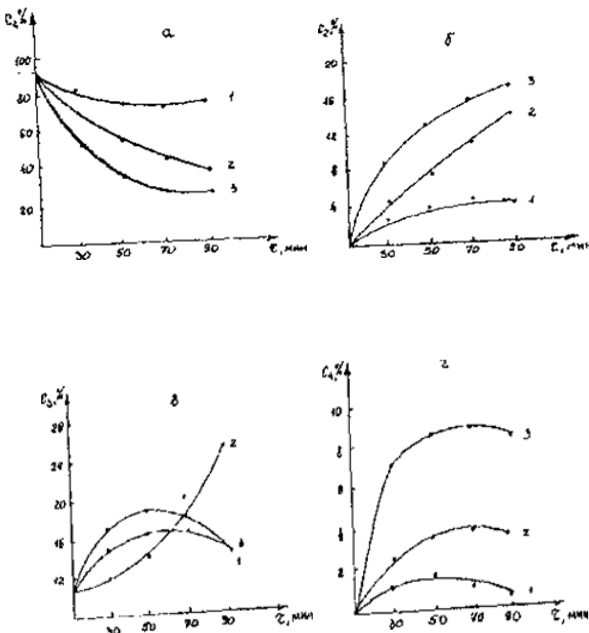
These data show that the thermogravimetric method (DTA) allows us to successfully study the effect of various factors on the thermal decomposition of coal. The heterogeneity of the chemical structure, including the difference in the organo-mineral structure, leads to differences in the thermal destruction of the Kender-Lyk and Shubarkol coals. Thus, by changing the organo-mineral structure of the coal due to catalytic additives (catalyst), it is possible to control the process of thermal decomposition and kinetic parameters within certain limits.

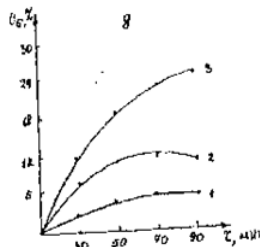
5.3. The kinetics of hydrogenation of Karazhambas highviscosity oil

The study of the kinetic patterns of destructive hydrogenation of high-viscosity oil is essential in the development of the scientific basis of hydrogenation and its implementation.

Figure 20 (a-e) shows the kinetic curves for the hydrogenation of high-viscosity oil in the presence of pyrite. As follows from Fig. 21, with an increase in temperature and an increase in contact time, the yield of the fraction increases to 453 K in the temperature range 573–623 K from 2 to 32%, respectively. In the entire temperature range under study, the gaseous products grow from 3 to 27% and the carbides from 1 to 11%.

Considering the literature data on the kinetics of hydrogenation of coal and heavy oil residues, we can suggest the following schemes for the transformation of high-viscosity oil (HVO) in catalytic hydrogenation processes under low pressure of hydrogen (Fig. 20).





a) C1 fraction above 573 K; b) C2 fraction up to 453K;
 a) C3 fraction 453-573K; d) C4 carboids; d) C5 gaseous products
Figure 20. Dependence of the fraction yield on the reaction time under various isothermal conditions: 1-573K, 2-598K, 3-623K

In accordance with the proposed scheme (Fig. 21), the kinetic model №1 has the following form:

$$\left\{ \begin{array}{l} \frac{d[C_1]}{dt} = -(k_1 + k_2 + k_3 + k_4)C_1 + k_5C_3 \\ \frac{d[C_2]}{dt} = k_1C_1 + k_6C_3 \\ \frac{d[C_3]}{dt} = k_2C_1 - k_6C_3 - k_8C_5 \\ \frac{d[C_4]}{dt} = k_3C_1 - k_7C_4 \\ \frac{d[C_5]}{dt} = k_4C_1 + k_7C_4 \end{array} \right. \quad (57)$$

where C_1, C_2, C_3, C_4, C_5 are the mass fractions of the corresponding components ($C_1+C_2+C_3+C_4+C_5=1$).

The system of equations was calculated on IBMAT 486DX using the special “Search” program. The developed program makes it possible to calculate the kinetic dependences for the given initial conditions and to carry out an automated selection by the gradient method of the optimal values of the rate constants k_1-k_7 . The optimization of the rate constants was carried out from the condition of the minimum of the squares of deviations between the experimental and calculated values of the mass fractions of the HVO hydrogenation products. From the analysis of the results of the rate constants presented in Table 37, it can be concluded that the effect of the rate constants on the yield of the hydrogenation products of HVO is ambiguous. Thus, the fraction yield up to 180°C is mainly determined by the value of the rate constant k_1 . The yield of the fraction 180-300°C decreases with increasing temperature, the value of k_2 and k_3 increases to 325°C, then decreases and k_4 increases significantly. The rate constants of the reverse reaction k_5-k_7 with increasing temperature decrease. The formation of gaseous and solid products competes with the output of the light and medium fractions, and this trend is

noticeably increasing with increasing temperature. The total constant of the process of hydrogenation HVO k_z has a slight tendency to decrease.

Table 37

HVO hydrogenation rate constants

| Rate constant, min ⁻¹ | Process stage | Hydrogenation Temperature, K | | |
|--|-------------------------------|---------------------------------|--------|--------|
| | | 573 | 598 | 623 |
| k_1 | fr.above 573K→to 453K | 0,0054 | 0,0057 | 0,0069 |
| k_2 | fr.above 573K→ 453-573K | 0,0157 | 0,0163 | 0,0114 |
| k_3 | fr.above 573K→ solid product | 0,0058 | 0,0052 | 0,0044 |
| k_4 | fr.above 573K→gas product | 0,0021 | 0,0028 | 0,0034 |
| k_5 | fr.above 453-573K→fr. 573K | 0,0363 | 0,0335 | 0,0255 |
| k_6 | fr.above 453-573K→fr. to 453K | 0,0054 | 0,0027 | - |
| k_7 | solid product → gas product | 0,0187 | 0,0170 | 0,0114 |
| k_z | | 0,029 | 0,0272 | 0,0261 |

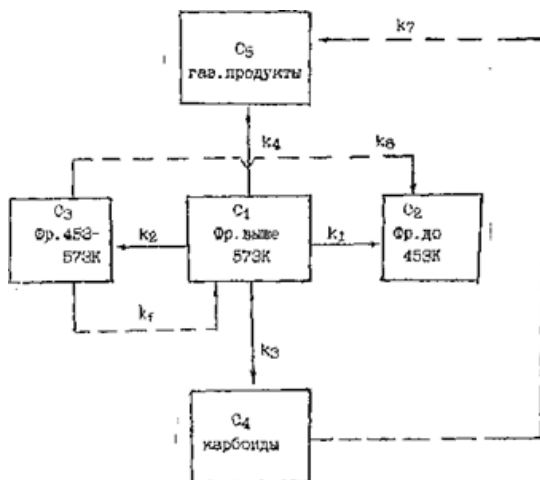


Figure 21. Kinetic conversion scheme organic mass of high viscosity oil

In accordance with the proposed scheme (Fig. 21), the kinetic model No. 2 has the following form:kc



$$\frac{d(\text{фракция до } 573 \text{ К})}{d\tau} = -k_c e e_{\text{Н}} \quad (58)$$

where k_c – speed constant.

$$\begin{aligned}\frac{d[C_1]}{d\tau} &= -(k_1 + k_2 + k_3 + k_4)C_1 + k_5 C_3 \\ \frac{d[C_2]}{d\tau} &= k_1 C_1 + k_6 C_3 \\ \frac{d[C_3]}{d\tau} &= k_2 C_1 - (k_5 + k_6)C_3 \\ \frac{d[C_4]}{d\tau} &= k_3 C_1 - k_7 C_4 \\ \frac{d[C_5]}{d\tau} &= k_4 C_1 + k_7 C_4\end{aligned} \quad (59)$$

where $/C_i/$ is the mass fraction of products at time t ; $/C_1/$ fraction above 573 K, $/C_2/$ fraction up to 453 K, $/C_3/$ fraction 453-573 K,

$/C_4/$ carboids, $/C_5/$ gas. products, $/C_i/ = 1$, k_i — hydrogenation rate constant, min-1; k_1 is the conversion constant of the fraction above 573 K to the fraction up to 453 K; k_2 is the conversion constant of the fraction above 573 K to fraction 453-573 K; k_3 is the conversion constant of the fraction above 573 K and the carbides; k_4 is the constant of converting the fraction above 573 K to gaseous products.

The system was calculated on an EC-1036 computer using the special “Search” program. The criterion for the relativity of the calculation is the minimization criterion as the sum of the squares of relative deviations:

$$F = \sum_{j=1}^N \sum_{i=1}^N \left[\frac{V_{\text{эксп}} - V_{\text{расч}}}{V_{\text{эксп}}} \right]^2 \quad (60)$$

where N is the number of measurements in the experiments, V_{exp} , V_{calc} experimental and calculated values of the content of components in the hydrogenate.

As a result of the calculation, a satisfactory agreement was obtained between the experimental data and the calculated values of the indicated products (Fig. 21 a – e). The calculated rate constants are given in table 38, where (Δ) is the standard deviation of the key velocities. Table 38 shows that the limiting rate of the hydrogenation of HVO is the stage of conversion of

the fraction above 573K to the fraction 453-573 K and the fraction above 573 K to carboids (k_1 and k_3).

The activation energy values were obtained by approximation of the Arrhenius equation, described by the linear function $\ln k = f(1/T)$ (Fig. 22).

The apparent activation energy of the process of converting HVO to liquid products increases from $C_1 \rightarrow C_3$ to $C_1 \rightarrow C_2$. The value of the apparent activation energy of the total transformation of the organic mass of high-viscosity oil is 73.8 kJ/mol, which is typical of a heterogeneous catalytic reaction. The apparent activation energy for the gas formation reaction, fractions up to 453K, fractions 453-573K, and carboids is presented in table 38.

Table 38
Constants of the hydrogenation rate of HVO and activation energy

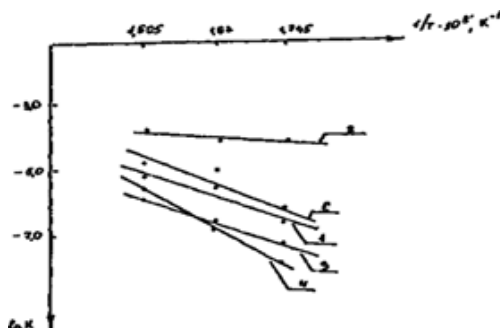
| T,K | Rate constants, min ⁻¹ | | | | | F | $\Delta, \%$ |
|---------------|-----------------------------------|----------------------|----------------------|----------------------|----------------------|-------|--------------|
| | k_c | k_1 | k_2 | k_3 | k_4 | | |
| 573 | $1,71 \times 10^{-3}$ | $1,0 \times 10^{-3}$ | $8,0 \times 10^{-3}$ | $2,0 \times 10^{-3}$ | $1,2 \times 10^{-3}$ | 0,217 | 10,4 |
| 598 | $5,46 \times 10^{-3}$ | $3,1 \times 10^{-3}$ | $1,6 \times 10^{-3}$ | $1,0 \times 10^{-3}$ | $2,7 \times 10^{-3}$ | 0,149 | 8,6 |
| 623 | $6,15 \times 10^{-3}$ | $6,5 \times 10^{-3}$ | $1,8 \times 10^{-3}$ | $2,7 \times 10^{-3}$ | $4,4 \times 10^{-3}$ | 0,163 | 9,0 |
| E, kJ/mo l | 73,8 | 46,1 | 47,1 | 147,5 | 75,2 | | |

Note: F the minimization criterion is taken as the sum of the squares of relative deviations.

From the data obtained it follows that the least energycomplicated processes of destruction of the organic mass of highviscous oil with the formation of light and medium fractions. Therefore, in order to carry out the process in the direction of obtaining light fractions, it should be limited to a low process temperature.

An analysis of two kinetic HVO hydrogenation models showed that model №1 has a high relative error (8–15%) deviations of the calculated data from experimental data and, therefore, the kinetic model

№2is more correct.



1. reaction of formation of fraction to 453K,
2. reaction of formation of fraction to 453 573K,
3. the reaction of the formation of carbides,
4. the reaction of formation of gaseous products
- C. reaction of formation of the total fraction to 573K

Figure 22. Dependence of the rate constant of the process of hydrogenation of HVO from inverse temperature

5.4.Kinetics of the process of hydrogenation of high-viscosity oil (fraction <200 °C)

In article [94], the possibility of optimizing the process of hydrogenation of high-viscosity oil (HVO) from the Karazhambas field in a synthesis-gas medium in the presence of an iron sulfide catalyst, pyrrhotite, was studied.

Using the method of mathematical planning of experiments based on nonlinear multiple correlation and statistical analysis of the system of acting factors, it was possible to obtain data on the kinetics of this process with the minimum number of experiments [94]. For the study, we used a plan based on the structure of a supergreco-latin square, with the processing of particular functions of a linear and nonlinear form. The union of these functions is possible with the help of the Protodyakonov equation, which guarantees the equality of the generalized function to zero with the zero value of any of the particular functions. The introduction of the generalized function into the exponent was limited to it from above one at a time, which is a necessary condition for conducting kinetic analysis.

Lets write the generalized equation in exponential form:

$$Y_p = \exp -1,138(Y_1 \times Y_2 \times Y_3 \times Y_4)^{-0,364} \quad (61)$$

where $Y_1=f(X_1)$, $Y_2=f(X_2)$, $Y_3=f(X_3)$, $Y_5=f(X_5)$ – particular

functions of the HVO hydrogenation process.

Differentiating the generalized equation with respect to time, we obtain the equation of the rate of the process of hydrogenation of HVO

$$\frac{\partial y_p}{\partial x_2} = y_p \exp - 1,138 y_n^{-0,364} y_2^{-0,364} \quad (62)$$

To determine the activation energy, we find the values of the process rates at different temperatures, taking in the multifaceted equation the duration of the process (X_2), corresponding to the yield of the light fraction:

$$\ln Y_p = -1,138(Y_1 x Y_2 x Y_3 x Y_5 x 19,12)^{-0,364} \quad (63)$$

$$y^{0,364} = \frac{-1,138[Y_1 x Y_2 x Y_3 x Y_5 x 19,12^{-2}]^{-0,364}}{\ln Y_p} \quad (64)$$

Found expression is substituted into the equation:

$$\frac{\partial y_p}{\partial x_2} = y_p \ln Y_p (-0,364) 5 \times 10^{-2} x Y_1 x Y_3 x Y_5 x 19,12^{-3} \left[\frac{\ln Y_p}{-1,138} \right]^{2,747} \quad (65)$$

This equation can be analyzed in the Arrhenius coordinates for any given value of the parameters included in the multivariate equation. The dependence of the HVO hydrogenogenization process rate on the temperature in these coordinates when the light fraction reaches 27% and the factors $X_1 = 0.02$, $X_3 = 0$, $X_4 = 0.08$ is described by a straight line (Fig. 23):

$$\ln \frac{\partial y_p}{\partial x_2} = -4,43 - 2695,3 \frac{1}{T} \quad (66)$$

For the temperature range of 350–425°C, the activation energy of 49.7 kJ/mol was found, which is typical of heterogeneous catalytic hydrocracking processes of heavy hydrocarbon feedstock.

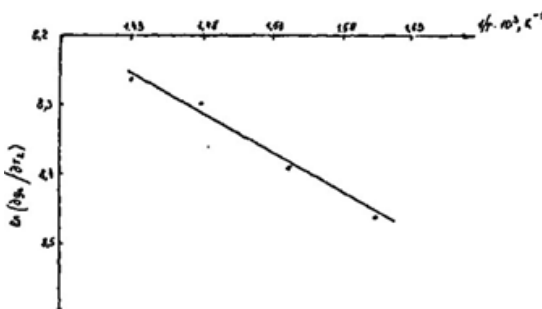


Figure 23. The dependence of the speed $\ln \partial V_p / \partial X_2$ of hydrogenation process of HVO from inverse temperature

Thus, a kinetic model of the HVO hydrogenation process has been developed, which allows determining the influence of technological parameters on this process.

5.5. Kinetic model of high viscosity oil hydrogenation

According to preliminary estimates of economic efficiency, oilbituminous rocks and high-viscous oils abroad and in the CIS countries are considered as the main source for obtaining hydrocarbon raw materials for the long term and scientific research is intensively conducted [95]. In addition, highly viscous oils can be used as a passer agent (hydrogen donor) during coal liquefaction processes.

In [96], it was shown that to facilitate the technical conditions of the process of hydrogenation of coal, heavy oil residue (HOR), highviscosity oil (HVO) (hydrogen pressure, temperature, catalyst), modern data on the structure of the organic mass of coal, HOR, HVO should be used. While studying the kinetics of the hydrogenation of coal and HOR, the authors proceeded by analogy with the refining processes and the products obtained during liquefaction were divided into a number of representative groups that approximately reflect the difference in the average molecular weight and chemical composition.

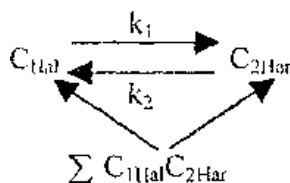
The kinetic description of the transformation of the organic mass of a heavy hydrocarbon feedstock (coal, HVO, HOR) is of great scientific and practical importance. In the literature [89, 90] and [97], the kinetics of the hydrogenation of petroleum bitumen and the kinetics of the hydrogenation of HVO are investigated in the presence of a catalytic additive of pyrite and pyrrhotite.

However, analysis of the literature data shows that there are

practically no studies on the kinetics of hydrogenation of HVO using the catalytic additive of pyrite on the distribution of hydrogen in hydrogenation products as a function of time.

We carried out the results of the kinetics of hydrogenation of HVO in the presence of an iron sulfide catalyst using data from PMR spectroscopy and elemental analysis.

According to the PMR spectroscopy of hydrogenate and feedstock, proton concentrations of aliphatic and aromatic hydrocarbons were found, it was found that with increasing temperature and contact time, an increase in the concentration of aromatic and decrease in aliphatic protons was observed. There is a kinetic scheme for the hydrogenation of high-viscosity oil and a system of differential equations that describes the change in proton concentration with time for each of the components of the scheme below:



$$\frac{d[C_1\text{Hal}]}{dt} = -k_1[C_1\text{Hal}] + k_2[C_2\text{Hal}] \quad (67)$$

$$\frac{d[C_2\text{Hal}]}{dt} = -k_2[C_2\text{Hal}] + k_1[C_1\text{Hal}] \quad (68)$$

where / C_i / is the weight fractions of products at time t, also for aromatic protons / C_{Har} / and aliphatic protons / C_{Hal} /; $C_{\text{Har}}C_{\text{Hal}}$ total concentration of aromatic and aliphatic protons of hydrocarbons; k_1 — conversion rate constants, min^{-1} ; k_2 aromatic protons to aliphatic, k_1 aliphatic protons to aromatic.

As a result of calculating the equation, a satisfactory correspondence was obtained between the experimental and calculated values. The calculated rate constants for the hydrogenation of HVO are given in table 39.

Table 39

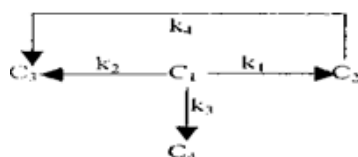
Kinetic data of aliphatic and aromatic proton changes during catalytic hydrogenation of high-viscosity oil

| τ , min | T,K | C _{Hal} exp. | C _{Hal} coun. | C _{Char} exp. | C _{Char} coun. | k _i | | F | $\Delta, \%$ |
|-----------------|-----|--------------------------|---------------------------|---------------------------|----------------------------|----------------|-------|---|--------------|
| | | | | | | k_1 | k_2 | | |
| 0 | | 0,97 | 0,97 | 0,03 | 0,03 | | | | |

| | | | | | | | | | |
|----|-----|------|------|------|------|-----------------------|-----------------------|-------|------|
| 5 | | 0,97 | 0,97 | 0,03 | 0,03 | | | | |
| 10 | 623 | 0,96 | 0,97 | 0,04 | 0,03 | $3,09 \times 10^{-4}$ | $1,03 \times 10^{-5}$ | 0,131 | 1,14 |
| 15 | | 0,96 | 0,96 | 0,04 | 0,03 | | | | |
| 30 | | 0,96 | 0,96 | 0,03 | 0,04 | | | | |
| 60 | | 0,95 | 0,95 | 0,05 | 0,04 | | | | |
| 0 | | 0,97 | 0,97 | 0,03 | 0,03 | | | | |
| 5 | | 0,96 | 0,97 | 0,04 | 0,03 | | | | |
| 10 | 648 | 0,96 | 0,96 | 0,03 | 0,03 | $5,08 \times 10^{-4}$ | $2,2 \times 10^{-5}$ | | |
| 15 | | 0,96 | 0,96 | 0,04 | 0,03 | | | | |
| 30 | | 0,95 | 0,95 | 0,05 | 0,04 | | | | |
| 60 | | 0,94 | 0,94 | 0,05 | 0,06 | | | | |
| 0 | | 0,97 | 0,97 | 0,03 | 0,03 | | | | |
| 5 | | 0,97 | 0,96 | 0,07 | 0,03 | | | | |
| 10 | 673 | 0,94 | 0,96 | 0,05 | 0,04 | $9,4 \times 10^{-4}$ | $3,4 \times 10^{-5}$ | 0,529 | 2,3 |
| 15 | | 0,95 | 0,96 | 0,05 | 0,04 | | | | |
| 30 | | 0,91 | 0,94 | 0,08 | 0,05 | | | | |
| 60 | | 0,93 | 0,92 | 0,07 | 0,08 | | | | |

The magnitude of the rate constant of the direct reaction of the hydrogenation of HVO is an order of magnitude higher than the rate constant of the reverse reaction. The activation energy values were obtained by approximating the Arrhenius equation. The value of the apparent activation energy is 73.1 and 87.6 kJ/mol.

The kinetic curves of HVO hydrogenation in the temperature range of 623-673 K are shown in Figure 24 (a, b). Analysis of the kinetic curves shows that with an increase in time and temperature, there is an increase in the concentration of hydrogen in the hydrosulfate from 27.8% to 34.0%, gaseous from 6.3 to 11.2%, solids from 0, 4 to 1.8%, respectively. The scheme for the conversion of HVO in the process of catalytic hydrogenation can be represented as follows:



The following systems of differential equations describe the change in hydrogen concentration over time for each of the components of the scheme:

$$\left\{ \begin{array}{l} \frac{dC_1}{d\tau} = -k_1 C_1 - k_2 C_2 - k_3 C_1 \\ \frac{dC_2}{d\tau} = k_1 C_1 - k_4 C_1 \\ \frac{dC_3}{d\tau} = k_2 C_1 - k_4 C_2 \\ \frac{dC_4}{d\tau} = k_3 C_1 \end{array} \right. \quad (69)$$

$$dC_1/d\tau = (k_1 + k_2 + k_3)C_1 \quad (70)$$

$$\left\{ \begin{array}{l} \frac{dC_2}{d\tau} = k_1 C_1 \\ \frac{dC_3}{d\tau} = k_2 C_1 \\ \frac{dC_4}{d\tau} = k_3 C_1 \end{array} \right. \quad (71)$$

where $/C_i/$ is the mass fraction of hydrogen in the feedstock and in the products at time t ; $/C_2/$ hydrogen content in HVO; $/C_3/$ hydrogen content in hydrogenation product; $/C_4/$ hydrogen content in gaseous products; $/C_1/$ is the hydrogen content in the solid product; $/C_i/ = 1$, k_1

rate constant of hydrogenation, min^{-1} ; k_1 is also HVO in hydrogenated; k_2 also HVO in gaseous products; k_3 is also HVO in solid products.

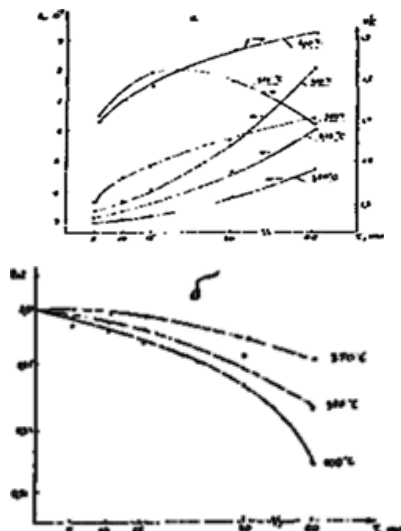


Figure 24. Kinetic accumulation curves of aromatic (a) and aliphatic (b) protons in the hydrogenation

The system was calculated on an EC-1036 computer; the minimization criterion and the standard deviation were used as the criterion for relativity of the calculation. As a result of the calculation of the system, a satisfactory correspondence was obtained between the experimental data and the calculated values of the indicated products (Fig. 25a-d). The rate constants k_1-k_3 calculated at different temperatures are given in table 40, where ($\Delta, \%$) the standard deviation does not exceed 10%.

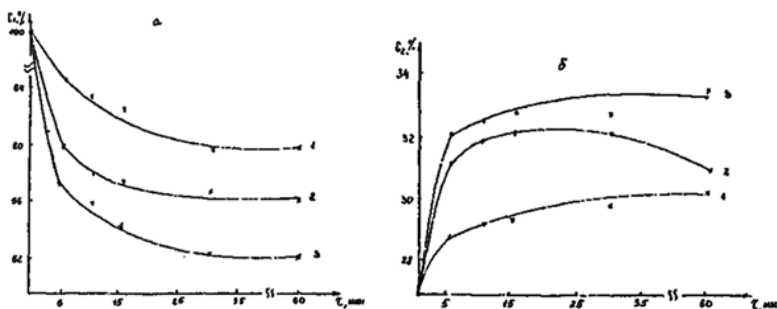


Figure 25 (a). The kinetic curves of hydrogenation HVO: 1 623K
2 648K, 3 673K: a) the concentration of hydrogen in HVO; b) in hydrogenate

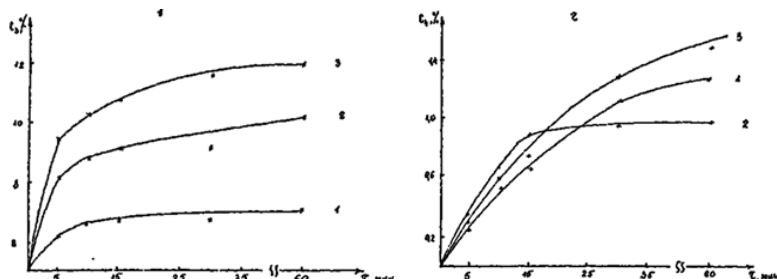


Figure 25 (b). Kinetic curves of HVO hydrogenation: 1 623K,
2 648K, 3 673K: b) in the gaseous product, d) in the solid product

In [98], it was shown that by the value of k_i it is possible to judge the contribution of each constant to the yield of liquid products. The calculated rate constants in table 40 show that k_i contributes significantly to the yield of the hydrogenate.

Table 40

Constants of the hydrogenation rate of HVO and activation energy

| T,K | Rate constant, min ⁻¹ | | | F | Δ, % |
|----------|----------------------------------|-----------------------|-----------------------|--------|------|
| | k ₁ | k ₂ | k ₃ | | |
| 623 | 1,29x10 ⁻³ | 6,64x10 ⁻³ | 1,77x10 ⁻³ | 0,1103 | 8,3 |
| 648 | 1,42x10 ⁻³ | 8,63x10 ⁻³ | 4,0x10 ⁻³ | 0,1525 | 9,8 |
| 673 | 1,85x10 ⁻³ | 1,28x10 ⁻³ | 5,59x10 ⁻³ | 0,1236 | 8,8 |
| E,kJ/mol | 66,4 | 109,3 | 181,1 | | |

The activation energy values were obtained by approximation of the Arrhenius equation, described by the linear function $k = f(1/T)$. The magnitude of the apparent activation energy of the process in the temperature interval 623–673 K is equal to 66.4 kJ/mol, which is typical of heterogeneous catalytic processes of heavy hydrocarbon feedstock. The obtained values of the apparent activation energy of 73.1 and 66.4 kJ / mol using PMR spectroscopy and elemental analysis are consistent with the data described in [99].

5.6. Kinetics of demetallization of high viscosity oil

For the kinetic analysis of the demetallization process of highly viscous oil, a generalized equation was used, which relates the recovery rate (αV , Ni) to the solid phase with all the factors studied.

To find the dependence of the extraction of vanadium and nickel from highly viscous oil into the solid phase on the inverse temperature at one given degree, the equation was somewhat transformed, as provided for [100]. Differentiating the equation in time, we found the rate of demetallization and HVO.

For vanadium:

$$\frac{\partial Y_V}{\partial x_2} = 1,003 \times 10^{-3} x V_c x \ln V_c \left(-\frac{\ln V_c}{0,145} \right)^{2,475} x \left(\frac{Y_1 x Y_3 x Y_4 x Y_5}{Y_p^3} \right)^{4,0872} \quad (72)$$

where $V_c = \exp(-0,148/Y_n^{1,65})$

For nickel:

$$\frac{\partial Y_{Ni}}{\partial x_2} = 3,95 \times 10^{-5} x V_c x \ln V_c \left(-\frac{\ln V_c}{0,207} \right)^{6,916} x \left(\frac{Y_1 x Y_3 x Y_4 x Y_5}{Y_p^3} \right)^{10,163} \quad (73)$$

where $V_c = \exp(-0,21/Y_n^{1,47})$

To obtain the dependence of the process rate on temperature, it is necessary to ensure the constancy of the surface area of phase separation, which in the first approximation is equivalent to the constant degree of

extraction of vanadium and nickel in the solid phase under equal conditions. Given the degree of extraction for vanadium in the differential equation from 0.35 to 0.81, and for nickel from 0.4 to 0.88, we obtain a number of dependences of the rate of extraction of vanadium and nickel in the solid phase on temperature (tables 41, 42).

The dependence of the extraction rate of vanadium and nickel on the temperature is given in tables 41, 42. At all extraction levels (vanadium, nickel), graphically rectilinear dependences are obtained with an equal inclination angle, which indicates the same process mechanism. After processing the data using the least squares method in Arrhenius coordinates, the corresponding values were calculated for various degrees of extraction of vanadium and nickel from HVO to the solid phase:

| | | | | |
|---|-------|-------|-------|-------|
| The degree of extraction of vanadium α | 0,35 | 0,46 | 0,61 | 0,81 |
| Activation energy, kJ/mol | 81,9 | 83,1 | 83,09 | 83,05 |
| Degree of Nickel recovery, α . | 0,40 | 0,52 | 0,68 | 0,88 |
| Activation energy, kJ/mol | 194,5 | 194,6 | 194,9 | 194,4 |

Table 41
**The rate of extraction of vanadium from HVO in the solid phase,
 $W, \text{d/min}$**

| The degree of extraction α , D. unit. | W, d/min at temperatures, K | | | |
|--|-----------------------------|------------------------|------------------------|-------------------------|
| | 623 | 648 | 673 | 698 |
| 0,35 | 1,27x10 ⁻³ | 3,878x10 ⁻³ | 1,226x10 ⁻² | 3,706x10 ⁻² |
| 0,46 | 1,95x10 ⁻³ | 5,942x10 ⁻³ | 1,882x10 ⁻² | 5,986x10 ⁻² |
| 0,61 | 2,086x10 ⁻³ | 6,361x10 ⁻³ | 2,016x10 ⁻² | 6,402x10 ⁻² |
| 0,81 | 1,575x10 ⁻³ | 4,849x10 ⁻³ | 1,531x10 ⁻² | 4,8476x10 ⁻² |

The values of the calculated activation energy for the extraction of vanadium and nickel in the solid phase indicate the absence of external diffusion difficulties and indicate the process in the kinetic region

Table 42
The rate of extraction of nickel from HVO in the solid phase, $W, \text{d/min}$

| The degree of extraction α , D. unit. | W, d/min at temperatures, K | | | |
|--|-----------------------------|------------------------|------------------------|------------------------|
| | 623 | 648 | 673 | 698 |
| 0,40 | 4,12x10 ⁻⁷ | 5,889x10 ⁻⁶ | 9,009x10 ⁻⁵ | 1,243x10 ⁻³ |
| 0,52 | 4,807x10 ⁻⁷ | 6,931x10 ⁻⁶ | 1,064x10 ⁻⁴ | 1,459x10 ⁻³ |

| | | | | |
|------|------------------------|------------------------|------------------------|------------------------|
| 0,68 | $5,678 \times 10^{-7}$ | $8,140 \times 10^{-6}$ | $1,240 \times 10^{-4}$ | $1,720 \times 10^{-3}$ |
| 0,88 | $6,59 \times 10^{-7}$ | $9,53 \times 10^{-6}$ | $1,450 \times 10^{-4}$ | $1,996 \times 10^{-3}$ |

According to [100], the proportion of non-porphyrin compounds of vanadium and nickel is higher than that of porphyrin. These compounds can be represented as complexes of vanadyl or nickel with ligands of the pseudoporphyrin structure containing 2 or 4 nitrogen atoms in the coordinating center. In the literature there are no data on the mechanism of catalytic hydrodemetallization of heavy oils, heavy oil residues. Using the method of molecular mechanics, we attempted to study the mechanism of demetallization of high-viscosity oil. As the initial model, we used the non-porphyrin structures of the vanadyl-containing complexes presented in the review.

The molecular mechanics method allows to calculate the total energy and geometric orientation of the vanadyl-containing complex. The initial model of the vanadyl-containing complex and the calculated value of the total energy minimization. Unlike vanadyl-porphyrin complexes, their structure is located in one plane, and non-porphyrin complexes of vanadium are located in different planes lying at an angle to each other. This significantly complicates the hydrodemetallization of the non-porphyrin vanadyl complex. According to calculations by the method of molecular mechanics, the addition of atomic hydrogen to the five-membered cycle (ligand-benzothiophene) is thermodynamically most preferable. The total energy of minimization is 472,056 kJ/mol, whereas the addition of atomic hydrogen to remove quinoline or isoquinoline ligands from vanadium is 472.931 kJ/mol and 518.885 kJ/mol, respectively. As a result of the attachment of atomic hydrogen to the five-membered cycle, the removal of the sulfur bond from vanadium occurred. The total energy of the complex formed due to the detachment of the benzothiophene ligand was 17.195 kJ/mol.

CHAPTER 6. DEVELOPMENT OF THE THEORY OF THE ORGANIC CAVITATION OF COAL AND A HEAVY OIL RESIDUE

6.1 Influence of catalytic cavitation treatment on the individual chemical composition of the primary coal tar

In this section, we investigated the effect of cavitation on the organic mass of coal and HOR. Primary coal tar was a model of the organic mass of coal and HOR.

During heat treatment of coal in the temperature range of 400–600 °C, primary resins are released. The yield of the primary resin from the coal of the Shubarkol mine is 9–12% by dry weight of the starting material.

In contrast to primary tar, high-temperature stone-carbon tar has a higher density of > 1,160 kg/m³ and is a mixture of multicore aromatic compounds. In primary tars, a higher content of the fraction of o.c.-170 °C and phenols (15–20%). However, unlike high-temperature coking tars, there are no industrial technologies for primary tars to produce marketable products in the CIS.

For the processing of high-temperature resins, traditional methods are used dehydration, fractionation and two-sphenolization.

At present, interest has grown in unconventional methods of processing heavy and solid hydrocarbons (coal, high-viscosity oil, oil residues and coal tar).

The study of mechanochemistry, the influence of dynamic loads and shock waves is complex. These phenomena are accompanied by heating of the substance, an increase in pressure and entropy.

As a catalytic additive, x/h ferrous sulfate crystalline hydrate ($\text{FeSO}_4 \times 7\text{H}_2\text{O}$) and nickel sulfate crystalline hydrate ($\text{NiSO}_4 \times 6\text{H}_2\text{O}$) were used as an aqueous solution in the form of aqueous solutions with a concentration of 1% and 2%, respectively. Solutions of the salt of iron sulfate and nickel were added in an amount of 3 v /% to the initial weight of the primary tar. The catalytic effect of metal salts in the process of cavitation treatment on the individual composition of the primary resin was considered separately. To obtain PHCA used one of the methods proposed in the work. During cavitation treatment of the mixture consisting of aqueous solutions of iron or nickel salts and primary resin, conditions are created that ensure the formation of a catalytic-active form of PHCA. The duration of cavitation treatment of the primary CT was carried out for 0–5 minutes. The individual chemical composition of the primary coal tar is presented in table 43.

Table 43

Individual chemical composition of the primary coal tar

| The holding time on the chromatogram | Compound | The relative content of the compounds in the primary coal tar, wt.% |
|--------------------------------------|-------------------------|---|
| 3,92 | 1,3-dimethylcyclohexane | 4,3 |
| 5,04 | Ethylbenzene | 6,9 5 |
| 8,35 | Octagidro1H-inden | 3,6 2 |
| 9,17 | 1,2,3-trimethylbenzene | 20, 62 |
| 16,60 | Isoquinoline | 7,8 4 |
| 20,19 | 1,2-methylnaphthalene | 17, 03 |
| 25,99 | 4-methyldiphenyl | 13, 29 |
| 26,88 | Isopropyl naphthalene | 6,2 8 |
| 28,76 | Fluoren | 6,3 3 |
| 33,95 | Compound | 3,7 4 |
| Total | | 100 |

Note: the table does not show compounds whose content in the chromatogram is below 1%.

The conditions for conducting experiments to study the effect of catalytic-cavitation treatment of the primary CT are given in table 44, where the experiment number, temperature, duration of treatment, amount of water and catalyst solution added to the primary coal tar are indicated.

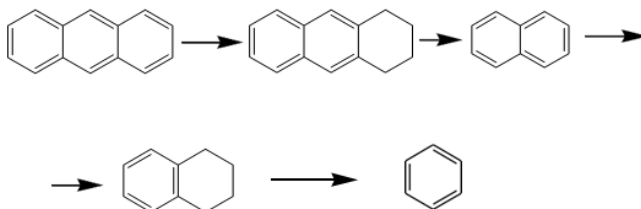
In the general case, the phenomenon of cavitation is associated with the appearance in the liquid under certain conditions of numerous cavitation bubbles that pulsate, oscillate, grow, decrease, collapse and at the same time mix with the flow of liquid.

Table 44

Experimental conditions for catalytic-cavitation treatment of CT in the presence of PHCA (the number of CT is 0.5 liters. With a density of 200°C 1042 kg/m³)

| Nº exp.. | T, °C | Duration of treatment (τ), min. | Amount of water, % | Amount of 1% solution of PHCA, (FeSO ₄ , Ni-SO ₄)) | Amount of 2% solution of PHCA, (FeSO ₄ , Ni-SO ₄) |
|----------|-------|--|--------------------|---|--|
| 1 | 60 | 7 | - | - | - |
| 2 | 70 | 5 | - | - | - |
| 3 | 60 | 3 | 10 | - | - |
| 4 | 60 | 7 | 10 | - | - |
| 5 | 70 | 3 | 10 | - | - |
| 6 | 70 | 0 | 10 | 3 | - |
| 7 | 70 | 1 | 10 | 3 | - |
| 8 | 70 | 2 | 10 | 3 | - |
| 9 | 70 | 3 | 10 | 3 | - |
| 10 | 70 | 4 | 10 | 3 | - |
| 11 | 70 | 5 | 10 | 3 | - |
| 12 | 60 | 7 | 10 | - | 3 |
| 13 | 70 | 0 | 10 | - | 3 |
| 14 | 70 | 1 | 10 | - | 3 |
| 15 | 70 | 2 | 10 | - | 3 |
| 16 | 70 | 3 | 10 | - | 3 |
| 17 | 70 | 4 | 10 | - | 3 |
| 18 | 70 | 5 | 10 | - | 3 |

The results given in table 44 show that as the temperature rises from 60 to 70°C without adding water to the CT, the total concentration of naphthenic and aromatic hydrocarbons increases from 35.5 to 72.09% and the concentration of polycyclic aromatic compounds sharply decreases from 54.5% in the original CT to 17.92% in the hydrogenate. This is apparently due to the destruction of polycyclic hydrocarbons, as shown in the review by I.V. Kalechic. The author has shown that hydrogenation of polycyclic hydrocarbons is accompanied by decomposition reactions, for example, naphthalene and its homologs are transformed in three directions: demethylation (naphthalene from methyl and dimethylnaphthalenes), hydrogenation and destruction (monocyclic arenas are formed), also stepwise anthracene destruction.



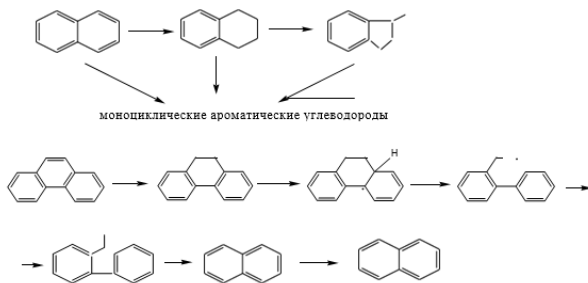
The decrease in the concentration of naphthenic and monoaromatic hydrocarbons may be a consequence of the dissociation of water and the development of the reaction of their secondary oxidative destruction with the release of gaseous products.

The addition of water in the amount of 10% to the CT and an increase in the duration of cavitation treatment from 3 to 7 minutes leads to a significant decrease in the total concentration of cycloalkanes and one-ring aromatic hydrocarbons from 72.1 to 52.9% and an increase in the concentration of polyaromatic solids from 17.9 to 48.9%, respectively.

The dependence of the yield of ethylnaphthalene and 2,6dimethylnaphthalene on the duration of the catalytic-cavitation treatment is extreme, reaching a maximum value for ethylnaphthalene 2.5% (processing time 4 minutes) and for 2,6-dimethylnaphthalene 7.2% (processing time 3 min.).

Investigation of the effect of treatment time (in the interval from 1 to 5 minutes) on the change in the concentration of polycyclic hydrocarbons such as diphenyl, acenaphthene, dibenzofuran, and fluorene shows that their concentration does not change significantly with an increase in the treatment time. The total yield of the concentration of naphthalene and its derivatives increases from 49.1 to 50.5% from the processing time. High concentrations of naphthalene and its derivatives, apparently, allows to see the competition between the cracking and polycondensation reactions of the initial substances that make up the tar due to the directional influence of the catalysts of iron sulfate and nickel sulfate.

It is known that aqueous solutions of nickel sulfate salts promote hydrogenation decomposition and have highly acidic properties, and also naphthalene and phenanthrene are thermolized according to the following scheme:



As was to be expected, the main differences between the behaviors of catalysts during the cavitation treatment of the primary resin are associated with the formation of iron and nickel sulfides.

As is known, the nature of the catalyst is important in the process of hydrogenation of a heavy hydrocarbon feedstock. Apparently, during cavitation treatment of the primary CT, aqueous solutions of salts of metals of iron and nickel boil, and intensive evaporation of water from the solution begins and crystallization of the salt begins.

As the water is removed, globules form. In the process of cavitation in the presence of PHCA, globules of metal salts are reduced and sulfided to form sulfides of metals of iron and nickel. In the process of cavitation treatment of the primary CT, the resulting sulfides of iron and nickel have a shape close to spherical, and thus provide a high concentration of active centers. The activity and selectivity of action PHCA is shown in tables 45-46.

Table 45
**Chemical composition and yield of compounds (wt.%) In the
hydrogenation of tar in the presence of catalyst NiSO₄ × 6H₂O**

| № of the chromatogram peak | The name of the compound | The relative content of substances in the CT before and after cavitation, % (to the sum identified) | | | | | |
|----------------------------|--------------------------|---|--------------|--------------|--------------|--------------|--------------|
| | | Hydrogen. 13 | Hydrogen. 14 | Hydrogen. 15 | Hydrogen. 16 | Hydrogen. 17 | Hydrogen. 18 |
| 2 | Naphthalene | 15,41 | 10,46 | 9,65 | 9,83 | 10,01 | 15,25 |
| 3 | 1-methylnaphthalene | 31,83 | 32,39 | 31,6 | 34,38 | 31,22 | 32,08 |
| 5 | Diphenyl | 3,9 | 3,44 | 3,70 | 3,16 | 4,62 | - |
| 6 | 2- | 1,34 | 1,42 | 1,47 | - | 2,46 | 1,47 |

| | | | | | | | |
|----|-------------------------|------|-------|-------|-------|-------|-------|
| | ethylnaphthalene | | | | | | |
| 7 | 2,6-dimethylnaphthalene | 6,1 | 4,85 | 4,61 | 7,23 | 5,93 | 3,72 |
| 10 | Acenafthen | 25,6 | 30,08 | 30,9 | 29,09 | 29,27 | 31,38 |
| 11 | Dibenzofuran | 7,14 | 8,82 | 8,07 | 7,56 | 8,28 | 7,45 |
| 12 | Fluoren | 8,68 | 8,54 | 10,00 | 8,75 | 8,21 | 8,65 |

Table 46

Chemical composition and concentration of compounds (wt.%) In the initial CT and hydrogenates of the tar obtained after cavitation treatment in the presence of the catalyst $\text{FeSO}_4 \times 7\text{H}_2\text{O}$

| № of the chromatogram peak | The name of the compound | The relative content of substances in the CT before and after cavitation, % (to the sum identified) | | | | | |
|----------------------------|--|---|-------------|-------------|--------------|-------------|-------------|
| | | Exodus CT | Hydrogen. 1 | Hydrogen. 2 | Hydrogen. 3. | Hydrogen. 4 | Hydrogen. 5 |
| 2 | 1,3-dimethylcyclohexane | 4,3 | 10,65 | 8,89 | 5,07 | 5,81 | 5,29 |
| 3 | Ethylbenzene | 6,95 | 14,92 | 12,56 | 8,16 | 9,27 | 8,60 |
| 9 | Octagidro 1N-inden | 3,62 | 5,50 | 4,87 | 4,34 | 4,37 | 4,48 |
| 10 | 1,2,3-trimethylbenzene | 20,6 | 41,02 | 36,82 | 33,45 | 34,48 | 34,54 |
| 17 | Isoquinoline | 7,84 | 7,35 | 6,65 | 7,22 | 6,97 | 7,01 |
| 18 | 1,2-dimethylnaphthalene | 17,0 | 10,29 | 9,97 | 16,41 | 15,59 | 15,78 |
| 23 | 4-methyldiphenyl | 13,2 | 10,28 | 9,93 | 12,92 | 11,70 | 12,48 |
| 24 | Isopropynaphthalene | 6,28 | - | 4,99 | 6,11 | 5,67 | 5,82 |
| 25 | Fluoren | 6,33 | - | 5,31 | 6,32 | 6,13 | 6,0 |
| 26 | Mixture of anthracene and phenanthrene | 3,74 | - | - | - | - | - |

Thus, the results of studies of catalytic-cavitation treatment of primary CT in the presence of PHCA allow us to conclude that the processing of the tar involves changing the direction of the reaction of destruction and hydrogenation of the resin associated with the destruction of aromatic structures and the formation of hydroaromatic hydrocarbons and the release active radicals of hydrogen atoms, which increase the reactivity of the primary CT. It is possible that the wave cavitation treatment of the primary tar in the presence of PHCA is a continuous series of thermolysis and hydrogenation of unsaturated and saturated compounds, successively proceeding and interconnected, where the polycyclic hydrocarbons are hydrogenated step by step, and then the rings are destroyed, the hydrogenated compounds break, which leads to various rearrangements and the formation of active radicals and hydrogen.

6.2 Catalytic-cavitation treatment of a model object (hexane) in the presence of β -FeOOH, Fe (OA)₃ nanocatalysts

The cavitation treatment of hexane was carried out according to the procedure described in Section 3.2 in a 0.05 l ultrasonic cavitator at an initial atmospheric pressure and a duration of 10 minutes. Nanocatalysts β -FeOOH, Fe (OA)₃ were used as catalytic systems. The results of cavitation treatment of hexane are shown in table 47.

Table 47

**The content of the products after cavitation treatment of hexane
in the presence of β -FeOOH, Fe(OA)₃**

| Product s | Content t% | | |
|------------------------|------------------|------------------|----------------------|
| | Without catalyst | β FeOOH | Fe (OA) ₃ |
| Hexane | 94.15 | 63.2 7 | 69.12 |
| Nonan | 1.04 | - | - |
| Undecane | 2.25 | 12.4 2 | 3.25 |
| Dodecane | 0.11 | 0.62 | 0.56 |
| Tridecan | 0.05 | 0.19 | 0.19 |
| Tetradecane | 0.08 | 0.97 | 0.08 |
| Hexadecane | 0.3 | 1.94 | - |
| 4-methylpentene-2 | - | 0.03 | - |
| 3-ethyl-4-methylhexane | 1.45 | - | 0.01 |

| | | | |
|------------------------|-----------|-----------|-------|
| 3,5-dimethyloctane | - | - | 6.79 |
| 3-methyldecane | 0.02 | 0.62 | 2.26 |
| 6-ethyl-2-methyldecane | - | 2.92 | - |
| 4,6-dimethylundecane | 0.19 1 | 15.1 1 | 17.11 |
| 2-nonenon | 0.27 | 0.05 | 0.27 |
| 2-decanon | 0.36 | 1.86 | 0.36 |

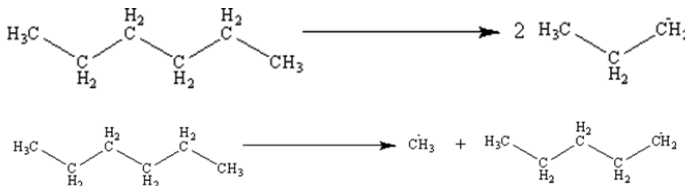
In the case of cavitation treatment without a catalyst, 1.45% 3ethyl-4-methylhexane, 1.04% nonane and 2.25% undecane were identified. In the presence of β -FeOOH catalyst, the content of undecane was 12.42% and 15.11% of 4,6-dimethylundecane. In the case of the Fe(OA)₃ nanocatalyst, the content of 3,5-dimethyloctane was 6.79%, 4,6-dimethylundecane 17.11%, undecane 3.25% and 3-methyldecane -2.26%. The data obtained confirm that as a result of the cavitation treatment of hexane, the following compounds were found: tridecane, tetradecan, pentadecan, hexaecane and heptadecan.

This again confirms the fact that during wave action the destruction of molecules occurs, caused by micro-cracking of molecules and ionization processes. As a result of these processes, "activated" particles are accumulated in the system: radicals, ions, and ionic-radical formations.

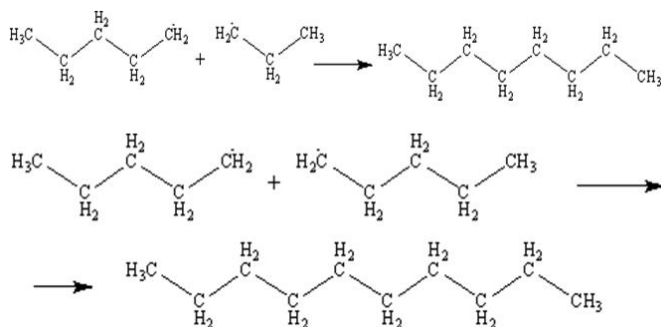
The lifetime of the activated formations, as a rule, little, however, some of them have a definite stability and are able to individually exist for a certain time. The process of the disappearance of the radicals proceeds in two ways: in the result of disproportionation and recourse.

Characterizing the destruction of hexane during cavitation, it can be compared with the transformation of the decane:

1. Immediately, the hexane proceeding process proceeds according to the free-radical mechanism initiated by the phenomenon of cavitation. Most intensely, the C – C bond breaks up in the middle of the molecule and at the first carbon atom:



2. The lifetime of the formed radicles of the krayne is small, the presumed breakage of the kinetics circuit is affected by the scheme:



In the result of multiple repetitive growth and breakage of the chain in a reaction system, a series of n-paraffins is accumulated.

Thus, cavitation treatment of the model object of hexane was carried out in the presence of nanocatalysts. The degree of conversion of the model object in the presence of β -FeOOH and Fe(OA)₃ was 36.73% and 30.88%, respectively. The use of β -FeOOH and Fe(OA)₃ nanocatalysts in the process of cavitation treatment of hexane exceeds its conversion compared with the absence of a catalyst (5.85%). The results indicate sufficient activity and selectivity of β -FeOOH and Fe(OA)₃ nanocatalysts.

CONCLUSION

1. The optimal conditions for the catalytic-cavitation treatment of the primary CT in the presence of PHCA FeSO₄ H 7H₂O were determined: temperature 40-45 °C; the amount of water added 11-12 vol.%; emulsion drop radius 2.0-2.5 microns; the amount of added PHCA 3.0-3.5%; processing time 3.0-4.0 minutes; in the presence of PHCA NiSO₄ 6H₂O: temperature 50-55.0 °C; amount of added water is 7-8.0% by volume; emulsion drop radius 1.5-1.7 microns; the amount of added PHCA 3.0-4.0%; processing time 5.0 min.

2. It was shown that during catalytic-cavitation treatment of primary coal tar, the direction of the reaction of destruction and hydrogenation changes, associated with the destruction of aromatic structures and the formation of hydroaromatic hydrocarbons and release of active radicals of hydrogen atoms, which increase the reactivity of the primary tar.

3. Using elemental structural analysis, thermodynamic indicators and the enthalpy of formation for the primary resin and its narrow fractions were calculated. The main directions of rational processing of this type of hydrocarbon raw materials are determined.

4. A mechanism for the conversion of hexane, which flows through a free-radical mechanism, initiated by the phenomenon of cavitation, more intensely breaks the C-C bond in the center of the molecule at the first carbon atom, is proposed.

REFERENCES:

1. Zhubanov K.A. Deep processing of hydrocarbon raw materials the prospect of the development of the petrochemical industry
K.A. Zhubanov // Industry of Kazakhstan. 2001. №4. p. 60-63.
2. Chistyakov A.N. Chemistry and technology of coal tar processing /
A.N. Chistyakov. Chelyabinsk.: Metallurgy, 1990. 10 p.
3. Makarova G.I. Chemical technologies of solid combustible minerals /
G.I. Makarova, GD Kharlamovich. M.: Chemistry, 1986. 493 c.
4. Izmailov, A.V. Theoretical foundations of chemical technology /
A.V. Izmailov. M.: Chemistry, 1972. Vol. 6, № 2. P. 290-294.
5. Maloletnev A.S. Production of commodity phenols by hydrogenation of
coal from the Kansk-Achinsk basin / A.S. Maloletnev, M.A. Gulnalieva
// Chemistry of solid fuels. 2007. -№ 3. C.21-29.
6. Molchanov, I.V. Light resin of high-speed pyrolysis of brown coal as a
raw material for the production of solvents of electrical insulating
varnishes / I.V. Molchanov, V.F. Korniliev // X and the mission of solid
fuel. № 5. 1988. p. 43-45.
7. Kostyuk V.A. Dephenolisation of hydrogenated brown coal in a
continuous countercurrent / V.A. Kostyuk, I.I. Slavinskaya // Chemistry
of solid fuel. № 2. 1987. p. 78–82.
8. Gogoleva, T.Ya. Chemistry and processing of coal tar
/ T.Ya. Gogoleva, V.I. Shustikov. M.: Metallurgy, 1992. 256 p.
9. Zelenin, N.I. Chemistry and technology of shale resin /
N.I. Zelenin, V.S. Feinberg, K.B. Chernyshev. L.: Science, 1968. 220 p.
10. Pokopova, Yu.V. Chemistry and technology of shale phenols /
Yu.V. Pokopova, V.A. Proskuryakov, V.I., Levanovsky. L.: Science,
1979. 157 p.
11. Kharlamovich, G.D. Chemical products of coking coal
G.D. Kharlamovich, G.A. Shub, V.V. Moscow and others. Sverdlovsk.:
"The Middle Ural book publishing house", 1967. Vol.4. p. 383-389.
12. Gavrilov Yu.V. Recycling of solid natural Ene River gonositeley /
JV Gavrilov, N.V. Korolev, S.A. Sinitzin. Moscow, 2001. 160 p.
13. Makarov G.N. Chemical technology of solid fuels /G.N. Makarov,
G.D. Kharlampovich. Moscow: Chemistry, 1986. 496 p.
14. Kalechits I.V. Chemicals from coal / I.V. To a lechits. Moscow:
Chemistry, 1980. – 616 p.
15. Maloletnev A.S. Hydrogenation of coal from promising fields in
Mongolia / A.S. Maloletnev, D.Yu. Ryabov // Chemistry of solid fuels.
2015. №4. p. 35–39
16. Kuznetsov P.N. Methods for obtaining coal pitch / PN. Kuznetsov,
L.I. Kuznetsova // Chemistry of solid fuels. 2015. -№4, pp. 16-29.

17. Maloletnev A.S. Production of synthetic liquid fuels by coal hydrogenation / A.S. Maloletnev, A.A. Krichko, A.A. Garkusha. M.: Nedra. 1992. 128 p.
18. Chizhevsky A.A. The effect of dispersion in the linear induction rotator on the properties of coal and its products of hydraulic genizatsionnoy processing / AA Chizhevsky, N.L. Goldenko, T.M. Khrenkova et al. // Complex processing of coal.Tr. IGI. M.: ITOTT. 1988. — pp. 33–37.
19. Ekaterina L.I. Properties of liquidphase oxidizinge Niatar oil in the presence of catalysts / L.I modifiers. Ekaterizhina, L.N. Vishnyakova,// Jornal «Chimistry of solid fuels». 1984.№1. – P. 63-68.
20. Radchenko O.A. Physical and chemical properties and with digging coal / O.A. Radchenko. M. Because of the AI USSR, 1962. 220 p.
21. Tayanchin A.S. Hydrogenation of Borodino brown coal of mestorozheniya Kansk-Achinsk basin with a small response / AS Time Tayanchin, A.A. Krichko, S.S. Makarevi.dr. // Processing of coal to produce synthetic fuels. Tr. IGI. M.: IOTT, 1986. p. 5-15.
22. Gagarin C. G. Selfassociate concept mules Timur coal structure / SG Gagarin, A.A. Krichko // Chemistry TVE p dogo fuel. 1984. №4. p. 3-8
23. Gagarin A.S. Structural transformations of the organic mass of brown coal during low-temperature hydrogenation in tetralin medium / A.S. Gagarin, P.N. Kuznetsov. Proceedings of the conference "Prospects for the development of chemical processing of combustible minerals" (KhPGI-2006). SankPetersburg. Chem. Ed., 2006. p. 2014.
24. Kuznetsov B.N. Deep processing of brown coal to produce liquid fuels and carbon materials / B.N. Forge of e ATCs. Novosibirsk: And the building of the SB RAS, 2012. 212 p.
25. Lipovich V.G. Chemistry and coal processing / VG Lipovich, G.A. Kalabin, I.V. Kalechits. Moscow: Chemistry, 1988. 336 p.
26. Sharypov V.I. Processing of coal into liquid products by the methods of hydrogenation and hydropyrolysis / V.I. Sharypov,N.G. Beregovtsova, B.N. Kuznetsov // Chemistry of solid fuels. 2014.№ 2. P. 44–49.
27. Diffuse catalytic burner. Post 3 [Text]:scientific publication/ Hiroki Sadamori, seichi Ito, Hiroshi Jinno// Nanre Kekaysi/ J.Fuel Soc. Jap. – 1989.-.Vol.68. N.3. – p. 226-235.ISSN 03693775
28. Maloletnev, A.S. Hydrogenation of coal from the Chaydakh deposit of the Lena basin / A.S. Maloletnev, P.N. The Forge is, AEC, S.M. Kolesnikova et al. // Chemistry of solid fuels. 2013. № 3. p. 37–42.
29. Kopytov M.A. Joint cracking lignite and m and Zuta in the presence of isopropyl alcohol / MA Kopytov, A.K. Golovko// Chemistry of solid fuel. 2013. № 6. p. 59 63.

30. Maloletnev A.S. The structure of coal hydrogenation products obtained in the presence of oil and coal used pastoo verters / A.S. Maloletnev, A.M. Gyulmaliev // Chemistry of the first fuel is firm. 2013. № 4. p. 40 42.
31. Glushchenko I.M. Theoretical foundations of the technology of gravel fossils / I.M. Glushchenko. Moscow: Metallurgy, 1990. 296 p.
32. Wang Li, Huang Peng, Huang Mujie, Zheng Jianguo. It was used in direct coal liquefaction// Meiton xuebaoj.of.China Coal Soc. – 1999. - Vol.24, № 4. – P. 420-423.
33. Osipov A.M. Thecatalytic properties of iron serosoderzh boiling compounds and the hydrogenation of brown coal / AM Osipov, Z.V. Boyko, L.I. Afanseva et al. // Chemistry solid then n Lebanon. 1994. № 2. p. 11-14.
34. Sharma RK, MacFadden IS, Stiller AH, Dadyburjor DB Direct coal liquefaction with use of a mixture of aerosol iron su 1 fide and metal catalyst// Energyand Fuels.1998. Vol 12, № 2. – P. 312-319.
35. Platonov V.V. Catalysis in the liquefaction of coal /V.V. Plat o new, OA Klyavina, V.D. Okushko // The problem of catalysis in coal and mission: Sat. scientific.T ores. Academy of Sciences of Ukraine. Kiev, 1992. p. 21-30.
36. Moshida Isao, Kavamoto Naoki, Kishino Masahiro. Thi s is a combination of heat resistant and low temperature combination. Fuel. - 1986.-Vol.65, No.1. –P. 81-85.
37. Yulin M. K. Catalytic systems fo rhydro zation process e lignite under hydrogen pressure 6Mpa / MK Yulin,S.G. Gagarin, A.A. Khrichko et al. // Chemistry of solid fuels. 1995. -№ 2. p. 22-27.
38. Wang Li, Huang Peng, Huang Mujie, Zheng Jianguo. It was used in the direct coal liquefaction //Meiton xuebaoj. of. China Coal. Soc. – 1999. – Vol. 24, №4. – P.420-423.
39. Landau, M.V. Seroustochivyh selection of catalysts for hydrogenation processes Principles and nefteperer Botko / MV Landau, V.Ya. Kruglikov. In the book: Catalysts for the processes of production and transformation of sulfur compounds. Novosibirsk.: Institute of Catalysis SB RAS, 1979. P.108-109.
40. Polubentseva, M.F. Liquefactionlignite Preece m Corollary iron catalyst and hydrogen donor / MF The floor bentseva, VV Duganova, B.A. Bajenov et al. // Chemistry solid then n Lebanon. 1997. № 6. p. 62-70.

41. Yokogama S., Yoshida T., Narita H., Yoshida R. The cat alytic effect of the natural pyrites for coal liquefaction. The catalytic activity of finely divided pyrites // J. Fuel Sos.Jap.1989.Vol.68, № 10.p. 881-882.
42. Karmanov, P.A. Catalytic effect of mineral componentson the liquefaction of mechanically activated coals / P.A. Karmanov // The problem of catalysis in coal chemistry.: Sat. scientific.tr. AN Ukraine and us. Kiev.: IFHOU, 1992. P. 86-92.
43. Tsodikov, M.V. Study of the catalytic properties of Ni and Fecontaining catalysts for the hydrogenation of brown coal / M.V. Tsodikov, M.A. Perederin, MM Grosjean // Solid Fuel Chemistry. 1990. № 1. p. 49-55.
44. Zekel, L.A. Basics of the Synthesis and Application of Pseudo Molecular Catalysts for the Hydrogenation of Coals and Crude Oil / L.A. Zekel, A.S. Maloletnev, A.A. Ozerenko et al. // X and the mission of solid fuel. 2007. №1. pp. 35-42.
45. Landau, M.V. Hydrogenation of aromatic carbohydrates of species on nickel-tungsten sulfide catalysts at low pressure in the presence of sulfur / M.V. Landau, A.N. Zenchenkov, V.Ya. Kruglikov et al. // Petrochemistry. 1981. T.XX 1, No. 6. Pp. 835-839.
46. Kairbekov, Zh.K. Catalysts for the hydrogenation of coal based on sulfur compounds of iron and other metals / Zh.K. Kairbekov, E.N. Yakupova, A.ZH. Kairbekov et al // Bulletin of the Kazakh State University. Ser.x them. 2000. № 1. p. 26-33.
47. Krichko, A.A. In-depth processing of coal and heavy oil residues / A.A. Krichko, A.S. Maloletnev, S.N. Hajiyev // Russian Chemical Journal (J. Ros.x them. Malvinas them. DI Men leyev). 1994. T.XXXVIII, No. 5. P. 100-104.
48. Krichko, A.A. Hydrogenation of coal liquefaction products on a HBC catalyst / A.A. Krichko, B.K. Nefedov, M.V. Landau// Chemistry of solid fuels. 1990. № 2. p. 66-69.
49. Krichko, A.A. Pseudohomogeneous catalysts, synthesis and formation features / A.A. Krichko, A.A. Ozerenko, S.B. Frosin and others // Catalysis in industry. 2007. №2. p. 30-36.
50. Krichko, A.A. Useof a pseudohomogeneous catalysis tori for deep processing of oil feedstock and coke / AA Krichko, A.A., Ozerenko, A.S. Maloletnev et al. // K and catalysis in industry. 2007. №3. pp. 23-32.
51. Zekel, L.A. Molybdenum-containing catalytic systems and systems for hydrogenation processing of coal/ L.A. Zekel // Chemistry of solid fuels. 2001. №5. pp. 49-56.

52. Zinel, L.A. Bases synthesis and application of gene pseudogene catalysts for the hydrogenation of coal and oil with Darya s / LA Zekel, A.S. Maloletnev, A.A. Ozerenko et al. // Chemistry of solid fuels. 2007. № 1. P.35-42.
53. Machinsky A.S. Cavitation devices for wastewater treatment / A.S. Machinsky, A. Yakhova, N.N. Marutovskaya. M.: TSNIIT Eneftekhim, 1991. 240 p.
54. Nesterenko, A.I. On the use of cavitation for the cracking of hydrocarbons / A.I. Nesterenko, Yu.S. Berlizy // Chemistry of fuels and oils. 2008. №4. pp. 41-43.
55. Fedotkin I.M. The use of a technolo gist and cavitation processes iCal / IM Fedotkin, A.F., Nemchin. Kiev.: " Visha School", 1984. 68 p.
56. Kuznetsov O.L. The use of ultrasound in the oil industry / O.L. Kuznetsov, S.A. Efimova. M.: Nedra, 1995. 192 p.
57. Baykenov M.I. Study of the effect of cavitation at its second-OPERATION coal tar by liquid chromatograms and IFE / MI Baikenov, TB Omarbekov, Sh.K. Amerkhanova et al. // Chemistry of solid fuels. 2008. №1. pp. 41-45.
58. Ivchenko V.M. The use of supercavities about us for processing semi-finished products / V.M. Ivchenko, A.F. Nemchin // Applied fluid mechanics and hydrophysics. 1975. Vol. 1. p. 39-50.
59. Birkhoff G. Jets, traces and caverns / G. Birkhoff,E. Sarentllo. M.: Mir, 1964. 456 p.
60. Besov A.S. Degradation of hydrocarbons in the cavitation zone, in the presence of an electric field during the activation electrolyte solutions GOVERNMENTAL d / AS Besov, K.Yu. Koltunov, S.O. Brulev // Letters to the Journal of Physics and Technology. 2003. V. 29, Vol. 5. p. 71-76.
61. Nadirov N.K. Intensification of oxidation in oils sokovyazkih s / N. Nadirov, T.N. Kovalchuk // Bulletin of the National Academy of Sciences of Kazakhstan. 1995. № 5. p. 7477.
62. Patent 3207. RK. From 10C 3/04. The method of obtaining bits from mov / TN Kovalchuk, N.K. Nadirov, N.A. Nikolenko. 1996.
63. Kolpakov, L.G. Cavitation in centrifugal pumps when pumping oil and petroleum products / L.G. Kolpakov, Sh.I. Rahm and Tullin. M.: Nedra, 1980. 143 p.
64. Knapp R.Cavitation/R. Knapp,J. Daily, F. Hammit. M.: Mir, 1974. 668 p.
65. Nuumachi F. The Influence of Cavitation on the Accuracy of the Venturi Water Meter Reading/ F. Nuumachi, R. Kobayashi, S. Kamiyama // Proceedings of the American Society of Mechanical Engineers. Series 4: Tech Ceska and mechanics, 1962. № 3. – C.62.

66. Taniguchi K., Tanibayashi. Cavitation Tests on a Series of Supercavitating Propellers /K.Taniguchi,Tanibayashi. Proc. 1962 Jahr Symp. on Cavitation and Hydralic Machinery. Sendai (Japan), 1963. pp. 475-497.
67. Rozhdestvensky, V.V. Cavitation / V.V. Christmas. L.: Shipbuilding, 1977. 247 p.
68. Pernik, A.D. Problems of cavitation / A.D. Pernik. L.: Shipbuilding, 1966. 300 p.
69. Baykenov, M.I. The use of cavitation wave effects in the processing of coal tar / M.I. Ba th KENOVA, TB Omarbekov, Sh.K. Amerkhanova et al. // Vestnik KarSU Ser.x them. 2006. T.44, № 4. p. 54-56.
70. Musina, G.N. Processing of coal tar, etc. on radiation from coals Shubarkol cut / GN Musina, M.I. Baykenov, V.A. Group // Bulletin of the KarGU Ser.x them. 2006. T.44, № 4. P. 43-46.
71. Musina, G.N. Mechanochemical Activation of organ ic e tion weight coal tar and coal and catalytic Hydrogen tion / GN Musina, M.I. Baykenov, V.A. Groups and others. // Bulletin of Peoples' Friendship University of Russia. 2007. № 3. p. 79-84.
72. Patrakov, Yu.F. The effect of cavitation treatment coal on their physico-chemical properties and the ability to e skom Conventional thermal dissolution / YF Patrakov,N.I. Fedorova, S.A. Sem e // new solid fuel chemistry. 2007. № 1. p. 3-8.
73. Musina, G.N. Processing of coal tar into petrochemical and fuel products / G.N. Musina, M.I. Baykenov, V.A. Groups and others // News of the scientific and technical society " Kakhak ". Proceedings of the III International Scientific Conference "Modern trends and science in Ce n tral Asia. Almaty, 2007. –№ 17. – C. 127-129.
74. Khrenkova, T.M. Mechanicalchemical activation of coal / T.M. Khrenkova. M.: Nedra, 1993. 176 p.
75. AU. 1748336. USSR. Cavitation Reactor/ P and Schenko LI, Klimnik N.G. 1990.
76. Ivchenko, V.M. The use of supercavities about us for processing semi-finished products / V.M. Ivchenko // Applied Hydromechanics and Hydrophysics, 1975. Issue 1. p. 39-50.
77. Patent2078116 With 1, cl. 6C10G. USSR RU. Method cr e King oil and petroleum products and plant for its implementation / A.F. Kladov Publ. 1997.
78. AU. A 1 1377281, cl. C10G7/06. THE USSR. Methodlane rabotki oil. / Kurochkin A.K., Gimayev R.N., Valitov R.B. – 1984.
79. Chernozhukov, N.I. Technology of oil and gas processing / N.I. Chernozhukov // Ed. A. A. Gureeva and B. I. Bondarenko. 6th ed., Trans. and add. M.: Chemistry, 1978. 424 s.

80. Bogomolov, A.I. Chemistry of oil and gas / A.I. Bogomolov // Ed. Proskuryakova V. A. St. Petersburg, Chemistry, 1995. 446 s
81. Sergienko, S.R. High molecular weight compounds of oil / S.P. Sergienko. Moscow, 1964.
82. Gong, R.B. Oil bitumens / R.B. Gong. Moscow, 1973.
83. Grudnikov, I.B. Modern technology for the production of oxidized bitumen. Pectoral Moscow, 1980.
84. Rudnev, BM Oil residues / V.M. Rudnev. In and forge. <http://www.wikiznanie.ru>
85. Shmandy V.M. Perspective directions Pereire Botko and heavy oil residues / VM Shmandy, A.M. Yatsenko, A.A. Sparrows, etc. - Kremenchug State's polite nical Institute. <http://www.kgpi.ru>.
86. Methods of industrial production of oil and tar. Building materials and household goods. <http://www.ssa.ru>
87. Galiev R.G. On a new approach to deepening the processing of heavy oil residues/ R.G. Galiev,A.I. Lugansky, F.V. Tretyakov et al. Specialized journal Exposition Oil Gas. <http://www.expoz.ru>
88. Evdokimova, N.G. Preparation road bitumen to the bitumen m paundirovaniem reoxidation with tar / NG Evd about Kimova, K.V. Kortyanovich, B.S. Zhirnov et al. / Oil and gas business. <http://www.ogbus.ru>
89. Evdokimova, N.G. Some features of the liquidphase oxidation of petroleum residue sludge process / NG Evd about Kimova, M.Yu. Bulatnikova, R.F. Galiev / Oil and gas business. <http://www.ogbus.ru>
90. Bituminous emulsions. / LLC "RTF". <http://www.rtf-info.ru>
91. Wisbreaking. / LLC PetersburgNefteStroy Design and Construction Company. <http://www.ptrs.ru>
92. Visbreaking / Sibneft. <http://eburg.gazprom-neft.ru>
93. Bikbulatov, A.M. Stages in the development of e tive production of petroleum coke by delayed coking unit (for example, Novo-Ufa refinery) / A.M. Bikbulat about VA / Oil and gas business. <http://www.ogbus.ru>
94. Coking heavy oil residue / Wikipedia ru <http://wikipedia.org>
95. Coking and commodity production. Oil, gas and stock market. <http://www.ngfr.ru>
96. Gilyazetdinov, L.P. Physical andchemical bases of tehn ogy processing/ L.P. Gilyazetdinov, M.Al-Dzhoma // Chemistry and technology of fuels and oils. – 1994.-№3. – p.27-29.
97. Sunyaev, Z.I. Oil disperse systems / Z.I. Slyunyaev et al. M.: Chemistry, 1990.

98. Ashmarin, I.P. Rapid methods of statistical mod and developments and a planning experiments / IP Ashmarin, N.N. You and the lions. L.: Izd. L GU, 1972. 80 p.
99. Gulmaliev, A.M. Theoretical foundations of coal chemistry / A.M. Gulmaliev, G.S. Golovin, T.G. Gladun. M: Publishing House of MGGU, 2003. 556 p.
100. Gagarin, S.G., Gladun, T.G. Estimation of the enthalpy of formation of the organic mass of brown coal / SG Gagarin, T.G. Gladun // Chemistry of solid fuel. 2002. № 5. p. 11-20.

MONOGRAPH

Musina Gulnaz Nurgaliyevna

Candidate of Chemical Sciences, Professor Department "Chemistry and Chemical Technologies", Karaganda State Technical University

Ibatov Marat Kenesovich

Doctor of technical sciences, professor

Department "Transport Engineering and Logistic Systems" Karaganda State Technical University

Takibayeva Altynaray Temirbekovna

Candidate of Chemical Sciences

Department "Chemistry and Chemical Technologies", Karaganda State Technical University

Rakhimberlinova Zhanara Baltabaevna

Candidate of Chemical Sciences

Department "Chemistry and Chemical Technologies", Karaganda State Technical University

Baykenov Murzabek Ispolovich

Doctor of Chemical Sciences, Professor Department of Chemical Technology and Ecology

Karagandy State University named after EA Buketov

INDUSTRIAL CHEMISTRY IN MANUFACTURE

Subscribe to print 08/05/2020. Format 60×90/16.

Edition of 300 copies.

Printed by “iScience” Sp. z o. o.

Warsaw, Poland

08-444, str. Grzybowska, 87

info@sciencecentrum.pl, <https://sciencecentrum.pl>



ISBN 978-83-66216-28-0



9 788366 216280